The two cytosolic adapter proteins ADAP and SKAP55: new insights into their role in T cell adhesion, migration and interaction with antigen-presenting cells

❋ ❋ ❋

DISSERTATION

zur Erlangung des akademischen Grades

doctor rerum naturalium
(Dr. rer. nat.)

genehmigt durch die Fakultät für Naturwissenschaften
der Otto-von-Guericke-Universität Magdeburg

von Diplombiologin **Amelie Witte**
geb. am **15.04.1983** in **Güstrow**

Gutachter: Prof. Dr. rer. nat. Jan Tuckermann
Dr. rer. nat. Stefanie Kliche

eingereicht am: 21.02.2017
verteidigt am: 20.10.2017

Amelie Witte
Niemöller-Privatweg 3a
39112 Magdeburg

Eigenständigkeitserklärung

Hiermit erkläre ich, dass ich die von mir eingereichte Dissertation mit dem Titel

The two cytosolic adapter proteins ADAP and SKAP55: new insights into their role in T cell adhesion, migration and interaction with antigen-presenting cells

selbstständig verfasst, nicht schon als Dissertation verwendet habe und die benutzten Hilfsmittel und Quellen vollständig angegeben wurden.

Weiterhin erkläre ich, dass ich weder diese noch eine andere Arbeit zur Erlangung des akademischen Grades *doctor rerum naturalium* (Dr. rer. nat.) an anderen Einrichtungen eingereicht habe.

Magdeburg, den 10.11.2017

A. Witte

Diplombiologin Amelie Witte

ABSTRACT

The β2-integrin LFA-1 plays a crucial role in the immune system. It mediates the homing of T cells to secondary lymphoid organs and the interaction of T cells with antigen-presenting cells. Both processes are essential for the participation of T cells in the adaptive immune response. Stimulation of T cells via the T cell receptor or the chemokine receptor CXCR4 activates LFA-1 and thereby increases its binding capacity for the ligand, ICAM-1. This signaling cascade is termed inside-out signaling. ICAM-1-bound LFA-1 transmits signals into the T cell (outside-in signaling) to promote the adhesion, migration, activation, differentiation and proliferation of T cells. Several studies have identified the two cytosolic adapter proteins ADAP and SKAP55 as key regulators of LFA-1 activation. Both proteins form the backbone of two complexes that translocate to the plasma membrane (PM) upon T cell receptor and chemokine receptor stimulation. By binding to the cytoplasmic tails of LFA-1, these complexes induce a conformational change within the integrin, leading to its activation.

Activation of T cells leads to the phosphorylation of several tyrosines within ADAP, which mediate interactions with SH2 domain-containing signaling molecules such as SLP-76, Nck and Fyn. Tyrosine 571 of ADAP has been identified as a phosphorylation site in numerous phospho-proteomic studies. In the first part of my study, we identified the syk family kinase ZAP70 as an interaction partner of this phospho-tyrosine. While T cell receptor-dependent signaling events such as T cell interaction with antigen-presenting cells and adhesion were not affected by mutation of Y571, CXCR4-mediated migration and F-actin polymerization are compromised, but not the adhesive capacity of T cells.

SKAP55 exhibits a central PH domain. PH domains are best known to mediate protein/lipid (phosphatidylinositol (PI)) interactions to facilitate PM targeting of proteins. In the second part of my study, I analyzed the PI-binding properties of the PH domain of SKAP55. While *in vitro* studies showed that the isolated PH domain of SKAP55 has a preference for PIP_3, my *in vivo* data indicate that PM targeting of the SKAP55 PH domain does not dependent of PIP_3. Two residues within the PH domain of SKAP55 were identified that regulate PM recruitment of SKAP55, lysine 152 (K152) and aspartic acid 120 (D120). D120 facilitates the retention of SKAP55 in the cytoplasm of non-activated T cells, while K152 mediates PM targeting via actin-binding upon T cell stimulation. Surprisingly, the K152-dependent interaction of actin promotes the binding of Talin to LFA-1, thus regulating inside-out signaling of LFA-1.

ZUSAMMENFASSUNG

Das β2-Integrin LFA-1 vermittelt die Einwanderung von T-Zellen in sekundäre lymphatische Organe und deren Interaktion mit Antigenpräsentierenden Zellen. Beide Prozesse sind für die Teilnahme von T-Zellen an der adaptiven Immunantwort essentiell. In T-Zellen führt die Stimulation des T-Zellrezeptors oder des Chemokinrezeptors CXCR4 zur Aktivierung von LFA-1 und erhöht so dessen Affinität zu seinem Liganden ICAM-1. Die zur LFA-1-Aktivierung führende Signalkaskade wird *Inside-out signaling* genannt. Die Bindung von ICAM-1 an LFA-1 vermittelt ein kostimulatorisches Signal in die T-Zelle (*Outside-in signaling*) und reguliert so die Adhäsion, Migration, Aktivierung, Differenzierung und Proliferation von T-Zellen. Die molekularen Mechanismen, die die Aktivierung von LFA-1 regulieren sind bisher noch nicht vollständig verstanden. Verschiedene Studien belegen, dass die beiden Adapterproteine ADAP und SKAP55 an der LFA-1-Aktivierung beteiligt sind. Beide Adapterproteine besitzen weder enzymatische noch transkriptionelle Aktivität, enthalten aber Tyrosinmotive und Domänen, die es ihnen ermöglichen Interaktionen mit anderen Proteinen oder Lipiden einzugehen.

ADAP besitzt mehrere Tyrosinmotive, die nach der T-Zellaktivierung phosphoryliert werden. Diese phosphorylierten Tyrosine ermöglichen die Interaktion von ADAP mit Proteinen, die eine SH2-Domäne besitzen (z.B. mit den Adapterproteinen SLP-76 und Nck oder der Src-Kinase Fyn). Eine in mehreren Phosphoproteom-Studien identifizierte Phosphorylierungsstelle ist das Tyrosin 571 (Y571) in der hSH3-Domäne von ADAP. Der Interaktionspartner dieses Tyrosins sowie dessen funktionelle Relevanz bei T-Zellrezeptor- und CXCR4-induzierten Signalprozessen sind bis heute nicht bekannt und wurden daher im ersten Teil dieser Arbeit untersucht. Die im Zusammenhang mit dieser Arbeit durchgeführten Phosphoproteom-Studien (Arbeitsgruppe von Prof. C. Freund (Freie Universität Berlin)) identifizierten die Syk-Kinase ZAP70 als Bindungspartner des phosphorylierten Y571 von ADAP. In Immunpräzipitationsstudien konnte ich die durch T-Zellrezeptor- bzw. CXCR4-Stimulation induzierbare Interaktion dieser Kinase mit ADAP in T-Zellen bestätigen. Um weiterführend die funktionellen Konsequenzen der ADAP Y571-Phosphorylierung zu untersuchen, habe ich Suppressions-/Re-expressions-vektoren verwendet. Der Einsatz dieser Vektoren ermöglicht die shRNA-vermittelte Reduktion der Expression von endogenem ADAP und die gleichzeitige Re-expression einer ADAP-Mutante, in der das Tyrosin 571 zu

Phenylalanin (Y571F) mutiert wurde. Die Y571F-Mutation verhindert hierbei die Phosphorylierung von ADAP an Y571. Mit diesen Suppressions-/Re-expressionsvektoren konnte ich zeigen, dass die Re-expression der ADAP Y571F-Mutante keinen Effekt auf die T-Zellrezeptor-induzierte Adhäsion, die Expression des Aktivierungsmarkers CD69 sowie die Interaktion von T-Zellen mit Antigen-präsentierenden Zellen hat. Die Re-expression der ADAP Y571F-Mutante führte auch nach CXCR4-Stimulation zu einer unveränderten Adhäsion. Im Gegensatz dazu zeigten Zellen, die die ADAP Y571F-Mutante re-exprimieren, eine verminderte CXCR4-induzierte Migration und einen reduzierten F-Aktingehalt.
Zusammenfassend konnte ich demonstrieren, dass die Phosphorylierung am Y571 von ADAP die Bindung von ZAP70 vermittelt und selektiv die CXCR4-induzierte F-Aktin-abhängige aber Integrin-unabhängige T-Zellmigration reguliert.

SKAP55 enthält eine Dimerisierungsdomäne, eine PH-Domäne und eine SH3-Domäne. PH-Domänen sind dafür bekannt, dass sie die Bindung von Phospholipiden, wie Phosphatidylinositol-(3,4,5)-trisphosphat (PIP_3), vermitteln und damit die Rekrutierung an die Plasmamembran regulieren. Wir konnten zeigen, dass die isolierte SKAP55-PH-Domäne *in vitro* eine moderate Affinität für Phospholipide, mit einer Prävalenz für PIP_3, aufweist. Im zweiten Teil dieser Arbeit habe ich untersucht, ob die Bindungseigenschaften der PH-Domäne für PIP_3 für die Rekrutierung an die Plasmamembran ausreichen. Ich konnte zeigen, dass in T-Zellen die isolierte PH-Domäne von SKAP55 konstitutiv an der Plasmamembran lokalisiert und dass die Rekrutierung an die Plasmamembran nicht von PIP_3 abhängig ist. Vielmehr scheint eine indirekte Assoziation der PH-Domäne (vermittelt durch Lysin 152 (K152)) mit Aktin für die Membranrekrutierung von Bedeutung zu sein. Mit Hilfe der Suppressions-/Re-expressionsvektoren konnte ich zeigen, dass die Mutation dieses Lysins zu Glutaminsäure (K152E) die T-Zellrezeptor-vermittelte Adhäsion, Interaktion mit Antigenpräsentierenden Zellen und die Aktivierung von LFA-1 verhindert. Im Gegensatz zu der konstitutiven Lokalisation der isolierten PH-Domäne von SKAP55 an der Plasmamembran, lokalisiert das Vollelänge SKAP55-Molekül im Zytoplasma der T-Zelle. Hier konnte ich die Bedeutsamkeit von Asparaginsäure 120 (D120) innerhalb der PH-Domäne von SKAP55 demonstrieren. Die Mutation dieser Aminosäure zu Lysin (D120K) führt zur konstitutiven Membranlokalisation von SKAP55. Mit Hilfe von Suppressions-/Re-exressionsvektoren konnte ich zeigen, dass die Re-expression der D120K-Mutante von SKAP55 und die damit verbundene Lokalisation von

SKAP55 an der Plasmamembran in unstimulierten T-Zellen zu einer spontanen LFA-1-Aktivierung, Adhäsion an ICAM-1 und Interaktion mit Antigenpräsentierenden Zellen führt. Diese Ergebnisse legen die Vermutung nahe, dass eine autoinhibitorische Interaktion innerhalb von SKAP55 existiert, die die Rekrutierung dieses Proteins an die Plasmamembran reguliert. Dabei interagiert die N-terminale Dimerisierungsdomäne mit der PH-Domäne und verhindert so die Rekrutierung von SKAP55 an die Plasmamembran.
Zusammenfassend konnte ich zeigen, dass die SKAP55-vermittelte Aktivierung von LFA-1 über zwei Aminosäuren (D120 und K152) innerhalb der PH-Domäne von SKAP55 reguliert wird. Zum einen hält D120 SKAP55 in unstimulierten Zellen im Zytoplasma und damit LFA-1 inaktiv. Zum anderen rekrutiert K152 SKAP55 in stimulierten Zellen an die Plasmamembran und führt über die Assoziation mit Talin und Aktin zur Aktivierung von LFA-1.

❊ ❊ ❊

TABLE OF CONTENT

	EIGENSTÄNDIGKEITSERKLÄRUNG	
	ABSTRACT	**I**
	ZUSAMMENFASSUNG	**II**
	TABLE OF CONTENT	**V**
1.	**INTRODUCTION**	**1**
1.1.	The immune system	1
1.2.	T cells	2
1.2.1.	T cell development in the thymus	2
1.2.2.	T cell homing	3
1.2.3.	T cell-APC interaction	6
1.3.	The actin cytoskeleton and integrins	7
1.3.1.	The actin cytoskeleton	7
1.3.2.	Integrins	9
1.3.2.1.	Inside-out/outside-in signaling	11
1.4.	Cytosolic adapter proteins	13
1.4.1.	ADAP	13
1.4.2.	SKAP proteins	17
1.4.2.1.	SKAP55	17
1.4.2.2.	SKAP-HOM	20
1.5.	Aims of this study	22
2.	**RESULTS**	**23**
2.1.	Analysis of ADAP tyrosine 571 (Y571) phosphorylation in T cells	23
2.1.1.	ZAP70 binds to the phosphorylated tyrosine 571 (Y571) of ADAP	23
2.1.2.	Consequences of tyrosine 571 (Y571F) mutation within ADAP for TCR-induced T cell activation	26
2.1.3.	Consequences of tyrosine 571 (Y571F) mutation within ADAP for CXCR4-induced T cell activation	28
2.2.	Lipid-binding properties of the SKAP55 PH domain and its relevance for plasma membrane targeting of SKAP55 and LFA-1-mediated adhesion/interaction with APCs	31

2.2.1.	PH_{SK55} translocates to the plasma membrane in a PIP_3-independent fashion	31
2.2.2.	Lysine 152 (K152)-mediated actin binding promotes plasma membrane recruitment of PH_{SK55}	36
2.2.3.	Lysine 152 (K152) is required for TCR-triggered adhesion and T-APC interactions	38
2.2.4.	Aspartic acid 120 (D120) prevents TCR-independent plasma membrane targeting of SKAP55	43
2.2.5.	Aspartic acid 120 (D120) of SKAP55 negatively regulates adhesion, T-APC interactions and LFA-1 activation	45
3.	**DISCUSSION AND OUTLOOK**	**54**
3.1.	DISCUSSION	54
3.1.1.	Y571 of ADAP interacts with ZAP70 and regulates CXCR4-induced migration	54
3.1.2.	D120 and K152 within the PH domain of SKAP55 regulate plasma membrane localization of SKAP55 and thus LFA-1 activation	63
3.2.	OUTLOOK	72
4.	**MATERIALS AND METHODS**	**74**
4.1.	MATERIALS	74
4.1.1.	Equipment and software	74
4.1.2.	Consumables	76
4.1.3.	Reagents	77
4.1.4.	Kits	79
4.1.5.	Antibodies	80
4.1.6.	Enzymes and their appropriate buffers	82
4.1.7.	Oligonucleotides	83
4.1.8.	Constructs	84
4.1.8.1.	Vectors and provided constructs	84
4.1.8.2.	Generated constructs	85
4.1.9.	Cells	86
4.2.	METHODS	87
4.2.1.	Isolation and cultivation of primary human T cells (CD3+)	87
4.2.2.	Cultivation of Jurkat E6.1 and Raji B cells	87
4.2.3.	Mycoplasma test	87
4.2.4.	Cryoconservation of Jurkat E6.1 T cells and Raji B cells	88

4.2.5.	Electroporation of Jurkat E6.1 and primary human T cells	88
4.2.6.	Stimulation and Wortmannin/LY294002 treatment	88
4.2.7.	Plasma membrane fractionation	89
4.2.8.	Cell lysis	89
4.2.9.	Protein concentration	90
4.2.10.	Immunoprecipitation	90
4.2.11.	SDS-PAGE	90
4.2.12.	Immunoblotting	91
4.2.13.	Cell biology assays	92
4.2.13.1.	Flow cytometry-based methods	92
4.2.13.1.1.	Surface staining	92
4.2.13.1.2.	TCR-induced CD69 upregulation	92
4.2.13.1.3.	Determination of the F-actin content	92
4.2.13.2.	Integrin-based methods	92
4.2.13.2.1.	mAb24-binding assay	92
4.2.13.2.2.	Adhesion assay	93
4.2.13.2.3.	Conjugation assay	93
4.2.13.2.4.	Transwell migration assay	93
4.2.14.	Confocal laser scanning microscopy (CLSM)	94
4.2.14.1.	Slide preparation	94
4.2.14.2.	Microscopy	94
4.2.14.3.	Image evaluation	95
4.2.14.3.1.	Plasma membrane localization studies	95
4.2.14.3.2.	LFA-1 clustering studies	97
4.2.15.	Statistical analysis	97
4.2.16.	Generation of competent *E. coli* DH10B	97
4.2.17.	Culture of *E. coli* DH10B	98
4.2.18.	Chemical transformation	98
4.2.19.	DNA preparation	99
4.2.19.1.	MAXI-DNA preparation	99
4.2.19.2.	MINI-DNA preparation	99
4.2.20.	DNA concentration	100
4.2.21.	Agarose gel electrophoresis	100
4.2.22.	PCR	101
4.2.22.1.	PCR for the generation of DNA fragments	101
4.2.22.2.	*In vitro* Mutagenesis	101
4.2.23.	Annealing of oligonucleotides	102
4.2.24.	Restriction digest	103

4.2.25. DNA extraction after restriction digest 103
4.2.26. Ligation 104
4.2.27. Sequencing 104

REFERENCES **106**

ABBREVIATIONS **117**

LIST OF FIGURES AND TABLES **125**

ACKNOWLEDGEMENTS **128**

CURRICULUM VITAE **130**

1. INTRODUCTION

1.1. The immune system

The human body possesses three layers of defense to protect itself from invaders: (i) the epithelial barrier, (ii) the innate immune system and (iii) the adaptive immune system.[1]

As a first line of defense, epithelial cell layers of skin and mucosa (digestive tract or respiratory tract) form physical, chemical and anti-microbial barriers to prevent pathogen entry. Once the epithelial barrier is penetrated, the host requires active protection by the immune system. It guards the human body against external threats like pathogens or toxins, as well as internal threats like infected or malignant cells. It comprises two parts, the innate and the adaptive immune system.[1]

The evolutionary older innate immune system is the first line of active defense and represents a basic resistance against pathogens without generating long-lived memory. It responds very quickly to factors that are common for many pathogens, like lipopolysaccharides (LPS), unmethylated deoxyribonucleic acid (DNA) and sugars. These factors are called pathogen-associated molecular patterns (PAMPs) and are recognized by specialized innate immune receptors called pattern-recognition receptors (PRRs). Humoral and cellular components contribute to innate immune responses. Cytokines, chemokines, acute-phase proteins and the complement system represent humoral factors promoting innate immunity. Basophils, eosinophils, neutrophils, mast cells, monocytes/macrophages, dendritic cells (DCs) and natural killer (NK) cells represent the cellular component of the innate immune system. DCs serve as a major link between innate and adaptive immunity by capturing, processing and presenting antigens to T cells (cells of the adaptive immune system).[1]

The adaptive immune system is activated when the innate immune system fails to eliminate the pathogen. Expression of a large and extremely diverse repertoire of antigen-specific cell-surface receptors enables cells of the adaptive immune system to respond to almost all pathogenic threats. Importantly, adaptive immune cells possess the ability to differentiate into long-lived memory cells, which provide rapid and efficient protection upon secondary infection with the same pathogen. Like the innate immune system, the adaptive immune system comprises humoral and cellular components. The humoral components are antibodies produced and

secreted by B cells, chemokines and cytokines. The cellular components are B cells and T cells.

1.2. T cells

T cells play a central role in cell-mediated immunity. Based on their expression of the surface markers cluster of differentiation 4 or 8 (CD4 or CD8), two major T cell subsets can be defined. $CD4^+$ T cells act as helper T cells (Th), which support a variety of other immune cells, such as B cells and macrophages. They recognize foreign peptides presented by major histocompatibility complex (MHC) class II molecules expressed on antigen-presenting cells (APCs), like DCs, macrophages and B cells. Depending on the surrounding cytokine milieu, Th cells can differentiate into several subsets, e.g. Th1, Th2, Th17 or regulatory T cells (Tregs).[1]
The cytokine interferon-γ (IFNγ) produced by Th1 cells activates macrophages, allowing a more potent destruction of intracellular microbes. Th2 cells produce IL-4, which stimulates B cells to produce antibodies. Th17 cells participate in an early phase of the adaptive immune system. They stimulate local epithelial cells to produce chemokines, which guide neutrophils to the site of inflammation.[1]
Regulatory T cells (Tregs) are a specialized Th subset, which counter-balances immune responses to prevent tissue damage and maintain immunological self-tolerance. Two types of Tregs have been identified: natural Tregs (nTregs), which develop in the thymus; and induced Tregs (iTregs), which develop from naïve peripheral $CD4^+$ T cells.[1]
$CD8^+$ cytotoxic T cells (Tc) recognize antigens presented by MHC class I molecules, which are expressed by all nucleated cells in the human body. Upon T cell receptor (TCR) ligation, $CD8^+$ Tc release cytotoxic factors like granzymes and perforin to lyse infected or malignant target cells.[1]
Some of the effector T cells (both $CD4^+$ as well as $CD8^+$) will eventually differentiate into long-living memory cells that are antigen-experienced and enable the immune system to respond faster and stronger to reoccurring infections.[1]

1.2.1. T cell development in the thymus

T cells are derived from hematopoietic stem cells in the bone marrow. T cell progenitors leave the bone marrow to mature in the thymus. Maturation can be monitored by the expression of the alpha and beta chain of the T cell receptor (αβ-TCR), CD4 and CD8. Early-committed thymocytes lack the expression of all three receptors and are called double-negative (DN) thymocytes. During their maturation, DN thymocytes recombine TCR α- and β-chain genes. Productive

recombination and successful protein synthesis are a prerequisite for proliferation and differentiation into double-positive (DP) thymocytes. Ultimately, they express a complete αβ-TCR, CD4 and CD8.[2,3]

These DP thymocytes are exposed to self-peptides bound by MHC class I and II molecules presented on cortical epithelial cells. The interaction of the TCR with self-peptide/MHC directs DP thymocytes in two different destinations. Thymocytes receiving TCR signals below a critical threshold undergo apoptosis (death by neglect), whereas those receiving appropriate signal intensities are positively selected and proceed with the next selection step. At the same time, TCR signal duration or strength determines the CD4-CD8 lineage decision: short/low signal intensity induces the CD8 T cell pathway, while long/moderate TCR signals induce $CD4^+$ T cells. [2,3]

Single-positive CD4 or CD8 thymocytes migrate into the medulla of the thymus, where they scan medullary epithelial cells and DCs for presented self-peptides. Potentially autoreactive thymocytes expressing TCRs with high affinity for self-peptide/MHC complex undergo negative selection via apoptosis. At the end of this selection process, only a minor fraction of thymocytes survives maturation and leaves the thymus as naïve (has not encountered cognate peptide), single-positive (CD4 or CD8) T cells.[2,3]

1.2.2. T cell homing

Having left the thymus, naïve T cells recirculate through secondary lymphoid organs (SLOs) such as the spleen, tonsils, lymph nodes (LNs) and Peyer's patches, etc. Blood lymphocytes enter SLOs (called homing) and return into the circulation via efferent lymphatic vessels. Entry of lymphocytes into SLOs is realized by special "homing receptors" on lymphocytes, named selectins, integrins and chemokine receptors and their ligands expressed on the endothelium.[4,5]

Homing of T cells into LNs occurs continuously throughout the whole life with on average 2.5×10^{10} lymphocytes passing each human LN every day.[6] The immigration of T cells into LNs occurs in four steps: rolling, firm adhesion, crawling and transmigration (**Figure 1.1: steps 1-4**).[4–7]

First selectins (like L-selectin (CD62L)) on the surface of naïve T cells bind to glycoproteins (e.g. peripheral lymph node addressin (PNAd)) expressed on endothelial cells of high endothelial venules (HEVs). HEVs are specialized blood vessels that regulate almost the entire entry of lymphocytes into LNs. These weak and dynamic interactions lead to rolling of the T cell along the endothelium and result in a velocity reduction of the T cell to increase the probability of encountering chemokines presented on the vessel wall (**Figure 1.1: step 1**).[4,5,7]

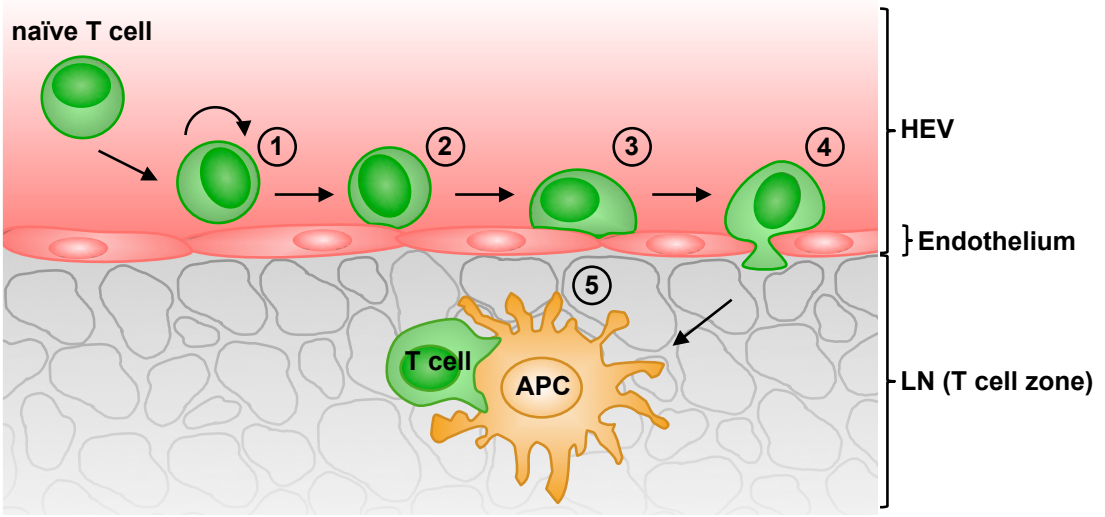

Figure 1.1: Homing and activation of T cells in lymph nodes. T cell homing occurs in four steps (1-4). **(1)** Rolling of the T cell along the endothelium is mediated by selectins expressed on T cells and glycoproteins expressed on endothelial cells of HEVs of LNs. **(2)** Chemokine-activated integrins enable firm adhesion of the T cell to the endothelium. Subsequently, the T cell crawls along **(3)** and migrates through the endothelium to get into the LN **(4)**. In the T cell zone of the LN, the encounter with an APC presenting cognate foreign-peptide/MHC-complexes activates the T cell to promote its proliferation and differentiation **(5)**. (modified from [4,7])

Naïve T cells express two chemokine receptors required for LN entry: C-X-C motif chemokine receptor 4 (CXCR4) and C-C motif chemokine receptor 7 (CCR7). CXCR4 binds C-X-C motif ligand 12 (CXCL12) and CCR7 binds C-C motif ligand 19 (CCL19) and C-C motif ligand 21 (CCL21).[7,8] All three ligands are considered as homeostatic, constitutively-expressed cytokines.[9] While HEVs solely produce CCL21, LN stromal cells in addition produce CCL19 and CXCL12, which are transcytosed and presented on the luminal side of HEVs.[7,8,10] The binding of these chemokines to their receptor induces signaling pathways that are only poorly understood, especially downstream of CCR7. CXCR4 and CCR7 are both G protein-coupled receptors (GPCR), which initiate different signaling pathways by the release of Gα and βγ subunits of the G protein.[9,11,12] Upon CXCR4 stimulation, the Gα subunit diffuses into the inner leaflet of the plasma membrane (PM), where it inactivates adenylate cyclase and thereby reduces the levels of intracellular cyclic adenosine monophosphate (cAMP). Studies with adenylate cyclase activators have revealed an inhibitory effect of cAMP on CXCL12-induced migration.[12] Additionally, src family kinases (SFKs) are believed to transmit CXCR4 signaling into the cell, although the identity of the src kinase as well as its activating mechanism remain subject to debate.[9,12] Data from Kumar et al. indicate that upon ligand binding CXCR4 associates with the TCR and uses its immunoreceptor tyrosine-based activation motifs (ITAMs) for signal transduction.[13] The src kinase lymphocyte-specific protein tyrosine kinase (Lck) phosphorylates the ITAMs of the TCR. This allows ξ-chain associated protein of

70kDa (ZAP70) recruitment to the ITAMs and subsequent activation of ZAP70 and IL2 inducible T cell kinase (Itk). The kinases Lck, ZAP70 and Itk activate several regulators that control cytoskeletal rearrangements (e.g. vav guanine nucleotide exchange factor 1 (VAV1)), cell survival (e.g. phosphatidylinositol-3-kinase (PI3K)), gene expression (e.g. phospholipase Cγ 1 (PLCγ1) and extracellular signal-regulated kinase (ERK1/2)) (**Figure 1.2**).[9,12] Furthermore, CXCR4 triggering initiates the formation of multiprotein complexes (containing e.g. adhesion and degranulation-promoting adaptor protein (ADAP)), which induce the activation of integrins and thereby adhesion and migration.[14]

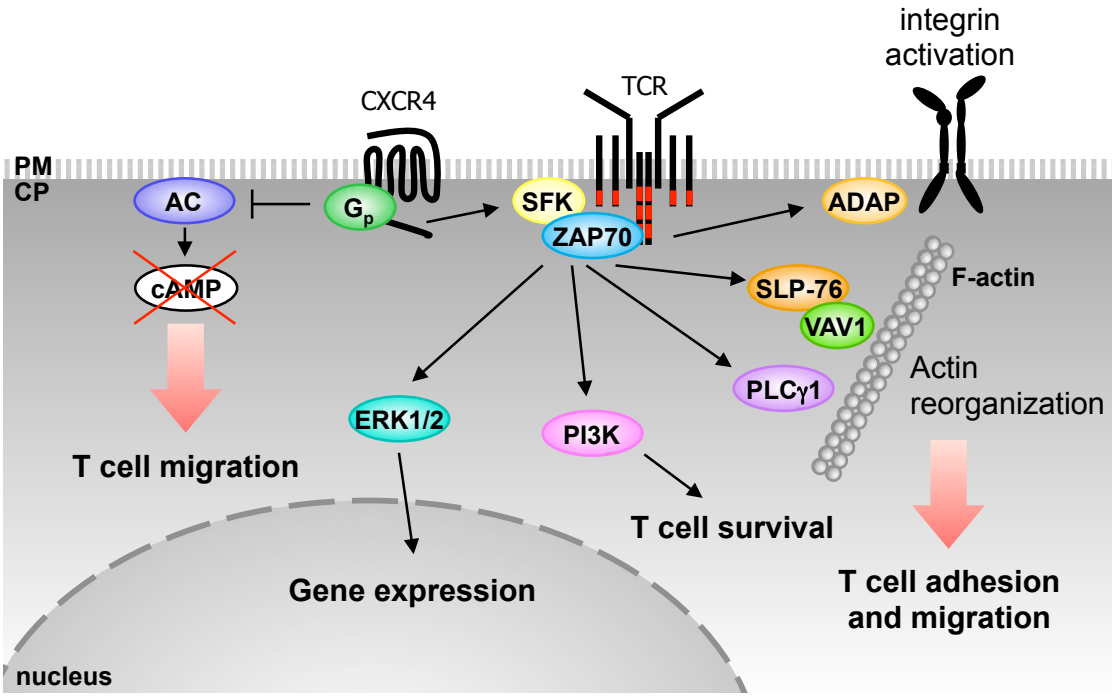

Figure 1.2: CXCR4-mediated signaling in T cells. Triggering of the chemokine receptor CXCR4 by its ligand leads to the activation of G proteins (G_p), which inhibit adenylate cyclase (AC) activity, thereby reducing cAMP levels and facilitating migration. Simultaneously, CXCR4 triggering activates SFKs that phosphorylate the ITAMs of the TCR. Binding of ZAP70 to the ITAMs allows its activation by SFKs. Eventually, ZAP70 in return regulates several signaling molecules involved in gene expression, cell survival, T cell adhesion and migration.[12,14] CP: cytoplasm, SLP-76: SH2 domain-containing leukocyte protein of 76kDa (modified from [12])

Activation of integrins by CXCR4 or CCR7 triggering results in the strong adhesion of T cells to the endothelium (**Figure 1.1: step 2**).[5,6] Subsequently, T cells crawl along and transmigrate through the endothelium into the LN (**Figure 1.1: step 3 and 4**).[4,7] They can passage either between (paracellular) or through (transcellular) endothelial cells.[5] For transmigration of T lymphocytes through the endothelium, the CCR7 receptor seems to co-operate with other chemokine receptors expressed on circulating naïve T cells, like CXCR4.[8,10]

1.2.3. T cell-APC interaction

Within LNs, T cells rapidly migrate (average three-dimensional velocity of 15μm/min) along the fibroblastic reticular cell (FRC) network.[7] FRCs produce CCL19 and CCL21 and guide T cells from the blood vessel to the T cell zone of the LN.[6–8] In the LN, T cells get in contact with foreign antigens bound to MHC presented on APCs. In the first eight hours after entering from the blood into the LN, T cells initially engage in transient (less than 10min) contacts with APCs. These contacts induce a change in T cell behavior, leading to progressively decreasing motility and prolonged T cell and APC (T-APC) interactions that can last for hours.[15] Here, the TCR engaged with its cognate (foreign-) peptide/MHC complex triggers a stop signal, which determines migration and induces long-lasting T-APC interactions (**Figure 1.1: step 5**).[16] These interactions result in a series of molecular rearrangements, finally leading to the formation of a distinct structure at the contact site between the two cells, termed the immunological synapse (IS).[17,18] The IS is organized like a shooting target, where the TCR and associated signaling molecules are localized in the center (central supramolecular activation cluster (cSMAC)). Integrins (like lymphocyte function-associated antigen-1 (LFA-1) and very late antigen-4 (VLA-4)) are enriched in the middle ring (called the peripheral supramolecular activation cluster (pSMAC)) of the IS, whereas a third distal region (called the distal supramolecular activation cluster (dSMAC)) consists of a circular array of filamentous actin (F-actin).[17,18]

During thymic T cell development, random recombination events at the TCR α and β chain loci ensure the expression of a single, unique TCRαβ for each naïve peripheral T cell. Consequently, the peripheral T cell pool contains a wide variety of TCRs specific to most – if not all – possible antigens.[19] Given that the cytoplasmic chains of the TCR are very short, the TCR co-operates with the CD3 complex to transduce signals into the T cell. TCRαβ themselves do not transduce signals upon peptide/MHC contact. This requires the CD3 complex, which comprises one delta/epsilon (δε) and gamma/epsilon (γε) heterodimer and one zeta/zeta (ξξ) homodimer.[19] Upon TCR engagement with a cognate peptide/MHC complex, Lck becomes activated and phosphorylates ITAMs of the TCR/CD3 complex. This is supported by the co-receptors CD4 and CD8, which deliver active Lck to the peptide-bound TCR.[19,20] Phosphorylation of the ITAMs leads to the recruitment of ZAP70 and its activation by Lck (phosphorylation of tyrosine 319 and 394). The adapter proteins linker for activation of T cells (LAT) and SH2 domain-containing leukocyte phosphoprotein of 76kDa (SLP-76) become phosphorylated by ZAP70 and form a signaling scaffold.[19,21] This scaffold includes a variety of regulators activating signaling pathways, as shown in **Figure 1.3**.

These regulators control integrin activation (e.g. ADAP),[19,21] cytoskeletal rearrangements (e.g. Nck (non-catalytic region of tyrosine kinase) and VAV1)[19,21,22] and gene expression (e.g. PLCγ1 and Itk).[19,22] Together, gene expression, activation of integrins and cytoskeletal rearrangements lead to full activation of T cells, proliferation and differentiation into effector T cells.[19]

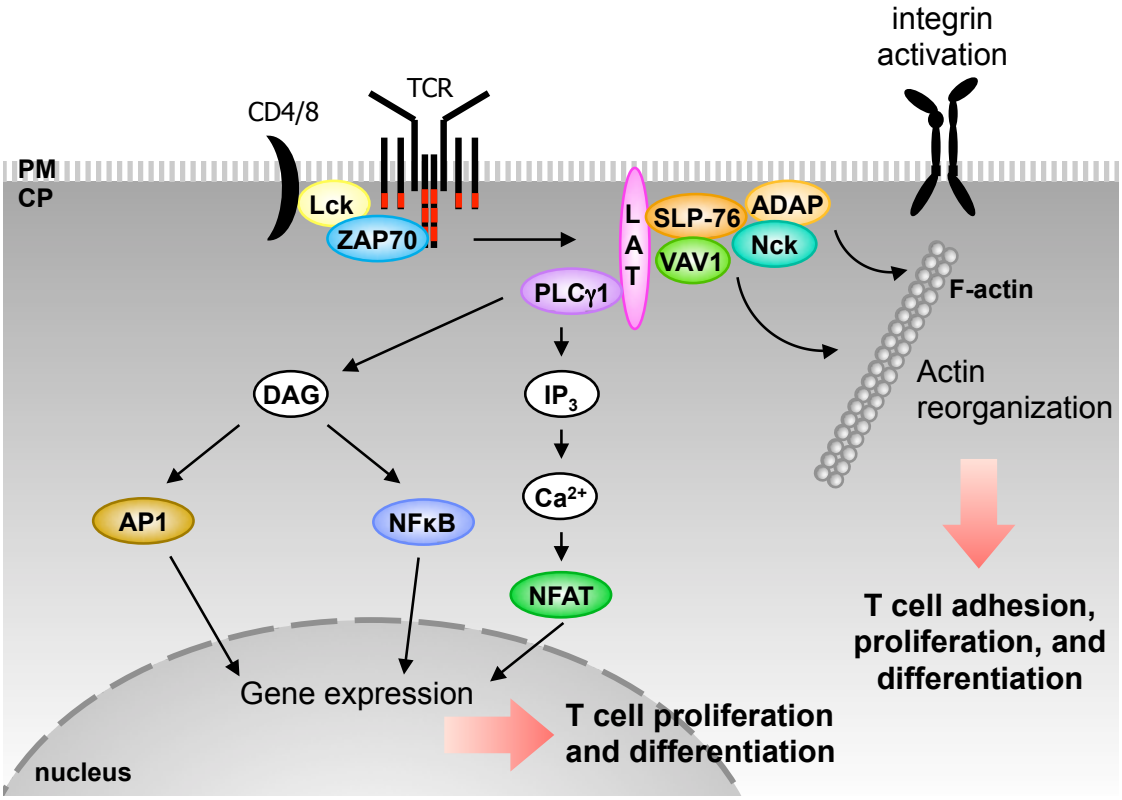

Figure 1.3: TCR-induced signaling pathways in T cells. TCR triggering activates the src kinase Lck. In turn, Lck activates ZAP70, which thereupon phosphorylates the adapter proteins LAT and SLP-76. A signaling scaffold associated around LAT and SLP-76 triggers several signaling pathways leading to T cell activation, proliferation and differentiation.[19-22] CP: cytoplasm; second messengers: Ca^{2+}: Calcium ions, DAG: diacylglycerol, IP_3: inositol-(1,4,5)-trisphosphate; transcription factors: AP1: activator protein-1, NFAT: Nuclear factor of activated T cells, NF-κB: nuclear factor kappa B

1.3. The actin cytoskeleton and integrins

In brief, T cell activation and effector function rely on different independent but coordinated cellular processes including migration, adhesion, the formation of an immunological synapse with defined central and peripheral signaling platforms, as well as the establishment of cell polarity for the directed secretion of cytokines and lytic granules. All of these processes crucially depend on the actin cytoskeleton and integrins.[5,23,24]

1.3.1. The actin cytoskeleton

Signaling pathways initiated by either the TCR or chemokine receptors like CXCR4 initiate dynamic cytoskeletal rearrangements, which induce morphological changes crucial for T lymphocyte adhesion, migration and

activation.[25,26] The circular floating T cell is covered with short microvilli build up by parallel bundles of actin filaments (**see Figure 1.4A**).[27] Molecules like L-selectin, which bind their ligand (PNAd) with low affinity, are localized at the tip of these microvilli, while molecules like the integrin LFA-1, which binds its ligand intercellular adhesion molecules 1 (ICAM-1) with high affinity, are excluded from the microvilli.[28,29] This distribution of adhesion molecules is thought to support rolling along the endothelium, while simultaneously minimizing unspecific adhesion.[30] Chemokine receptor stimulation triggers rapid microvilli collapse[31] and the activation of integrins, which involves the release of integrins from the actin cytoskeleton.[32] The T cell adheres and adopts a migratory phenotype (hand mirror shape) characterized by a leading edge at the front and a uropod at the rear (**see Figure 1.4B**).[25] T cells show an amoeboid movement where actin-rich protrusions at the front push forward while contractile structures at the rear pull.[16,25] When the migrating T cell encounters its antigen on an APC in the LN or spleen, migration is haltered and the cells rapidly polarize towards the intercellular contact area (**Figure 1.4C**).[16] The subsequent formation of the IS is accompanied by complex cytoskeletal changes and comprises the structural basis for T cell activation.[23]

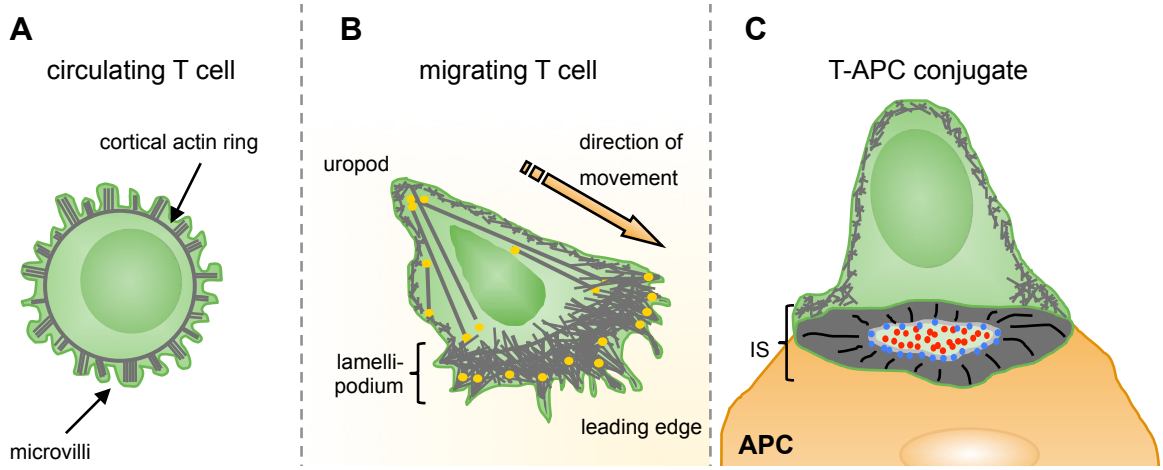

Figure 1.4: The actin cytoskeleton in T cells. By modulating its actin cytoskeleton, T cells can adopt different morphologies. **(A)** A floating T cell displays a circular phenotype with a cortical actin ring that produces microvilli.[27] **(B)** Upon triggering of chemokine receptors, T cells adopt a hand mirror-shaped form characterized by the lamellipodium at the leading edge and a uropod.[25] **(C)** Interaction of a T cell with an APC induces polarization of the T cell towards the APC and the formation of an immunological synapse (IS).[16] (modified from [33–35])

The actin cytoskeleton is a highly flexible system that undergoes permanent changes, where actin filaments are built up on one site (barbed (plus) end) and broken down on the other site of the filament (pointed (minus) end). Dynamic F-actin polymerization and depolymerization is realized by actin-severing (e.g. cofilin), actin-capping (e.g. Drosophila enabled/vasodilator-stimulated phosphoprotein (Ena/VASP) proteins and gelsolin), actin-regulatory

(e.g. Wiskott-Aldrich syndrome protein (WASp), WASp verprolin homologous (WAVE) and WASp-interacting protein (WIP)) and actin-nucleating proteins (e.g. actin-related protein 2/3 (Arp2/3) complex and formins).[16,23,25] Actin-severing proteins become activated downstream of cell-surface receptors and cleave F-actin, thereby providing globular/monomeric actin (G-actin) for new actin-filament growth. Actin-capping proteins bind to the barbed end of F-actin and prevent further actin polymerization. Actin-regulatory proteins regulate actin dynamics through their association with F-actin. Actin-nucleating proteins facilitate actin nucleation through binding either the barbed or pointed end of F-actin in conjugation with their binding to monomeric (G)-actin or G-actin-profilin complexes.[16,23,25]

1.3.2. Integrins

Integrins play a crucial role for T cell function. Upon activation by chemokines, integrins enable shear-resistant T cell adhesion, crawling and transmigration through the endothelium into SLOs (see **Figure 1.1** steps 2-4) or areas of inflammation. Integrins activated by TCR triggering provide the adhesive forces and signaling necessary to initiate and maintain T-APC interactions. Finally, integrins act as co-receptors that facilitate T cell activation, proliferation and cytokine secretion.[5,36,37]

Integrins are heterodimeric transmembrane receptors that comprise one α- and one β-chain. In mammals, 18 α- and 8 β-chains are known, forming 24 different integrins.[37–40] Two of the major integrins expressed on T cells are the β2-integrin LFA-1 (αLβ2 or CD11a/CD18) and β1-integrin VLA-4 (α4β1 or CD49d/CD29).[5,36,39] Binding of LFA-1 to its ligands ICAM-1-5[36,38] is important for T cell adhesion on HEVs, migration into peripheral LNs (pLNs) and T cell interactions with APCs.[37] VLA-4 binds to vascular cell adhesion molecule-1 (VCAM-1) and the extracellular matrix protein fibronectin.[36,38,41] Ligand binding by VLA-4 is involved in T cell adhesion to the extracellular matrix and migration of T cells to sites of inflammation.[36,41]

Integrins are expressed in three different conformations that exist in equilibrium in the PM but possess different affinities for their ligands: low affinity, intermediate affinity and high affinity conformation (**Figure 1.5A-C**).[5,36,37]

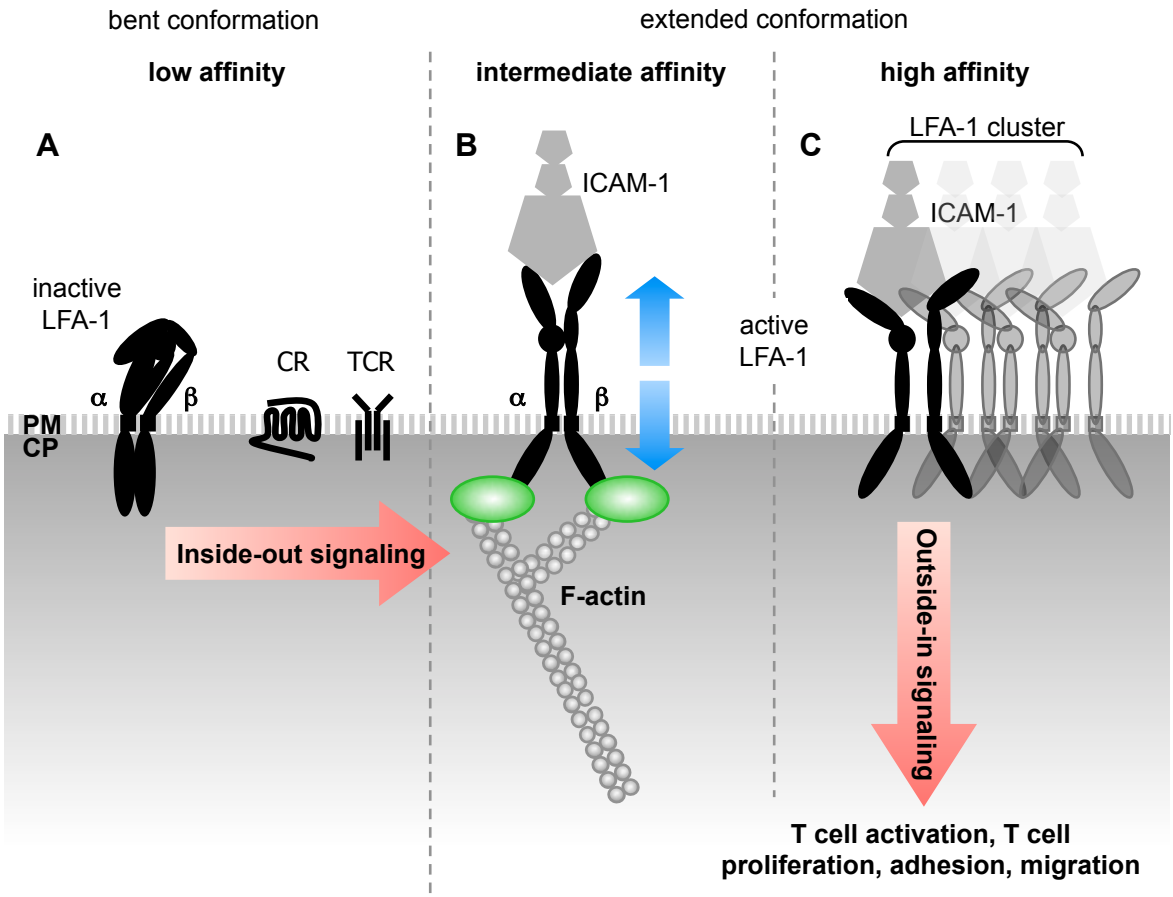

Figure 1.5: LFA-1 affinity and avidity regulation. (A) In its inactive state, LFA-1 is expressed in its bent/low affinity conformation. **(B)** Upon activation of the T cell by TCR or chemokine receptor (CR) stimulation, a signaling cascade is triggered (inside-out signaling), which induces the unfolding of LFA-1. The light green circles are a representation of two protein complexes (for details see **Figure 1.6**) that bind to the α- and β-chain of LFA-1 and regulate its activation by inducing conformational changes within the integrin and connecting LFA-1 with the actin cytoskeleton. Binding of the intermediate affinity LFA-1 to its ligand ICAM-1 and the actin cytoskeleton creates forces (blue arrows) that induce full activation of LFA-1 and high affinity binding to its ligand. **(C)** Active LFA-1 forms clusters that further increase adhesion (avidity regulation). High affinity ligand binding translates signals into the cell participating in T cell activation, proliferation, adhesion and migration (outside-in signaling). CP: cytoplasm (modified from [36,37,40])

Non-activated T cells hardly adhere to integrin ligands. Here, most of the integrins exist in an inactive state where the extracellular, ligand-binding headpiece bends down to the PM and the cytoplasmic domains are in tight contact with each other (**Figure 1.5A**). This allows only low affinity binding to the ligand.[37,38,40] Triggering of TCR or chemokine receptors initiates a signaling cascade called inside-out signaling, which induces the extension of the integrin to the intermediate affinity state (**Figure 1.5B**). Binding of the ligand to the intermediate affinity state induces a conformational change, leading to full activation of the integrin (high affinity).[37,38] High affinity integrins are characterized by separated cytoplasmic domains and an exposed/open headpiece.[38,40] Full activation of integrins is only realized by opposing forces supplied by the integrin-bound ligand and the

cytoskeleton (**Figure 1.5B**).[37] These conformational changes are accompanied by a 9,000-fold change in affinity of LFA-1 for ICAM-1.[42]

Active LFA-1 has been shown to form microclusters or to accumulate at one part of the cell (**Figure 1.5C**). An accepted view is that avidity regulation/cluster formation is another way to increase ligand binding by LFA-1 and thereby to strengthen the attachment to the endothelium or APC.[36–38] Ligand binding initiates conformational changes within the integrin, which send biochemical and mechanical signals into the cell to regulate multiple cellular functions. This is called outside-in signaling.[36–38] In T cells, the bidirectional signaling of integrins leads to the formation/stabilization of the immunological synapse to facilitate T cell activation, proliferation and cytokine secretion (e.g. interleukin-2 (IL-2)). Outside-in signaling is not fully understood but involves molecules that participate in inside-out signaling.[36,37]

The failure to express or activate the integrin LFA-1 can have life-threatening consequences, as shown by patients suffering from leukocyte adhesion deficiency (LAD) type I or III. Here, defective expression (LAD type I) or impaired activation of LFA-1 (LAD type III) causes severe recurring bacterial (most frequently by *Staphylococcus aureus* or gram-negative enteric bacteria) or fungal infections.[43]

1.3.2.1. Inside-out/outside-in signaling

Key players in LFA-1 activation upon TCR or chemokine receptor triggering are Talin, Kindlin-3, Rap1-GTP-interacting adapter molecule (RIAM), regulator for cell adhesion and polarization enriched in lymphoid tissues (RapL), Ras proximity 1 (Rap1) and mammalian sterile20-like kinase 1 (Mst1).[37,39,44] Knockdown or knockout (ko) of these molecules lead to severe consequences for T cell function (**summarized in Table 1.1**).

Table 1.1: Key players of integrin signaling.

	knockdown/knockout in T cells	known defects in humans
Talin (FERM-domain-containing protein)	impaired integrin activation[45,46] impaired adhesion, migration and conjugation with APCs[46–49] impaired F-actin polarization to the IS[49] impaired contact-dependent T cell proliferation and IL-2 production[49] impaired LN homing and trafficking[48,49]	
Kindlin-3 (FERM-domain-containing protein)	impaired development (reduced cellularity in thymus and spleen)[50] impaired LFA-1 activation[51]	LAD III[51,52]
Rap1 (small GTPase)	increased L-selectin-dependent rolling[53] impaired polarization of LFA-1, adhesion and migration[47,54,55] impaired T cell proliferation and cytokine production[53,54] impaired homing to LNs[53,55]	
RapL (Rap1-binding adaptor protein)	impaired adhesion and migration[47,56] impaired thymic emigration and LN homing[56]	
RIAM (Rap1-binding adaptor protein)	impaired adhesion[48,55] impaired homing to LNs [48,55] impaired T cell-dependent humoral immunity[55]	
Mst1 (kinase)	impaired LFA-1 clustering[57] impaired polarization, adhesion and T-APC interaction[57,58] impaired thymic emigration, homing to SLOs and intranodal migration[57]	autosomal recessive primary immunodeficiency (loss-of-function/loss-of-expression mutations)[59]

The molecules shown in **Table 1.1** together with the cytosolic adapter proteins ADAP and src kinase-associated phosphoprotein of 55kDa (SKAP55) form two signaling complexes that are involved in the activation of LFA-1 (subsequently referred to as LFA-1-activating complexes; **Figure 1.6**).[44] Adapter proteins exhibit no enzymatic or transcriptional activity but contain several protein/protein or protein/lipid interaction sites and thereby mediate the formation of signaling complexes.[44,60,61] One of these LFA-1-activating complexes comprises ADAP, SKAP55, RapL, Mst1 and Rap1, binding to the α-chain of LFA-1. The other complex contains ADAP, SKAP55, RIAM, Kindlin-3, Talin, Mst1 and Rap1 and binds to the β-chain of LFA-1 (**Figure 1.6**).[44,62]

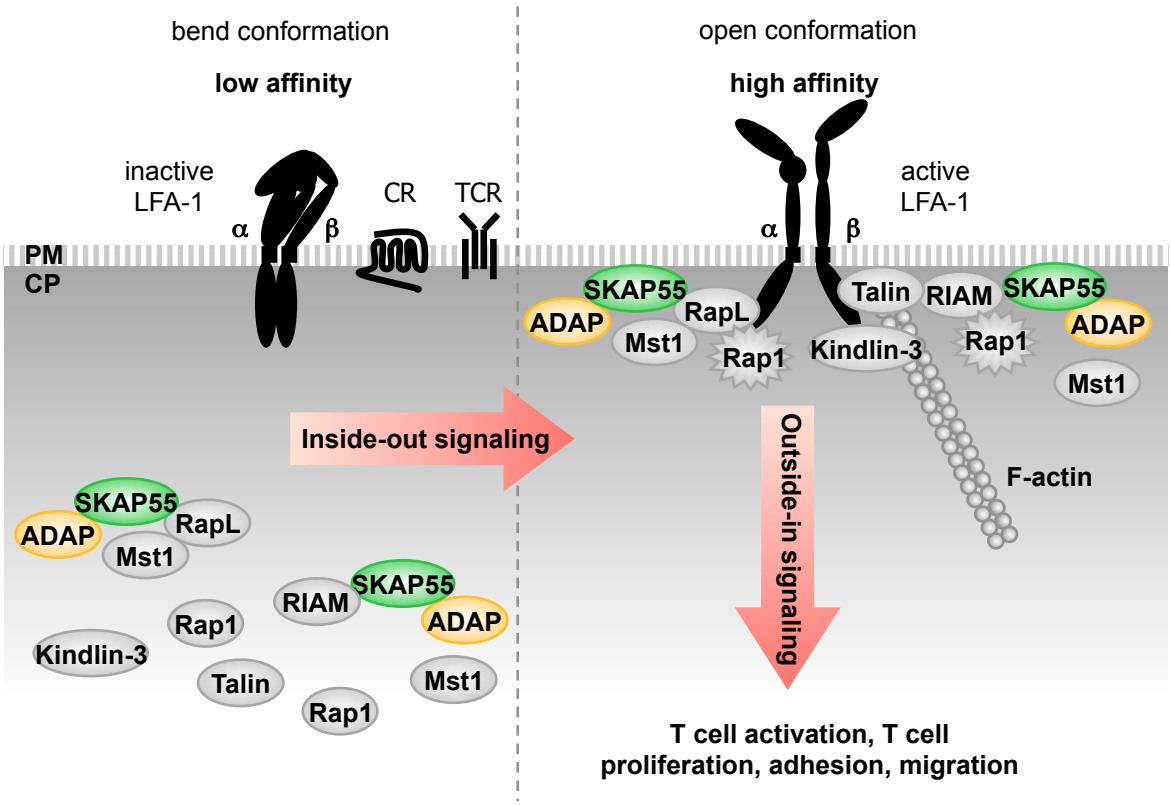

Figure 1.6: LFA-1-activating complexes. Upon TCR and Chemokine receptor (CR) triggering, two LFA-1-activating complexes are formed and recruited to the PM to bind to the cytoplasmic tails of LFA-1. One complex contains ADAP, SKAP55, RapL, Mst1 and Rap1 and binds to the α-chain of the integrin. The second complex binds to the β-chain and comprises ADAP, SKAP55, RIAM, Rap1, Mst1, Talin and Kindlin-3. Binding of these complexes to the integrin induces conformational changes within the integrin and connects LFA-1 to the actin cytoskeleton, leading to its activation (inside-out signaling). The fully-activated integrin binds its ligand with high affinity and translates signals into the cell participating in T cell activation, proliferation, adhesion and migration (outside-in signaling).[44,62] CP: cytoplasm

Both LFA-1-activating complexes are partially preformed in the cytoplasm of non-stimulated T cells and translocate to the PM upon stimulation.[62] They link integrins to the actin cytoskeleton and intracellular signaling pathways.[44,63] This enables integrins – like LFA-1 – to transduce signals into the cell (outside-in signaling), leading to adhesion, migration, T-APC interaction, T cell activation and proliferation.[37,44,63,64]

1.4. Cytosolic adapter proteins

1.4.1. ADAP

ADAP (also called: SLAP-130 (SLP-76-associated protein of 130kDa)[65] or FYB (Fyn-binding protein)[66]) is expressed in thymocytes, peripheral T cells and other hematopoietic cells.[65–67] Most recently, ADAP expression has been demonstrated outside the hematopoietic compartment in neuronal cells of the hippocampus.[68] As shown in **Figure 1.7**, ADAP possess an unstructured N-terminal region of unknown function, a proline-rich (PRO) domain, two helical src homology 3

(hSH3) domains, an Ena/VASP homology 1 (EVH1)-binding site and several tyrosine-based signaling motives.[69–74]

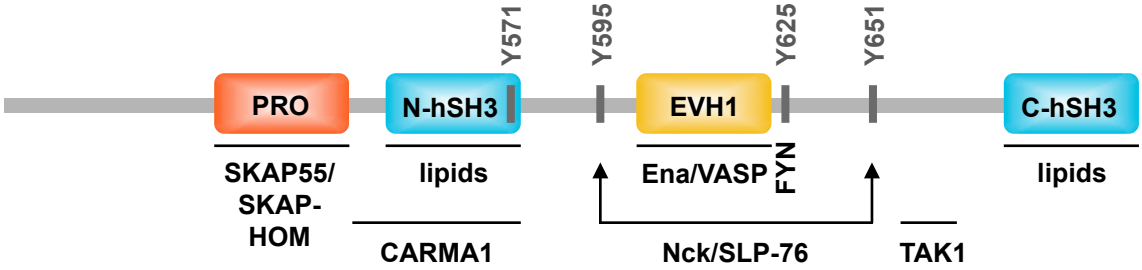

Figure 1.7: Structure of ADAP. ADAP consists of an unstructured N-terminal part, a PRO domain, two hSH3 domains, an EVH1-binding site, and several tyrosine-based signaling motives (Y). Identified interaction partners are listed below the domains/sites they are binding to. (modified from [21,74,75])

The tyrosines 595, 625 and 651 are well characterized. They are localized in the unstructured region between the two hSH3 domains of ADAP. Upon TCR triggering, ADAP becomes tyrosine-phosphorylated by the src kinase feline yes-related protein (Fyn)[75,76] and interacts with Fyn (YDGI, residues 625-628 of ADAP), Nck and SLP-76 (2 x YDDV, residues 595-598 and 651-654 of ADAP) in an src homology 2 (SH2) domain-dependent manner.[67,72,76–81] The interaction of ADAP with Nck connects the actin cytoskeleton to integrins.[79,82] As previously mentioned, forces provided by the actin cytoskeleton are essential for full activation of integrins (see **Figure 1.5B**).[37] Pauker and co-coworkers propose that Nck and ADAP both regulate actin polymerization and rearrangement by recruiting WASp to SLP-76 and stabilize their interaction.[82] The interaction of ADAP with SLP-76 is essential for T cell adhesion, migration, interactions with APCs, T cell activation and integrin clustering (avidity regulation).[67,75–77,83] Ligand binding of LFA-1 leads to an ADAP- and SLP-76-dependent re-organization of the actin cytoskeleton.[84,85] LFA-1 ligation (in the absence of TCR stimulation) leads to re-organization of the actin cytoskeleton into a ring-shaped structure, called an "actin cloud". Tyrosine-phosphorylated proteins accumulate in this actin cloud and enhance TCR signaling. Formation of the actin cloud involves the interaction of ADAP and LFA-1 and a functional ADAP/SLP-76 complex.[85] Additionally, SLP-76 is involved in the regulation of ADAP dephosphorylation by recruiting the phosphatase src homology phosphatase 2 (SHP-2) in the proximity of ADAP.[86]

The phosphorylation of several other residues within ADAP (Y559, Y571, Y755, Y757, Y771 and Y780) has been demonstrated.[75,77,87–90] Of special interest for my thesis is tyrosine 571 (Y571). Studies investigating the phosphorylation status of this residue are controversial, showing a significant[88,90] or negligible[89] increase upon TCR stimulation. Costimulation with CD28 has no effect on Y571 phosphorylation[91] and phosphorylation of this site does not depend on ZAP70.[89]

Y571 is localized at the rim of the N-terminal hSH3 domain (N-hSH3$_{ADAP}$, residues 490-579)[92] and the side-chain of Y571 is fully exposed. Therefore, phosphorylation of this residue might enable the binding of hitherto unknown interaction partners.[75]

hSH3 domains are an unusual variant of an src homology 3 (SH3) domain where an N-terminal α-helix packs against the β-sheet of the canonical SH3 domain structure. This increases the stability of the hSH3 domain.[74] These domains do not bind PRO domains; instead, the N-terminal α-helix displays several positively charged amino acid side chains that likely favor membrane lipid binding. Compared to N-hSH3$_{ADAP}$, the C-terminal hSH3 (C-hSH3$_{ADAP}$) domain shows higher affinity for lipids *in vitro* and might be involved in PM recruitment of ADAP.[71,93] Deletion of the N-terminal α-helices of both hSH3 domains leads to reduced T cell adhesion and migration. Complete loss of the C-hSH3$_{ADAP}$ domain has no effect.[71]

The EVH1-binding site (FPPPPDDDI motif, residues 616-624) is recognized by proteins of the Ena/VASP family.[73] These proteins are capping proteins involved in migration by modulating the actin cytoskeleton.[25,94]

The PRO domain (more precisely: residues 340-364 within the PRO domain) of ADAP mediates the interaction with the adapter proteins SKAP55 and SKAP-HOM.[69,70,95] This constitutive interaction with ADAP stabilizes the expression of both SKAP proteins by protecting them from degradation.[95–98] Therefore, the ADAP knockout mouse is a triple knockout that lacks ADAP, SKAP55 and SKAP-HOM.[95] In T cells, the interaction of ADAP with SKAP55 is essential for its integrin-regulatory functions. Upon deletion of the entire PRO domain or amino acids 340-364, ADAP-dependent adhesion to ICAM-1/fibronectin and T-APC interactions are impaired.[95,97,98]

We could show that there are two pools of ADAP identified in T cells: 70% of ADAP molecules are bound to SKAP55, thereby modulating integrin function; while 30% of ADAP molecules are not associated to SKAP55[70] and regulate nuclear factor kappa B (NF-κB) signaling by binding caspase recruitment domain-containing membrane-associated guanylate kinase protein-1 (CARMA-1) and transforming growth factor β-activated kinase (TAK1).[97–100]

CARMA-1/TAK1 binding to ADAP is induced by TCR/CD28-triggering.[99,100] ADAP ko T cells show defective CARMA1/B-cell lymphoma/leukemia 10 (Bcl10)/mucosa-associated lymphoid tissue lymphoma translocation protein 1 (MALT1) (CBM) complex formation and an impaired assembly of the protein kinase C theta (PKCθ)/CBM/TNF receptor-associated factor 6 (TRAF6) complex.[99,100] These complexes are essential for IL-2 production regulated by

NF-κB.[101,102] Additionally, Srivastava et al. have shown that the CARMA-1/TAK1 binding sites within ADAP are critical for T cell proliferation.[103] Deletion of the CARMA-1/TAK1 binding sites within full-length ADAP or the loss of ADAP leads to a complete block in gap1 phase/synthesis phase (G_1-S) transition after TCR/CD28 stimulation. This is due to an impaired accumulation of cyclin-dependent kinase 2 (Cdk2) and cyclin E.[103]

ADAP ko mice (also deficient for SKAP55 and SKAP-HOM[95]) show a defect in thymic positive and negative selection.[104] ADAP deficiency leads to defective T cell adhesion mediated by β1 and β2 integrins, reduced clustering of LFA-1 and defective T-APC interaction.[97,98,105,106] Additionally, studies have shown that ADAP is a positive regulator of T cell activation, proliferation and cytokine production (IL-2 and IFNγ).[105–108] We showed that CCL21-mediated migration, homing to SLOs and intranodal motility of ADAP ko T cells is impaired.[95] The impaired migration, activation and proliferation of T cells might be the reason why ADAP ko mice display increased allograft survival.[108,109] Experimental autoimmune encephalomyelitis (EAE) induction in ADAP ko mice is associated with reduced numbers of inflammatory cells in the central nervous system and a amelioration of disease. Data indicate that this is due to a radio-resistant non-hematopoietic cell type that retains T and B lymphocytes in LNs.[110] A study with ADAP ko mice revealed a negative role for ADAP by dampening the response of naïve $CD8^+$ T cells to lymphopenia and interleukin-15. Furthermore, this study demonstrated an antigen-independent function of ADAP, where it suppresses the generation of $CD8^+$ memory-like T cells.[111] Additionally, ADAP-deficiency enhances $CD8^+$ T cell cytotoxicity and facilitates tumor growth control.[112] Furthermore, Li and colleagues showed that ADAP is indispensable for autocrine transforming growth factor beta 1 (TGF-β1) production by $CD8^+$ T cells and that ADAP is essential for the protection against influenza virus infections.[113] By contrast, Pazmair and colleagues did not observe an impaired pathogen-specific immunity in *influenza A* or *Listeria monocytogenes*-infected mice adoptively transferred with ADAP-deficient $CD8^+$ T cells. In fact, they found that while ADAP ko $CD4^+$ T cells show severe impairment of TCR-triggered activation, proliferation and adhesion *in vitro*, their $CD8^+$ counterparts seemed to be almost unaffected by ADAP deficiency.[114]

In human patients, two studies by Levin et al. and Hamamy and colleagues identified homozygous mutations in the *FYB* gene.[115,116] In the first study, patients carry an ADAP nonsense mutation where guanine (G) 393 is mutated to adenine (A) (c.393G>A).[115] In the second case report, patients share a frameshift mutation caused by the deletion of 2 base pairs (bp, c.1385_1386del).[116] Both

mutations result in a premature stop codon and therefore translational termination presumably leading to a truncated ADAP molecule.[115,116] Interestingly, none of the patients developed immune defects or unusual infections but all of them showed small-platelet thrombocytopenia and an increased bleeding tendency.[115–117]

1.4.2. SKAP proteins

SKAP proteins include SKAP55 (also termed SKAP1[118]) and its homolog SKAP-HOM (SKAP55-homolog, also called: SKAP55-related (SKAP-55R)[69] or SKAP2[119]). Both proteins are 44% identical at the protein level, mainly in their pleckstrin homology (PH) and src homology 3 (SH3) domains (see **Figure 1.8**).[69,120]

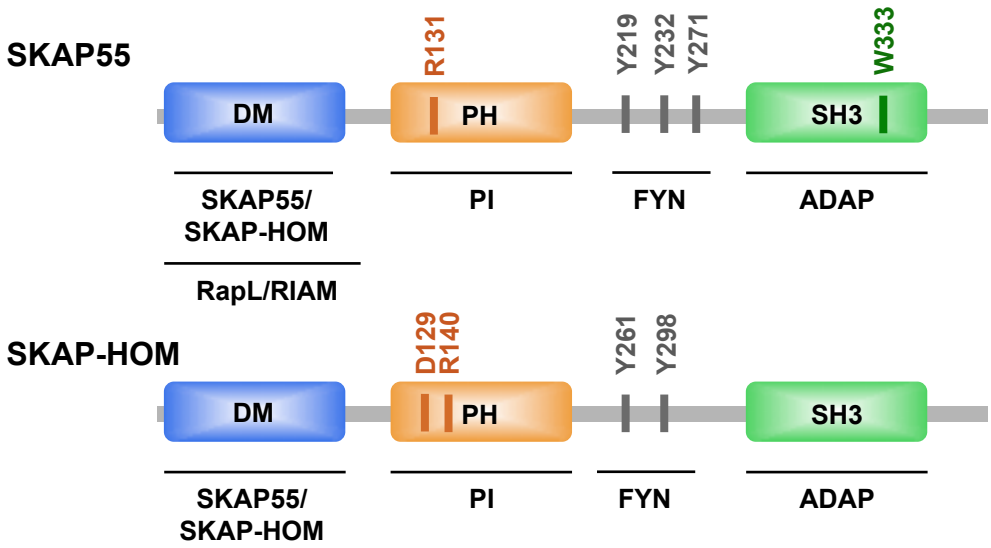

Figure 1.8: Structure of SKAP55 and its homolog SKAP-HOM. Both proteins contain a dimerization (DM) domain, a central PH domain, a SH3 domain and tyrosine-based signaling motives (SKAP55: Y219, Y232 and Y271[121,122]; SKAP-HOM: Y261 and Y298[120]). Tryptophane 333 (W333) within the SH3 domain of SKAP55 mediates the interaction with ADAP.[70,95,123] Arginine 131 (R131) in SKAP55[124] and arginine 140 (R140) in SKAP-HOM[125] have been described as enabling PM targeting of both proteins. Aspartic acid 129 (D129) in the PH domain of SKAP-HOM is involved in an auto-inhibitory mechanism that regulates the cellular localization of SKAP-HOM (for details see **Figure 1.9**).[125] Known interaction partners are listed below the domains/sites to which they bind. (adapted from [21,44,122])

1.4.2.1. SKAP55

SKAP55 is exclusively expressed in T cells[121,126] and contains a dimerization (DM) domain, a PH domain, three tyrosine-based signaling motives and a C-terminal SH3 domain (**Figure 1.8**).[69,121,122,127]

The SH3 domain (residues 300-356[121]) or more precisely, tryptophan (W) 333 of SKAP55 interacts with ADAP's PRO domain.[70,123] Marie-Cardine and colleagues could show that while only 70% of ADAP interact with SKAP55, depletion experiments revealed that there is no free SKAP55 in T cells.[70] The interaction with ADAP is essential for SKAP55 protein stability. ADAP ko T cells show normal

SKAP55 messenger ribonucleic acid (mRNA) levels but no detectable SKAP55 protein.[95] Loss of ADAP reduces the half live of SKAP55 protein from 90min to 15min. It seems that SKAP55 is a substrate of the proteasome- and caspase-driven proteolysis and that ADAP protects SKAP55 from degradation by stabilizing a protease/caspase-insensitive conformation or targeting it to subcellular compartments that are less accessible for proteolysis.[96] This suggests that ADAP and SKAP55 form a functional unit subsequently referred to as the ADAP/SKAP55 module.

SKAP55 also constitutively (under non-stimulatory and stimulatory conditions) interacts with the two Rap1-interacting proteins RapL (via its Sav/Rassf/Hpo (SARAH) domain)[128] and RIAM (via its (Ras-associating) RA and PH domain)[129] and it was shown that these interactions are essential for the translocation of Rap1 to the PM and integrin-mediated adhesion and T-APC interaction.[95,128,129]

Tyrosines 219, 232 and 271 within the linker region of SKAP55 have been described as potential phosphorylation sites. The EDIY[271]EVL motif has been predicted to mediate the interaction with the SH2 domain of Fyn and other src kinases,[121,127] although phosphorylation of these three tyrosines (Y219, Y232, Y271) has not been proven to date. Functional assays with a SKAP55 molecule where all three tyrosines are mutated to phenylalanine (Y to F) reveal no effect on T cell adhesion to ICAM-1 and fibronectin.[95,122] However, a study with the Y232F mutant showed that phosphorylation of this tyrosine induces an interaction of SKAP55 with CD45. Wu and co-workers published that overexpression of the Y232F mutant of SKAP55 in T cells abolishes the interaction of CD45 with Fyn, subsequently leading to reduced Fyn kinase activity and suppression of TCR-mediated IL-2 transcription.[130]

The role of the PH domain of SKAP55 (PH_{SK55}; residues 106-205[121]) remains controversial.[95,98,122,124] It has been proposed that PH_{SK55} binds phosphatidylinositol-(3,4,5)-trisphosphate (PIP_3) and that phosphatidylinositol (PI) binding is supposed to be required for stimulation-induced PM recruitment and LFA-1 binding. Arginine 131 (R131; see **Figure 1.8**) within PH_{SK55} was identified as the residue that enables PM recruitment. Mutation of arginine 131 to methionine (R131M) impairs PM recruitment of the SKAP55 mutant upon stimulation and leads to defective adhesion to ICAM-1.[124] In the same year, a study by Burbach and colleagues showed that deletion of the entire PH domain or R131M mutation within the PH domain of a SKAP55/ADAP chimera (SKAP55 residues 1-299 fused to ADAP residues 426-819) inhibits binding of the SKAP55/ADAP chimera to β2 integrins and strongly impairs T-APC interactions.[98] Burbach et al. hypothesized that an intact PH_{SK55} directs the

ADAP/SKAP55 module to the PM and thus towards integrin activation. Thereby, SKAP55 limits the ability of ADAP to interact with components of the NF-κB signaling pathway and act as a positive regulator of NF-κB activation.[98] In clear contrast, in 2006 we showed that overexpression of a SKAP55 mutant lacking the PH domain ($SKAP55_{\Delta PH}$) has no effect on adhesion to fibronectin and ICAM-1.[95] These findings were supported by a study in 2013, where SKAP55-deficient cells reconstituted with either $SKAP55_{\Delta PH}$ or a R131M-mutant of SKAP55 showed normal T cell adhesion and SLP-76 microcluster dynamics.[122] Since, further studies are necessary, my doctoral thesis focuses on unraveling the importance of this domain for T cell functions.

The DM domain of SKAP55 (DM_{SK55}; residues 1-60[122]) allows homo- and heterodimer formation with another SKAP55 or SKAP-HOM molecule, respectively.[122,131] DM_{SK55} is essential for SLP-76 cluster formation, stability and movement upon TCR stimulation. SKAP55 dimer formation has been shown to be required for T cell spreading, the formation of stable contacts and adhesion via the TCR in the absence of integrin ligands.[122] This might be due to an impaired interaction of SKAP55 with RIAM and RapL. While RapL directly connects the ADAP/SKAP55 module to the α-chain of LFA-1,[132] RIAM is required for the conformational activation of Talin[133] and its recruitment to TCR-induced adhesive junctions.[134] The importance of DM_{SK55} was not observed in a study from our lab using a SKAP55 molecule lacking its N-terminus (deletion of residues 1-105). Here, the N-terminal region of SKAP55 seems to be dispensible for TCR-mediated adhesion to ICAM-1 and fibronectin.[95]

SKAP55 ko T cells express normal ADAP levels.[135] They exhibit no major alterations in T cell maturation but otherwise have a phenotype comparable to ADAP ko T cells, showing reduced β1/β2 integrin-mediated adhesion, LFA-1 clustering, impaired polarization, T-APC interaction, IL-2/IFNγ production and proliferation.[134,135] In contrast to ADAP ko T cells, SKAP55-deficient T cells show normal migration *in vitro*.[118] These data suggest that the loss of SKAP55 might be compensated by SKAP-HOM, which is also expressed in T cells.[120,126] According to this theory, we are generating the double ko mouse that lacks the expression of SKAP55 as well as SKAP-HOM in T cells. Additionally, SKAP55-deficiency in $CD8^+$ T cells leads to increased cytotoxicity due to impaired programmed death-1 (PD-1) expression, resulting in enhanced tumor prevention in SKAP55 knockout mice.[112]

1.4.2.2. SKAP-HOM

In contrast to SKAP55, SKAP-HOM is ubiquitously expressed.[120,126] SKAP-HOM contains a DM domain, a PH domain, two tyrosine-based signaling motives and a C-terminal SH3 domain (**Figure 1.8**).[120]

Like SKAP55, SKAP-HOM interacts via its SH3 domain with ADAP,[120,123] whereby this interaction is also essential for stable protein expression of SKAP-HOM.[95]

Studies investigating the ability of SKAP-HOM to compensate for SKAP55 in T cells are controversial.[122,136] One study shows that knockdown of SKAP55 leads to impaired LFA-1 clustering and T-APC interactions, which was not reversed by expression of SKAP-HOM.[136] By contrast, a second study by Ophir and colleagues indicated that SKAP-HOM expressed at levels comparable to SKAP55 is able to rescue SLP-76 microcluster dynamics and T cell adhesion to fibronectin.[122]

Marie-Cardine and colleagues predicted that the N-terminus of SKAP-HOM (termed DM domain[125]) forms a coiled-coil structure mediating dimer formation.[120] Indeed, homodimerization with another SKAP-HOM molecule as well as heterodimerization with a SKAP55 molecule has been observed.[122,125] Additionally, Swanson et al. showed that the isolated PH domain of SKAP-HOM ($PH_{SK\text{-}HOM}$) binds preferentially PIP_3 and that PIP_3 binding is required for targeting the full-length SKAP-HOM molecule to actin-rich membrane ruffles. They identified arginine 140 (R140; see **Figure 1.8**), which is localized within $PH_{SK\text{-}HOM}$ and mediates the interaction of SK-HOM with PIP_3.[125] Interestingly, they observed a difference in the localization of full-length SKAP-HOM depending on whether they deleted its entire PH domain or single-mutated R140 within the PH domain. Deletion of the entire PH domain results in the localization at membrane ruffles as observed for the wild-type SKAP-HOM molecule. In contrast, mutation of R140 within the PH domain inhibits membrane recruitment and leads to diffuse cytoplasmic distribution.[125] They also found that PI binding by $PH_{SK\text{-}HOM}$ is strongly reduced when the PH domain is expressed together with the N-terminal DM domain. They identified a loop localized between the β1 and β2 strand of $PH_{SK\text{-}HOM}$, forming a helix that interacts with the DM domain.[125] The interaction of the two domains mediates an auto-inhibitory conformation that prevents PIP_3-triggered localization to actin-rich membrane ruffles in macrophages. They hypothesized that SKAP-HOM exists in two states: a closed, auto-inhibited conformation of the protein with cytoplasmic distribution (**Figure 1.9A**); and an open, PI binding state that localizes at actin-rich membrane ruffles (**Figure 1.9B**).[125] They identified aspartic acid 129 (D129; localized within $PH_{SK\text{-}HOM}$; see **Figure 1.8**), which mediates the inhibitory interaction with the DM domain. Mutation of D129 to lysine (D129K) induces the active state of the protein and leads to constitutive

membrane localization of SKAP-HOM that evokes hyperactive actin polymerization.[125,137] Combining both mutations D129K/R140M creates a SKAP-HOM molecule that is constitutively in an open/active state but unable to bind PIP_3. Studies with this double mutant revealed that it still localizes at membrane ruffles and induces the hyperactive polymerization of actin.[125,137] Swanson and colleagues hypothesized that PIP_3 binding by R140 alone is not sufficient for ruffle association but relieves the auto-inhibitory conformation of SKAP-HOM and expose a putative ruffle-targeting signal (e.g. a protein-protein interaction site in the DM domain).[125]

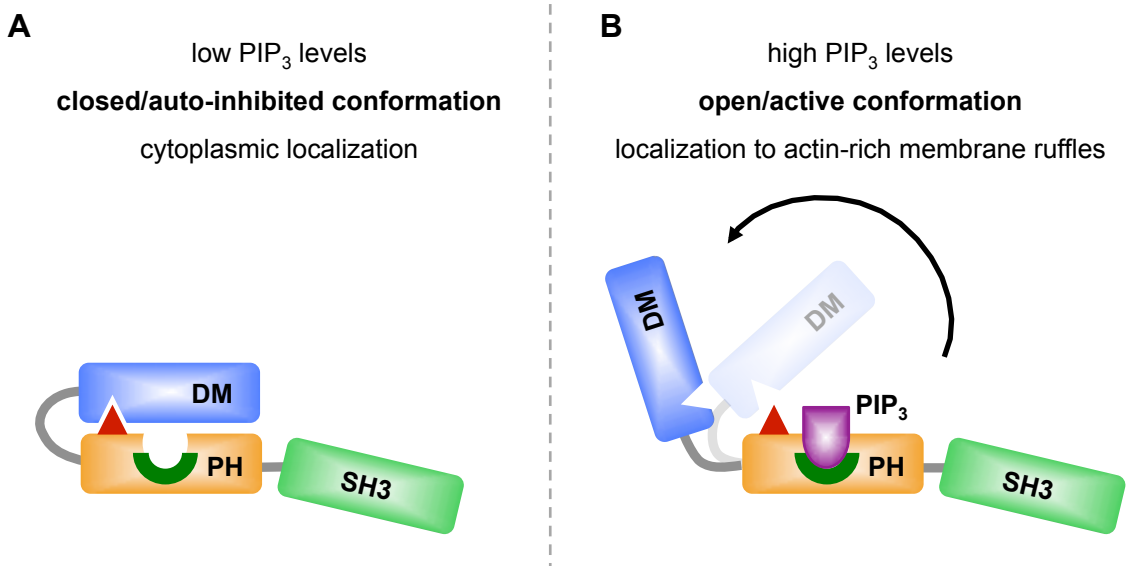

Figure 1.9: Model of a PIP_3-responsive molecular switch that controls the targeting of SKAP-HOM to actin-rich membrane ruffles. (A) At low PIP_3 levels, SKAP-HOM is in its closed/auto-inhibited conformation where aspartic acid 129 (D129; depicted in red) within $PH_{SK\text{-}HOM}$ mediates an interaction with $DM_{SK\text{-}HOM}$. In its closed conformation, SKAP-HOM is localized in the cytoplasm of the cell.[125] **(B)** At high PIP_3 levels, PIP_3 is bound by arginine 140 (R140; localized in the PI-binding pocket depicted in dark green), which relieves the interaction of $PH_{SK\text{-}HOM}$ with $DM_{SK\text{-}HOM}$ stabilizing the open/active conformation of SKAP-HOM and enables ruffle targeting.[125]

SKAP-HOM ko mice show normal T cell development and display no T cell defects. SKAP-HOM ko B cells on the other hand have a defective β1/β2 integrin-mediated adhesion and *in vitro* proliferation.[126] The differences for T cells and B cells might be due to a compensatory effect by SKAP55, which is expressed in T cells but not in B cells.[121,126]

1.5. Aims of this study

To participate in the adaptive immune response, T cells have to home to SLOs and interact with APCs.[6] Both processes have been linked to the activation of the integrin LFA-1,[37,63,138,139] actin cytoskeletal rearrangements[16,24,26] and the two cytosolic adapter proteins ADAP and SKAP55.[21,44,140]

In my study, I have addressed the following questions:

(i) What is the functional relevance of ADAP Y571 phosphorylation?

Tyrosine 571 (Y571) is localized at the rim of N-hSH3$_{ADAP}$. Controversial data have been published on the phosphorylation status of Y571, showing a significant[88,90] or negligible[89] increase upon TCR stimulation. The aim of the first part of my thesis was to validate ZAP70 as an interaction partner of ADAP and to monitor the importance of tyrosine 571 phosphorylation for T cell function upon TCR as well as chemokine receptor stimulation.

(ii) What is the functional role of the SKAP55 PH domain for TCR-mediated LFA-1 activation?

PH domains are known for their ability to bind specifically and with high affinity to lipids of the PM called posphoinositides (PIs), thereby targeting proteins to the membranes.[141–145] In the second part of my thesis, I focused on the PI-binding properties of PH$_{SK55}$ and its role for SKAP55 recruitment to the PM. My aim was to verify the involvement of lysine 116 (K116), lysine 152 (K152) and aspartic acid 120 (D120) in PI binding and ascertain whether these residues control the cellular localization of SKAP55 (cytoplasm (non-stimulated T cell) versus PM (stimulated T cell)).

The results of these studies are presented in section 2.

❊ ❊ ❊

2. RESULTS

My research study is divided into two parts: the first part deals with the role of tyrosine 571 of ADAP ($ADAP_{Y571}$) for T cell adhesion, interaction of T cells with APCs and regulation of the actin cytoskeleton, while the second part focuses on the PH domain of SKAP55 (PH_{SK55}), its lipid/protein-binding properties and relevance for integrin activation.

2.1. Analysis of ADAP tyrosine 571 (Y571) phosphorylation in T cells

TCR-mediated activation of T cells leads to ADAP phosphorylation at multiple tyrosine residues.[65,66,77,80,88,90] Some of these tyrosines have been described to mediate interactions with SH2 domain-containing signaling molecules, including SLP-76,[65–67,76,77] Nck[75,78,79] and Fyn.[66,80] Studies investigating the phosphorylation of tyrosine 571 of ADAP ($ADAP_{pY571}$) upon TCR stimulation are controversial[88–90] and no interaction partner(s) have been identified to date.

2.1.1. ZAP70 binds to the phosphorylated tyrosine 571 (Y571) of ADAP

Using the *in vitro*-phosphorylated N-$hSH3_{ADAP}$ domain (residues 486-579) as bait, pull-down experiments demonstrated a direct interaction between $ADAP_{pY571}$ and the N-terminal phospho-tyrosine binding pocket of the tandem SH2 domains of the spleen tyrosine kinase (syk) family kinase ZAP70 (N-$pYBP_{ZAP70}$).[146] ZAP70 is a protein tyrosine kinase that plays a crucial role in T cell development and function.[147–149] To verify whether ZAP70 interacts with ADAP in Jurkat T cells upon TCR or chemokine receptor stimulation, we performed co-immunoprecipitation experiments. Jurkat T cells were stimulated with OKT3 (monoclonal anti-TCR antibody) or recombinant CXCL12 (ligand for CXCR4[150]) and lysates were used for the immunoprecipitation of ZAP70. Western Blot analysis of precipitates revealed no co-precipitation of ZAP70 and ADAP in non-stimulated Jurkat T cells but an interaction of both molecules upon T cell activation (**Figure 2.1.1**). After TCR stimulation, the interaction of ZAP70 with ADAP peaked at 5min and strongly decreased thereafter. On the other hand, upon CXCR4 stimulation, the ADAP/ZAP70 interaction already peaked at 1min of stimulation and rapidly declined again within the next 4 minutes.

SKAP55 is an interaction partner that links ADAP to integrin activation.[95,98] As shown in **Figure 2.1.1**, staining for SKAP55 suggests that ZAP70 binds to the SKAP55-associated pool of ADAP upon TCR as well as CXCR4 stimulation. This indicates that the ADAP/SKAP55-associated pool of ZAP70 might be involved in integrin activation. It has been reported before that ZAP70 kinase activity is

critical for integrin activation.[151–155] ZAP70 kinase activity is commonly monitored by the phopshorylation of tyrosine 319. Tyrosine 319 is localized within the interdomain B of ZAP70 and becomes phosphorylated by Lck upon T cell stimulation. Phosphorylation of Y319 induces a conformational change within ZAP70, which is pivotal for full catalytic activity of the kinse.[156,157] **Figure 2.1.1** shows that only upon TCR stimulation ADAP-associated ZAP70 became phosphorylated at Y319. ZAP70 pY319 levels peaked at five minutes of TCR stimulation and subsequently decreased to almost undetectable levels at 10min. After CXCR4 stimulation, no Y319 phosphorylation of the ADAP-bound ZAP70 was detectable under the given conditions (**Figure 2.1.1**).

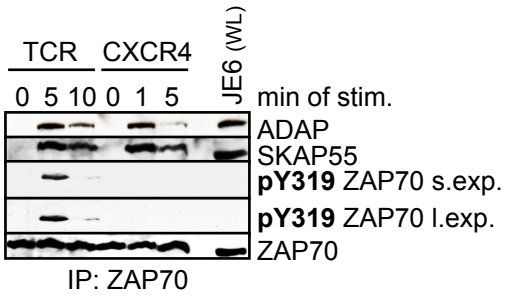

Figure 2.1.1: ZAP70 inducibly interacts with ADAP upon TCR and CXCR4 stimulation. Jurkat T cells were either left untreated, stimulated with anti-TCR monoclonal antibody OKT3 (TCR) or CXCL12 (CXCR4) for the indicated time points. Lysates were used for immunoprecipitation using an anti-ZAP70 antibody (IP:ZAP70). Precipitates were separated by sodium dodecyl sulfate polyacrylamide gel electrophoresis (SDS-PAGE), transferred and immunoblotted with the indicated antibodies. JE6 (WL): whole lysate of non-stimulated Jurkat JE6 T cells, served as positive control. l.exp.: long exposure, s.exp.: short exposure

These data indicate that ZAP70 interacts with ADAP upon TCR as well as CXCR4 stimulation. Our data also suggest that ADAP-bound ZAP70 only becomes activated upon TCR stimulation. ZAP70 molecules that interact with ADAP upon CXCR4 triggering seem to be kinase inactive (no pY319).

Since the interaction of ADAP and ZAP70 upon T cell stimulation was confirmed in T cells, it was of interest to ascertain whether the interaction of both proteins depends on the phosphorylation of ADAP at Y571. To address this question, a suppression/re-expression vector system (described in chapter **4.1.8.2.**) was used. This system allows the small hairpin RNA (shRNA)-mediated downregulation of endogenous ADAP and the simultaneous re-expression of an shRNA-resistant FLAG-tagged version of ADAP. To study the importance of $ADAP_{pY571}$, a suppression/re-expression vector was generated that encodes an ADAP where tyrosine 571 was mutated to phenylalanine (RE-AD_{Y571F}). This amino acid exchange prevents the phosphorylation of ADAP at position 571. In parallel, a control suppression/re-expression vector encoding wild-type ADAP (RE-AD_{WT}) was used (**Figure 2.1.2A**). **Figure 2.1.2B** shows a Western blot analysis of cell

lysates derived from Jurkat T cells transiently transfected with the indicated suppression/re-expression vectors. Expression of endogenous ADAP was reduced by 60%. In addition, these vectors allowed simultaneous re-expression of either FLAG-tagged RE-AD$_{WT}$ or RE-AD$_{Y571F}$ to comparable levels (**Figure 2.1.2B**).

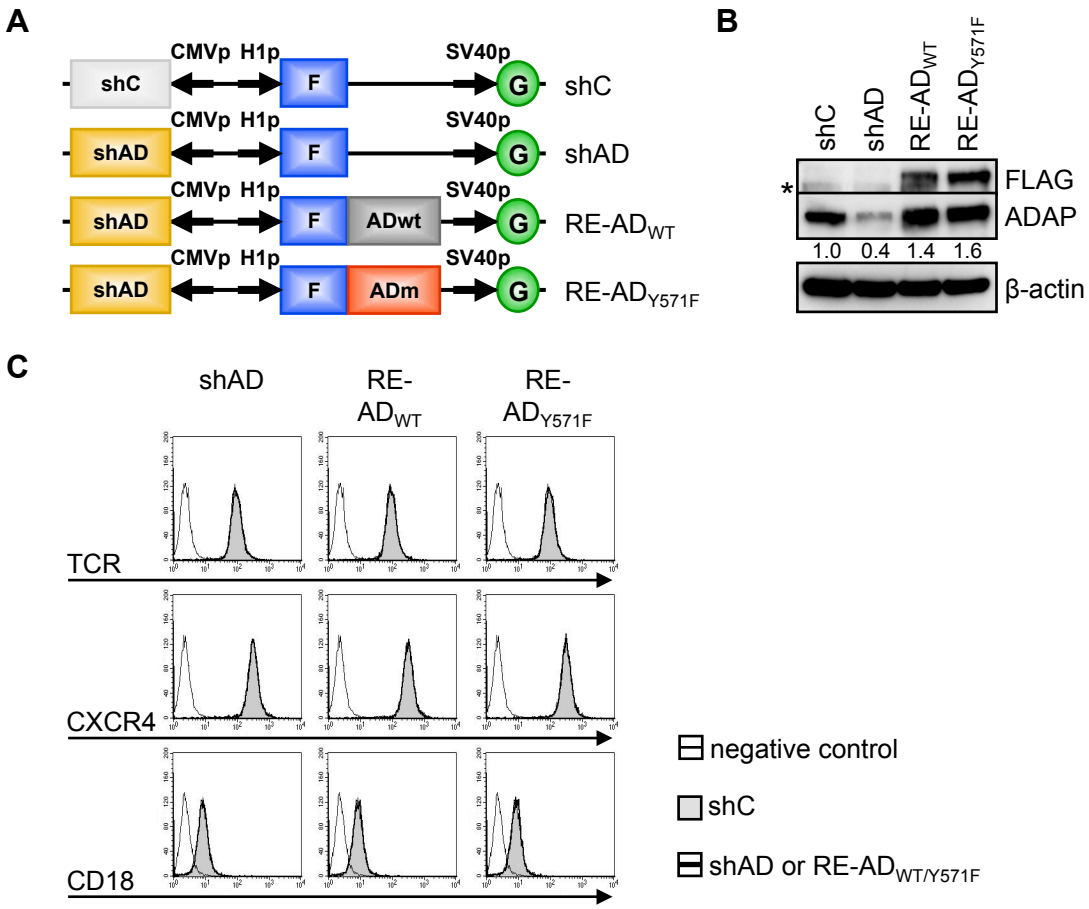

Figure 2.1.2: Suppression/re-expression vectors of ADAP. (A) Schematic representation of the suppression/re-expression vectors for ADAP used in this study. The vectors are composed as follows: shC: control vector encoding green fluorescent protein (GFP, G); shAD: vector encoding shRNA against ADAP (shAD) and GFP (G); RE-AD$_{WT}$: vector encoding shRNA against ADAP (shAD), shRNA-resistant FLAG-tagged wild-type ADAP (ADwt) and GFP (G); RE-AD$_{Y571F}$: vector encoding shRNA against ADAP (shAD), shRNA-resistant FLAG-tagged (F) Y571F-mutated ADAP (ADm) and GFP (G). **(B,C)** Jurkat T cells were transfected with the constructs shown in (A) and incubated for 48h. **(B)** Cell lysates were prepared, separated by SDS-PAGE, transferred and analyzed by immunoblotting for FLAG (re-expressed FLAG-tagged ADAP) and ADAP (endogenous and re-expressed ADAP) antibodies. Star (*) marks a non-specific band for FLAG blotting. Staining with an anti-β-actin antibody served as a loading control. The suppression of endogenous ADAP and re-expression of FLAG-tagged wild-type and mutant ADAP were quantified using the Kodak Image Station 2000R (Kodak ID Image software). **(C)** Cells were analyzed for their surface expression of TCR, CXCR4 and CD18 (LFA-1) by flow cytometry gating on GFP-positive cells. The gray, filled curves represent the shC-transfected control cells and the bold, black lines are cells transfected with the construct of interest (shAD, RE-AD$_{WT}$ or RE-AD$_{Y571F}$). The negative control (cells stained with secondary antibody only) is represented as a thin black line. One representative experiment out of two is shown.

If Y571 is required for the ADAP-ZAP70 interaction (see **Figure 2.1.1**), an RE-AD$_{Y571F}$ mutant should fail to co-precipitate ZAP70. Immunoprecipitation of re-expressed ADAP proteins from TCR-stimulated Jurkat T cells revealed a strong interaction between RE-AD$_{WT}$ and ZAP70 5min after stimulation. Again, ZAP70

bound to RE-AD$_{WT}$ showed no Y319 phosphorylation and thus no kinase activity. The interaction of ADAP and ZAP70 was reduced by 30% in cells expressing the RE-AD$_{Y571F}$ mutant (**Figure 2.1.3A**). Upon CXCR4 stimulation, ZAP70 only co-precipitated RE-AD$_{WT}$ but not RE-AD$_{Y571F}$ (**Figure 2.1.3B**). RE-AD$_{Y571F}$ molecules did not interact with ZAP70, indicating that Y571F mutation completely abolished the interaction of the two proteins (**Figure 2.1.3B**).

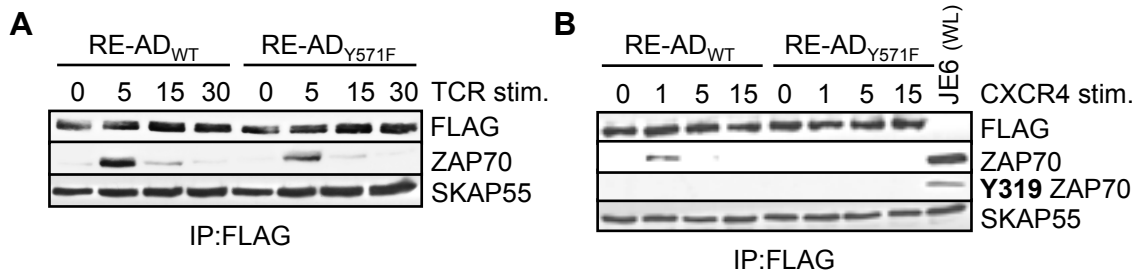

Figure 2.1.3: Tyrosine 571 (Y571) of ADAP mediates the ADAP-ZAP70 interaction. Jurkat T cells were transfected with the suppression/re-expression constructs shown in **2.1.2A**. Cells were left untreated or were stimulated with OKT3 (TCR) **(A)** or CXCL12 (CXCR4) **(B)** for the indicated time points. Lysates were used for immunoprecipitation using an anti-FLAG antibody (IP:FLAG). Precipitates of FLAG-tagged ADAP proteins were separated by SDS-PAGE, transferred and immunoblotted using the indicated antibodies (anti-FLAG, anti-SKAP55, anti-pY319 ZAP70 and anti-ZAP70). JE6 (WL): whole lysate of TCR-stimulated Jurkat JE6 T cells, served as positive control.

These data indicate that phosphorylation of ADAP at Y571 is mandatory for its interaction with ZAP70 upon CXCR4 stimulation.

2.1.2. Consequences of tyrosine 571 (Y571F) mutation within ADAP for TCR-induced T cell activation

ADAP knockout T cells exhibit defective TCR-triggered activation, reduced adhesion of β2 integrins to ICAM-1, defective LFA-1 clustering and impaired T-APC interaction.[97,98,105,106] To study the relevance of Y571 phosphorylation for adhesion to ICAM-1, Jurkat T cells were transfected with the suppression/re-expression vectors shown in **Figure 2.1.2A**. Transfectants were stimulated with OKT3 and seeded on ICAM-1-coated 96-well plates. After removing unbound cells, the percentage of cells bound to ICAM-1 was calculated. As compared to shC-transfected controls, the downregulation of endogenous ADAP in shAD-transfected cells strongly impaired ICAM-1-dependent adhesion. Re-expression of RE-AD$_{WT}$ rescued adhesion to ICAM-1 upon TCR stimulation. TCR-triggered T cells re-expressing RE-AD$_{Y571F}$ showed comparable adhesion as shC-transfected control cells (**Figure 2.1.4A**). To exclude an altered surface expression of the TCR complex or LFA-1 (CD18), transfected Jurkat T cells were stained with anti-TCR or anti-CD18 antibodies and were subsequently analyzed by flow cytometry. Since the suppression/re-expression vectors encode for green fluorescent protein (GFP) (**see Figure 2.1.2A**), transfected cells could be discriminated from non-transfected

cells. As shown in **Figure 2.1.2C**, no differences in TCR or CD18 expression were detectable when compared to the shC transfectants.

The interaction of T cells with APCs is regulated by ADAP.[83,97,98] To assess the influence of $ADAP_{Y571}$ phosphorylation on the formation of T-APC conjugates, Raji B cells were stained with DDAO-SE (red), loaded with or without superantigen (SA) and were incubated with transfected Jurkat T cells. Subsequently, the frequency of conjugates containing DDAO-SE-positive Raji B cells and GFP-positive Jurkat T cells was quantified by flow cytometry. As shown in **Figure 2.1.4B**, knockdown of ADAP (shAD) significantly reduced T-APC interactions as compared to control transfectants (shC; in line with ADAP ko studies[97,98]). Re-expression of $RE\text{-}AD_{WT}$ and $RE\text{-}AD_{Y571F}$ led to similar results (**Figure 2.1.4B**), demonstrating that the phosphorylation of $ADAP_{Y571}$ is not required for the interaction of T cells with APCs.

Since TCR-induced CD69 expression is impaired in ADAP-deficient T cells,[105,106] we wanted to test whether Y571F mutation affects CD69 surface expression. Jurkat T cells were stimulated with OKT3 for the indicated time points and analyzed for CD69 expression. As shown in **Figure 2.1.4C**, shC transfectants still expressing endogenous ADAP efficiently increased CD69 expression upon TCR stimulation. By contrast, the downregulation of endogenous ADAP in shAD-transfectants prevented CD69 upregulation (also shown for ADAP ko T cells[105,106]). Re-expression of $RE\text{-}AD_{WT}$ as well as $RE\text{-}AD_{Y571F}$ fully restored TCR-induced CD69 upregulation to control levels (**Figure 2.1.4C**).

Given that ADAP can – via binding to Nck and Ena/VASP proteins – modulate the actin cytoskeleton,[73,79,82] the role of $ADAP_{Y571}$ phosphorylation for TCR-induced actin polymerization was analyzed next. I measured the F-actin content of transfected T cells by intracellular phalloidin-staining after TCR stimulation. A significant reduction in TCR-induced F-actin content was observed upon ADAP knockdown (**Figure 2.1.4D**). However, again $RE\text{-}AD_{WT}$ and $RE\text{-}AD_{Y571F}$ were both able to completely rescue the phenotype (**Figure 2.1.4D**).

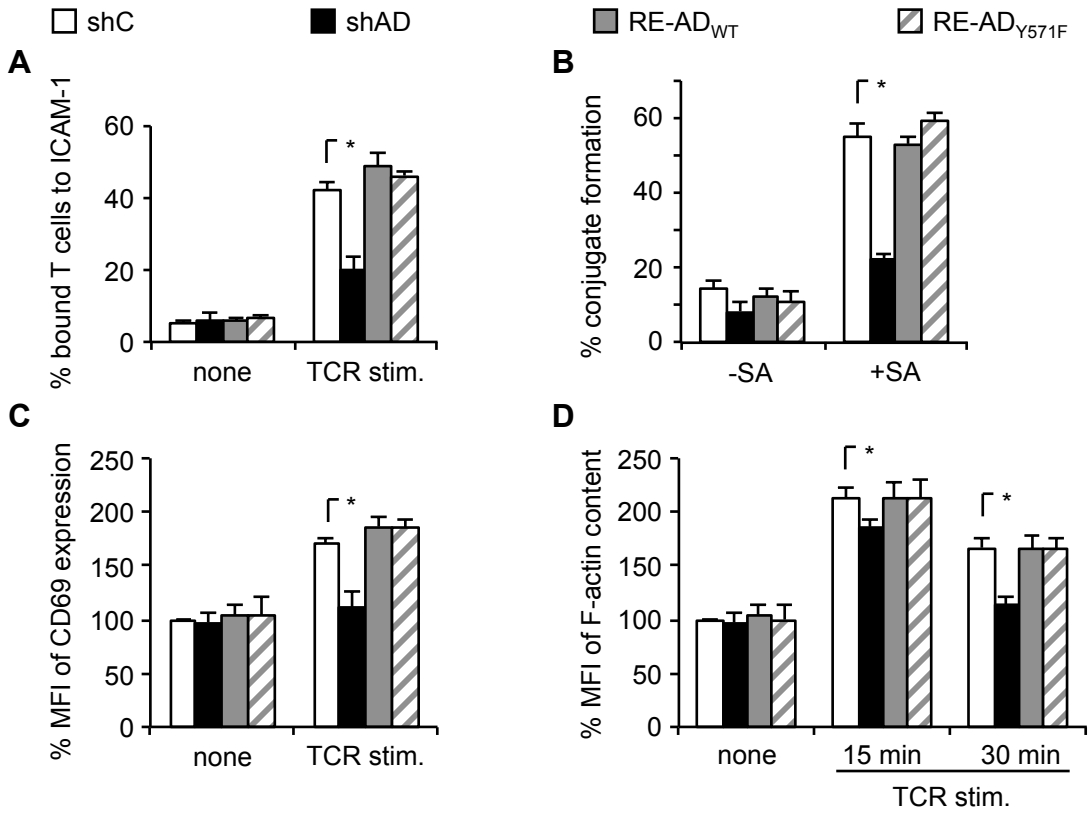

Figure 2.1.4: Tyrosine 571 (Y571F) mutation has no effect on TCR-induced adhesion, interaction with APCs, CD69 upregulation and F-actin content. (A-D) Jurkat T cells were transfected with the constructs shown in **2.1.2A** and incubated for 48h. **(A)** Non-stimulated (none) or OKT3-stimulated (TCR stim.) cells were analyzed for their ability to adhere to ICAM-1-coated plates. Adherent cells were counted and calculated as a percentage of input (2x10^5 cells). **(B)** Cells were analyzed for their ability to form conjugates with DDAO-SE (red)-stained Raji B cells that were loaded with (+) or without (-) superantigen (SA). The percentage of conjugates (double-positive events; a GFP-positive T cell interacting with a DDAO-SE-positive B cell) was assessed by flow cytometry. **(C)** TCR-induced CD69 upregulation was measured in non-stimulated (none) and OKT3 (plate-bound mAb) treated cells. Surface expression of CD69 was measured by flow cytometry gating on the transfected GFP-positive cells. **(D)** Cells were left untreated (none) or stimulated with OKT3 (TCR stim.), fixed, permeabilized, stained with phalloidin-Alexa Fluor®633 (F-actin) and analyzed by flow cytometry (gating on GFP-positive cells). The F-actin content of non-stimulated shC-transfected cells was set 100%. Data are presented as normalized mean fluorescence intensities (MFI). Error bars represent mean ± standard deviation (SD) of three independent experiments (*$p \leq 0.05$).

In summary, TCR-dependent phosphorylation of ADAP$_{Y571}$ does not control adhesion to ICAM-1, interaction with APCs, CD69 upregulation and F-actin polymerization.

2.1.3. Consequences of tyrosine 571 (Y571F) mutation within ADAP for CXCR4-induced T cell activation

We and others could show that ADAP promotes chemokine-dependent adhesion and migration *in vitro* and *in vivo*.[62,71,75] Triggering of the chemokine receptor CXCR4 by its ligand CXCL12 induces both adhesion and migration.[9] To address whether phosphorylation of tyrosine 571 regulates adhesion and/or migration, Jurkat T cells were transfected with suppression/re-expression vectors as described above (**Figure 2.1.2A**). Transfectants were stimulated with CXCL12 and

the percentage of cells bound to ICAM-1-coated plates was determined. As seen in **Figure 2.1.5A**, only knockdown of ADAP significantly reduced adhesion, whereas T cells transfected with RE-AD$_{WT}$ or RE-AD$_{Y571}$ showed normal adhesion levels (compared to shC).

To investigate directed migration, I seeded transfected Jurkat T cells in the ICAM-1-coated upper well of a Transwell chamber. The cells were incubated for two hours in the absence or presence of CXCL12 and the percentage of cells that migrated into the lower chamber was calculated. CXCL12-induced T cell migration was markedly reduced upon knockdown of ADAP but could be restored by re-expression of RE-AD$_{WT}$. Importantly, however, re-expression of RE-AD$_{Y571F}$ failed to do so (**Figure 2.1.5B**).

Migration of T cells along a chemokine gradient requires modifications of the actin cytoskeleton.[16,158,159] Similar to TCR stimulation, knockdown of ADAP significantly reduced F-actin levels 5 and 15min after chemokine receptor stimulation (**Figure 2.1.5C**). Re-expression of RE-AD$_{WT}$ restored F-actin content to control cell levels (**Figure 2.1.5C**). Interestingly, the RE-AD$_{Y571F}$ was unable to rescue F-actin content upon chemokine stimulation (**Figure 2.1.5C**). The effect of RE-AD$_{Y571F}$ re-expression on F-actin content increased over time. After 5min of stimulation, only a slight – albeit significant – difference was visible comparing F-actin content of RE-AD$_{WT}$ and RE-AD$_{Y571F}$-transfected cells, whereas at the 15min time point F-actin content of RE-AD$_{Y571F}$ transfectants was reduced to ~2/3 compared to RE-AD$_{WT}$ cells.

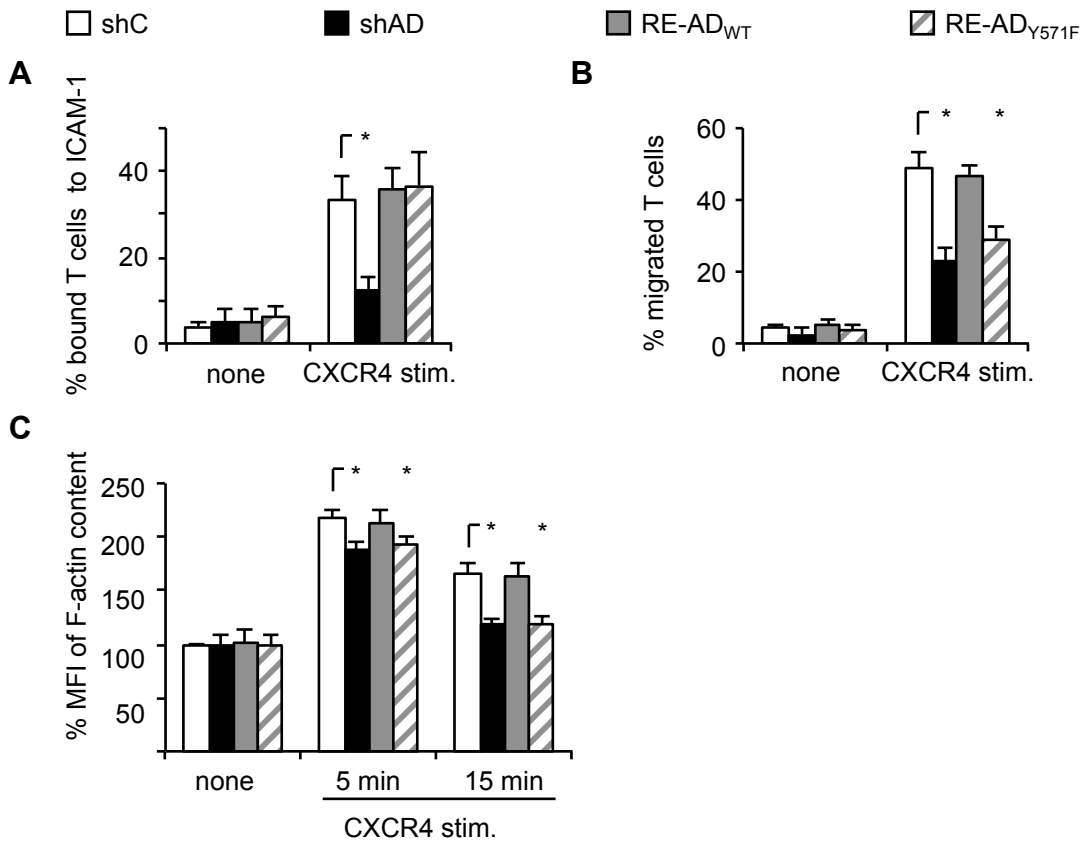

Figure 2.1.5: Tyrosine 571 (Y571) phosphorylation of ADAP regulates CXCR4-induced migration and F-actin content but not adhesion. (A-C) Jurkat T cells were transfected with constructs shown in **Figure 2.1.2A** and incubated for 48 h. **(A)** Non-stimulated or CXCR4 stimulated cells were analyzed for their ability to adhere to ICAM-1-coated plates. Adherent cells were counted and calculated as a percentage of input ($2x10^5$ cells). **(B)** Cells were seeded into the ICAM-1-coated transwell inserts. Subsequently, cells were incubated in the absence or presence of CXCL12 (CXCR4 stim.) in the lower chamber for 2h. Migrated T cells (located in the lower chamber) were counted and calculated as percentage of input ($2x10^5$ cells). **(C)** Cells were stimulated with CXCL12 (CXCR4 stim.), fixed, permeabilized, stained with Phalloidin-Alexa Fluor®633 (F-actin) and analyzed by flow cytometry. Data are presented as normalized MFI after gating on the transfected GFP-positive cells. The F-actin content of non-stimulated shC-transfected cells was set 100%. Error bars represent mean ± SD of three independent experiments (*$p \leq 0.05$).

Overall, these data indicate that ADAP$_{Y571}$ phosphorylation promotes actin-dependent T cell migration in response to CXCR4 signaling. Thus, we have identified a tyrosine phosphorylation site in ADAP that is solely required for chemokine but not TCR-induced T cell function.

2.2. Lipid-binding properties of the SKAP55 PH domain and its relevance for plasma membrane targeting of SKAP55 and LFA-1-mediated adhesion/interaction with APCs

On non-stimulated T cells, integrins like LFA-1 are expressed in a closed, inactive conformation. Upon TCR or chemokine receptor triggering, LFA-1 unfolds and becomes highly affine for its ligand ICAM-1.[36–38] Unfolding of integrins is induced by binding of LFA-1-activating complexes containing ADAP, SKAP55, RIAM, RapL, Rap1, Mst1, Talin and Kindlin-3 to the cytoplasmic tail of the integrin (see **Figure 1.6**). These complexes are already partially preformed but remain in the cytoplasm of non-stimulated T cells (published in [62] and unpublished data of our group). Activation of T cells by TCR or chemokine receptor stimulation induces the translocation of these complexes to the PM, where they can interact with the cytoplasmic tails of LFA-1 (published in [62] and unpublished data). The binding of these complexes to integrins is probably mediated by RapL (to the α-chain)[132] and Kindlin-3/Talin (to the β-chain)[50,160] and triggers conformational changes that result in the high affinity conformation of LFA-1.[37,39,44] Until today, it is not fully understood how the LFA-1-activating complexes are targeted to the PM.

Together with ADAP, the adapter protein SKAP55 forms the backbone of the two LFA-1-activating complexes shown in **Figure 1.6**. SKAP55 exhibits a PH domain.[69,121,127] PH domains are known for their ability to bind PIs and thus act as PM-targeting domains.[141–145] The importance of PH_{SK55} for integrin activation remains under debate. Two studies reported that deletion of the entire PH domain within SKAP55 or mutation of R131 (residue involved in membrane targeting of SKAP55) of SKAP55 impairs binding to CD18 (the β-chain of LFA-1), integrin-mediated adhesion and conjugate formation of T cells with APCs.[98,124] By contrast, two other studies stated that neither mutation or deletion of the PH domain within full-length SKAP55 nor expression of an isolated PH_{SK55} alters TCR-mediated adhesion.[95,122] Therefore, I was interested in shedding further light on PI binding and regulation of this domain.

2.2.1. PH_{SK55} translocates to the plasma membrane in a PIP_3-independent fashion

High affinity binding and recognition of PIs by PH domains has been described for phosphatidylinositol-(4,5)-bisphosphate (PIP_2) and PIP_3.[142] By using nuclear magnetic resonance (NMR) spectroscopy, the group of Prof. Christian Freund (Freie Universität Berlin) found that the purified isolated PH domain of SKAP55 has a moderate preference for PIP_3 ($PI(3,4,5)P_3$ (PIP_3-C4): dissociation constant (k_D)= 74 ± 12μM) compared to PIP_2 ((PIP_2-C4): k_D= 604 ± 202μM) binding

in vitro.[161] Additionally, they identified lysine 116 (K116), arginine 131 (R131) and lysine 152 (K152) as those residues that are localized in the vicinity of a putative PI-binding pocket and which displayed significant chemical shifts in NMR spectroscopy. The generation of potential non-binding mutants indeed revealed a significantly reduced PI-binding affinity for the R131M mutant while the K152E-mutated PH_{SK55} was no longer able to bind PIs at all.[161]

PIs like $PI(4,5)P_2$ and $PI(3,4,5)P_3$ are localized in the inner leaflet of the PM[143] and enable PM localization of PH domain-containing proteins.[142,143,145] The PI-binding affinities of PH_{SK55} are low compared to the well-characterized PH domains of e.g. phospholipase C delta (PLCδ; k_D ($PI(4,5)P_2$)= 190 ± 70nM) or Ak thymoma (AKT; k_D ($PI(3,4,5)P_{3)}$= 23 ± 6nM).[162] To test whether the isolated PH_{SK55} localizes at the PM, Jurkat T cells were transfected with constructs encoding for either GFP alone or the GFP-tagged isolated PH domains of AKT (G-PH_{AKT}), PLCδ (G-$PH_{PLCδ}$) and SKAP55 (G-PH_{SK55}). Subsequently, confocal laser-scanning microscopy (CLSM) analysis was performed to determine the ratio of fluorescence intensity at the PM of GFP-fusion proteins. In control transfectants, GFP showed a diffuse distribution, while – similar to G-PH_{AKT} and G-$PH_{PLCδ}$ – G-PH_{SK55} localized to the PM of non-stimulated Jurkat T cells (**Figure 2.2.1**).

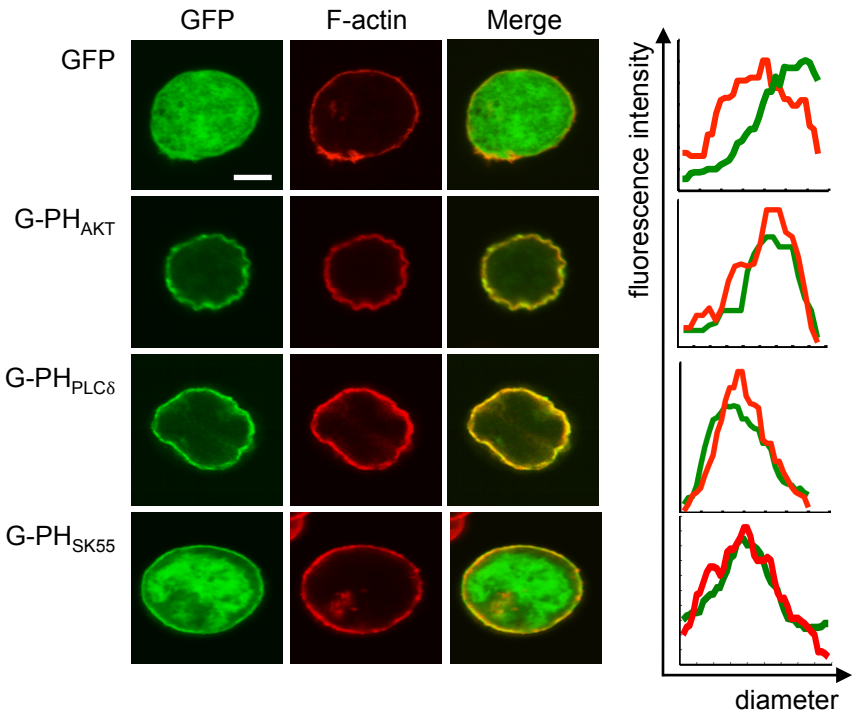

Figure 2.2.1: The isolated PH domain of SKAP55 localizes at the plasma membrane of T cells. Jurkat T cells were transiently transfected with constructs encoding either GFP alone or the GFP-tagged isolated PH domains of AKT (G-PH$_{AKT}$), PLCδ (G-PH$_{PLC\delta}$)) or SKAP55 (G-PH$_{SK55}$). Transfected cells were fixed, permeabilized and stained with phalloidin-tetramethylrhodamine (phalloidin-TRITC; visualizes F-actin). Confocal laser-scanning microscopy (CLSM) was performed and the fluorescence intensity of GFP/GFP-tagged protein and phalloidin-TRITC at the PM was measured using the DisplayOverlay04 software. White bar at the lower right corner: 5µm.

These data indicate that despite its moderate PI-binding affinities, the isolated PH domain of SKAP55 constitutively localizes at the PM of non-stimulated Jurkat T cells.

Subsequently, we investigated whether PM localization of PH$_{SK55}$ depends on PI(3,4,5)P$_3$. In Jurkat T cells, PI3K – which generates PI(3,4,5)P$_3$ by phosphorylating PI(4,5)P$_2$ – is constitutively active due to a lack of the phosphatases phosphatase and tensin homolog (PTEN) and SH2 domain-containing inositol 5-phosphatase 1 (SHIP-1), resulting in constantly high levels of PIP$_3$.[163,164] Treatment of Jurkat T cells with the selective PI3K inhibitor Wortmannin leads to an inhibition of PIP$_3$ production and reduced PIP$_3$-levels.[165,166] To investigate how changes in the availability of PIP$_3$ after inhibitor treatment affect PM targeting of G-PH$_{SK55}$, I compared its PI-binding behavior to the aforementioned PH domains of AKT (G-PH$_{AKT}$, high affinity binding of PIP$_3$)[162,167] and PLCδ (G-PH$_{PLC\delta}$, high affinity binding of PIP$_2$).[162,168] I performed CLSM studies in Jurkat T cells expressing GFP or the GFP-tagged PH domains in the absence or presence of Wortmannin. In untreated Jurkat T cells, both G-PH$_{AKT}$ as well as G-PH$_{PLC\delta}$ were targeted to the PM (**Figure 2.2.2A**). In line with previous reports,[162,169] G-PH$_{AKT}$ relocated to the

cytoplasm after PI3K inhibitor treatment (**Figure 2.2.2A**). By contrast, PM localization of G-$PH_{PLC\delta}$ and G-PH_{SK55} was not altered following Wortmannin treatment (**Figure 2.2.2A**). The inhibition of PI3K activity was monitored by Western Blot staining of cellular lysates for the phosphorylation of serine 473 of AKT (fully active AKT). Phosphorylation of this serine strongly depends on the activity of PI3K.[170] As shown in **Figure 2.2.2B**, Wortmannin treatment strongly reduced AKT S473 phosphorylation, indicating successful inhibition of PI3K. The localization data were confirmed using LY294002 (another PI3K inhibitor;[171] data not shown).

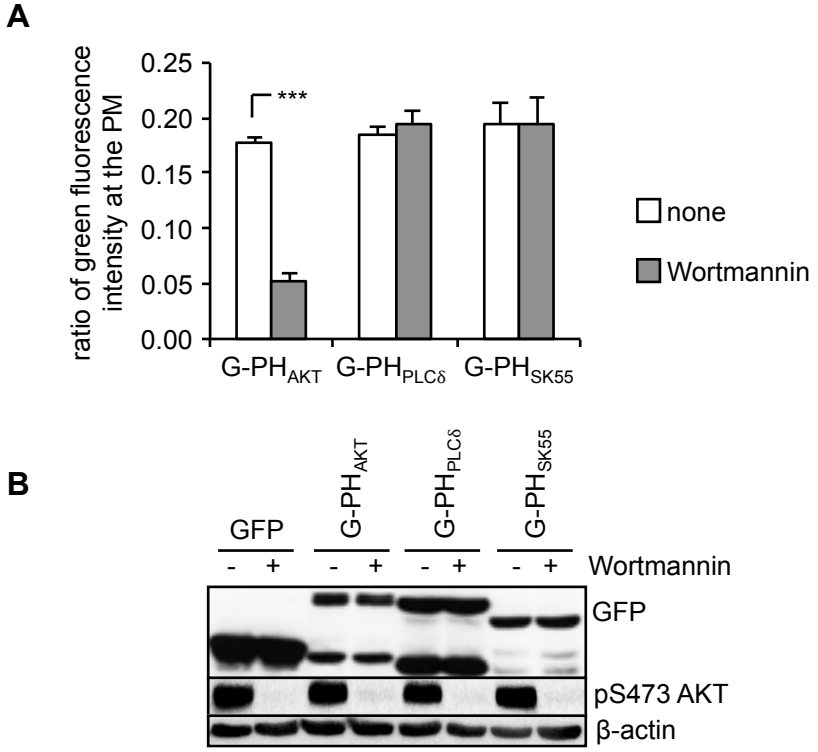

Figure 2.2.2: Plasma membrane localization of the isolated PH domain of SKAP55 is independent of PIP_3 in Jurkat T cells. (A) Jurkat T cells were transfected with constructs encoding GFP alone or the GFP-tagged PH domain of AKT (G-PH_{AKT}), PLCδ (G-$PH_{PLC\delta}$)) or SKAP55 (G-PH_{SK55}). 24h after transfection, Jurkat T cells were left untreated (none) or treated with 0.5µM Wortmannin for 1h. Cells were fixed, permeabilized, stained with phalloidin-TRITC (F-actin) and imaged by CLSM. A histogram tool (DisplayOverlay04) was used to determine the fluorescence intensity of GFP/GFP-tagged protein and phalloidin-TRITC at the PM of individual cells. The ratio of green fluorescence intensity at the PM after subtractions of GFP-background levels was calculated (see chapter 4.2.14.3.1.; n=3-4; mean ± SD; ***$p \leq 0.001$). **(B)** Transfected cells as described in (A) were lysed, separated by SDS-PAGE, transferred and analyzed by immunoblotting for pS473 AKT (served as readout for PI3K activity), GFP (GFP/GFP-tagged PH domains) and β-actin (served as a loading control). One representative experiment out of three is shown.

To confirm that the PM localization of G-PH_{SK55} occurs independent of PIP_3, primary human T cells were used. In these cells, the activity of PI3K and thus the levels of PIP_3 are very low under non-stimulated conditions. Upon TCR/CD28 stimulation, PI3K becomes active and PIP_3 levels increase.[172] As expected, G-PH_{AKT} molecules accumulated preferably in the cytoplasm rather than at the

PM in non-stimulated primary human T cells. Only upon TCR/CD28 stimulation, G-PH_{AKT} translocated to the PM and again relocated back to the cytoplasm, when PI3K was inhibited by Wortmannin treatment (**Figure 2.2.3A**). By contrast, G-PH_{SK55} and G-$PH_{PLC\delta}$ constitutively localized at the PM in non-stimulated cells (**Figure 2.2.3A**). Neither TCR/CD28 stimulation nor the addition of Wortmannin affected the localization of both domains. Successful stimulation and PI3K inhibition were monitored by immunoblotting against pS473 of AKT (**Figure 2.2.3B**).

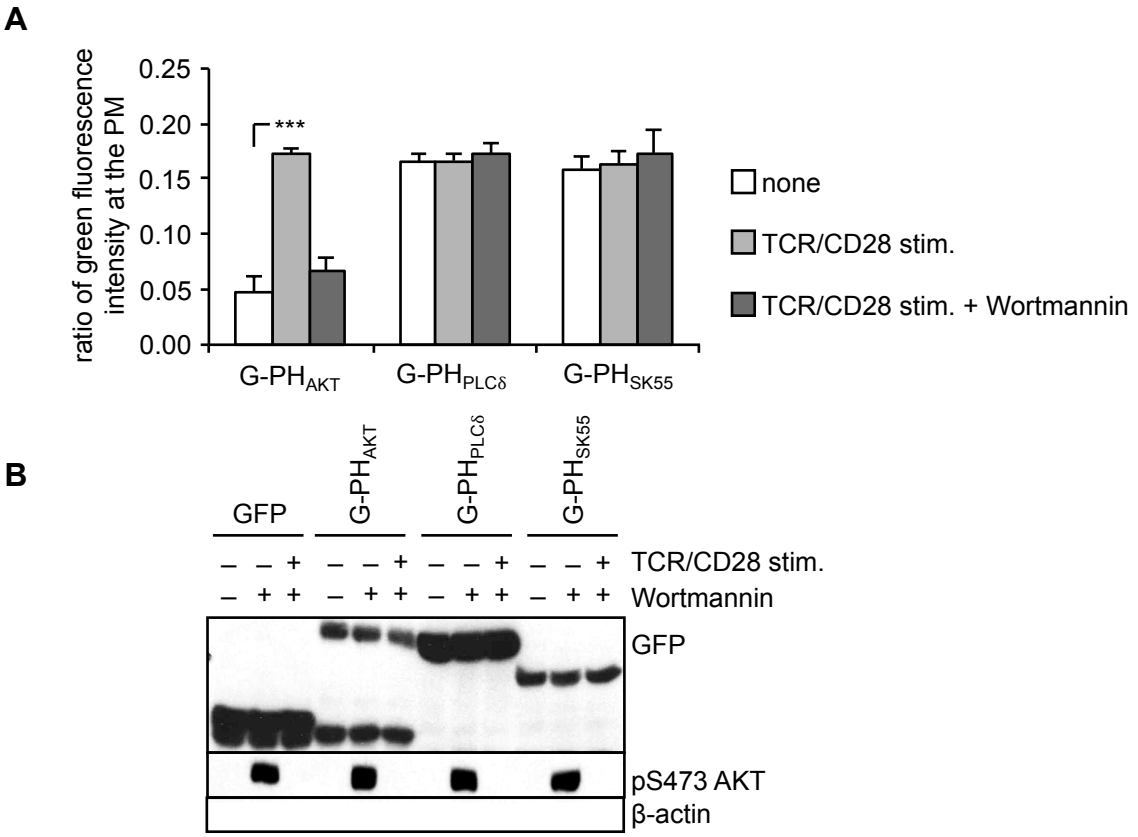

Figure 2.2.3: Plasma membrane localization of the isolated PH domain of SKAP55 is independent of PIP_3 in primary human T cells. (A) Primary human T cells isolated from healthy donors were transfected with constructs encoding GFP alone or the GFP-tagged PH domain of AKT (G-PH_{AKT}), PLCδ (G-$PH_{PLC\delta}$) or SKAP55 (G-PH_{SK55}). 24h after transfection, cells were left untreated (none) or stimulated with OKT3/CD28.2 (TCR/CD28 stim.) in the presence or absence of Wortmannin (100µM). Cells were fixed, permeabilized, stained with phalloidin-TRITC (F-actin) and imaged by CLSM. A histogram tool (DisplayOverlay04) was used to determine the fluorescence intensity of GFP/GFP-tagged protein and phalloidin-TRITC at the PM of individual cells. The ratio of green fluorescence intensity at the PM after subtractions of GFP-background levels was calculated (see chapter 4.2.14.3.1.; n=3; mean ± SD; ***$p \leq 0.001$). **(B)** Transfected cells from (A) were lysed, separated by SDS-PAGE, transferred and immunoblotted with anti-pS473 AKT (served as readout for PI3K activity), anti-GFP (GFP/GFP-tagged PH domains) and anti-β-actin (served as a loading control). One representative experiment out of three is shown.

These data indicate that G-PH_{AKT} localizes at the PM in a PIP_3-dependent fashion, whereas G-PH_{SK55} PM localization occurs independent of PIP_3 and could not be further reinforced by TCR/CD28 stimulation.

2.2.2. Lysine 152 (K152)-mediated actin binding promotes plasma membrane recruitment of PH_{SK55}

It was previously reported that of all PH domains identified, less than 10% bind PIs with high affinity and specificity.[142] Instead, some of these PH domains have been shown to mediate protein-protein interactions with actin. For example, the PH domains of bruton's tyrosine kinase (Btk), oxysterol-binding protein (OSBP), Itk (also termed Emt), pleckstrin and exchange factor for Arf6 (EFA6) bind directly to actin.[173,174] Therefore, we investigated whether the same holds true for PH_{SK55}. To test this, Jurkat T cells were transfected with constructs encoding either GFP, G-$PH_{PLC\delta}$ or G-PH_{SK55}. Lysates were generated and used for co-immunoprecipitation studies. G-$PH_{PLC\delta}$ (used as a negative control) did not co-precipitate actin, as previously reported by others.[174] In contrast to G-$PH_{PLC\delta}$, G-PH_{SK55} co-precipitated actin (**Figure 2.2.4A**), indicating that the isolated PH domain of SKAP55 interacts with actin.

Actin is a highly acidic protein that displays negatively charged amino acids on its surface.[175] Hence, we explored whether the identified positively charged residues within PH_{SK55} that mediate the interaction with the negatively charged PIs (PIP_2 and PIP_3) would also be involved in actin binding. To investigate this, we used the potential non-binding K116M (G-$PH_{SK55*K116M}$), R131M (G-$PH_{SK55*R131M}$) and K152E (G-$PH_{SK55*K152E}$) mutants (subsequently referred to as K*R-mutants). Jurkat T cells expressing GFP, the GFP-tagged PH_{SK55} wild-type (G-PH_{SK55}) or its K*R-mutants were lysed and used for co-precipitation studies. As shown in **Figure 2.2.4C**, these studies revealed that – similar to wild-type SKAP55 – K116M and R131M mutants still bound to actin, while K152E mutation completely interfered with the ability of PH_{SK55} to bind actin. To exclude that the different charges (K152E (negative) versus K116M (uncharged)) were responsible for the loss of actin binding, I also included a K152M (uncharged) mutant in this study. Like K152E, the K152M mutant showed no co-precipitation of actin (**Figure 2.2.4C**).

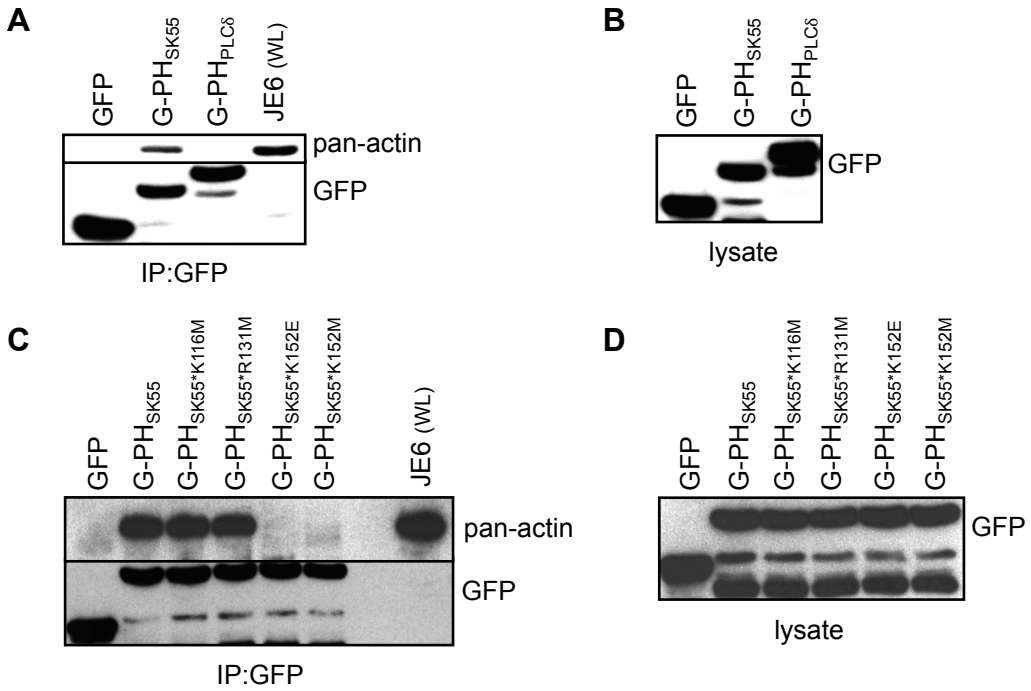

Figure 2.2.4: Lysine 152 (K152) of SKAP55 mediates the interaction of the isolated PH domain of SKAP55 with the actin cytoskeleton. (A,B) T cells were transfected with constructs encoding GFP alone or the GFP-tagged PH domain of PLCδ ($PH_{PLCδ}$)) or SKAP55 (PH_{SK55}). 24h after transfection, expression of the transfected constructs was assessed by immunoblotting with an anti-GFP antibody (left panel). Lysates were used for anti-GFP immunoprecipitation (IP:GFP). Precipitates of GFP/GFP-tagged PH domains were separated by SDS-PAGE, transferred and immunoblotted using the indicated antibodies (anti-GFP, anti-pan-actin). One representative experiment out of three is shown. **(C,D)** T cells were transiently transfected with either GFP, the GFP-tagged isolated wild-type ($G\text{-}PH_{SK55}$), K116M-mutated ($G\text{-}PH_{SK55*K116M}$), R131M-mutated ($G\text{-}PH_{SK55*R131M}$) or K152E-mutated ($G\text{-}PH_{SK55*K152E}$) PH domain of SKAP55. 24h after transfection, expression of the transfected constructs was assessed by immunoblotting with an anti-GFP antibody **(D)** and lysates were used for anti-GFP immunoprecipitation (IP:GFP) **(C)**. Precipitates of GFP/GFP-tagged PH domains were separated by SDS-PAGE, transferred and immunoblotted using the indicated antibodies (anti-GFP, anti-pan-actin). One representative experiment out of two is shown. JE6 (WL): whole lysate of non-stimulated Jurkat JE6 T cells served as positive control for detection of actin.

These data indicate that PH_{SK55} binds to actin and that this interaction is mediated by K152.

We next wanted to ascertain whether the K*R-mutants of PH_{SK55} still localize at the PM. Therefore, CLSM analysis was performed to study Jurkat T cells that expressed either GFP, GFP-tagged PH_{SK55} wild-type or its K*R-mutants. Cells expressing $G\text{-}PH_{SK55}$ served as a positive control for PM localization. As shown in **Figure 2.2.5A**, PM localization of $G\text{-}PH_{SK55*K116M}$ molecules was mildly but significantly reduced compared to the positive control. By contrast, membrane targeting of $G\text{-}PH_{SK55*K152E}$ (as well as $G\text{-}PH_{SK55*K152M}$) was completely abolished (**Figure 2.2.5A**). The R131M mutation showed a moderate effect on PM localization of PH_{SK55}. Similar results were obtained using non-stimulated primary human T cells (**Figure 2.2.5B**).

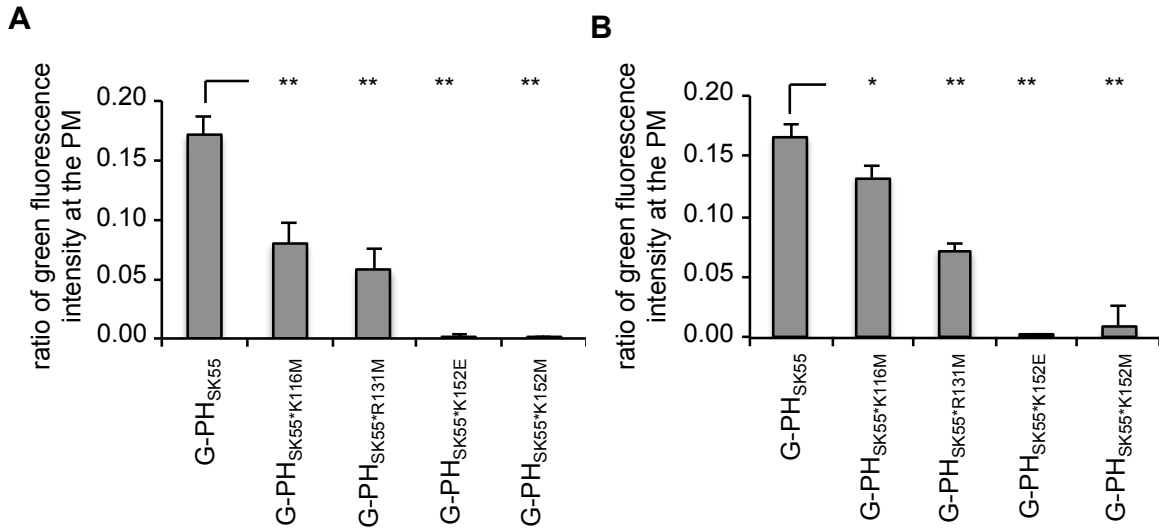

Figure 2.2.5: Lysine 152 (K152) regulates plasma membrane targeting of SKAP55. Jurkat **(A)** and primary human T cells **(B)** were transiently transfected with constructs encoding GFP alone, the GFP-tagged isolated wild-type (G-PH_{SK55}), K116M-mutated (G-$PH_{SK55*K116M}$), R131M-mutated (G-$PH_{SK55*R131M}$) or K152E-mutated (G-$PH_{SK55*K152E}$) PH domain of SKAP55. 24h after transfection, cells were fixed, permeabilized, stained with phalloidin-TRITC (F-actin) and imaged by CLSM. A histogram tool (DisplayOverlay04) was used to determine the fluorescence intensity of GFP/GFP-tagged protein and phalloidin-TRITC at the PM of individual cells. The ratio of green fluorescence intensity at the PM after subtractions of GFP-background levels was calculated (see chapter 4.2.14.3.1.; n=3-4; mean ± SD; *$p \leq 0.05$, **$p \leq 0.01$).

Taken together, these results suggest that K152 mediates the interaction with actin, which is critical for membrane recruitment of the isolated PH_{SK55}.

2.2.3. Lysine 152 (K152) is required for TCR-triggered adhesion and T-APC interactions

Given that PM recruitment of SKAP55 is essential for integrin activation,[124] we next investigated the individual contribution of the K*R-mutants within full-length SKAP55 for TCR-mediated adhesion and T-APC interactions. For this purpose, suppression/re-expression constructs were generated as shown in **Figure 2.2.6A**. These constructs encode for both an shRNA specific to knockdown endogenous SKAP55 and a cDNA that enables re-expression of an shRNA-resistant FLAG-tagged SKAP55 mutant. As shown in **Figure 2.2.6B**, the suppression/re-expression vectors are able to suppress 90% of endogenous SKAP55 and re-express SKAP55 mutants at levels comparable to control cells (shC and RE-$SK55_{WT}$).

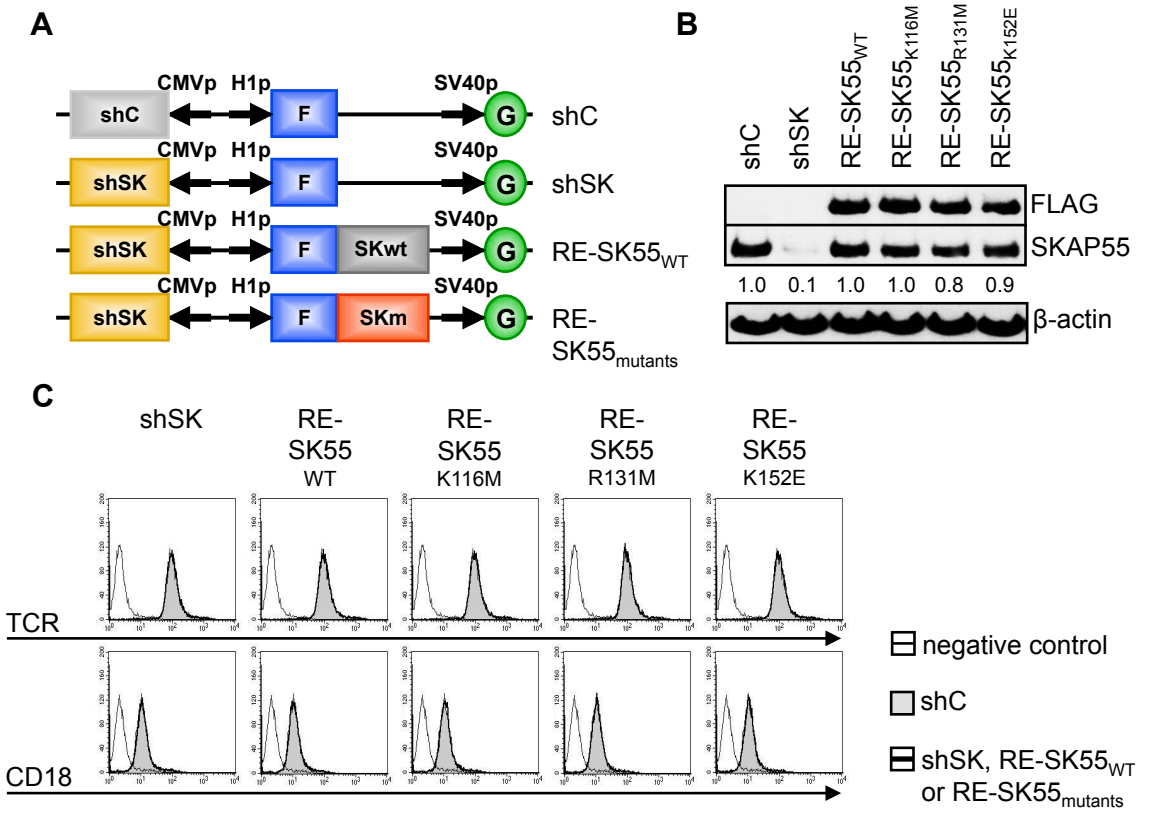

Figure 2.2.6: Suppression/re-expression vectors of arginine and lysine (K*R) mutants of SKAP55. (A) Schematic representation of the suppression/re-expression vectors for SKAP55. The vectors are composed as follows: shC: control vector encoding GFP (G); shSK: vector encoding shRNA against SKAP55 (shSK) and GFP (G); RE-SK55$_{WT}$: vector encoding shRNA against SKAP55 (shSK), shRNA-resistant FLAG-tagged (F) wild-type SKAP55 (SKwt) and GFP (G); RE-SK55$_{mutants}$: vector encoding shRNA against SKAP55 (shSK), shRNA-resistant FLAG-tagged (F) mutated SKAP55 (SKm; the used mutants are K116M, R131M or K152E) and GFP (G). **(B,C)** Jurkat T cells were transfected with the constructs shown in (A) and incubated for 48h. **(B)** Cell extracts were prepared, separated by SDS-PAGE, transferred and analyzed by immunoblotting for FLAG (re-expressed FLAG-tagged SKAP55) and SKAP55 (endogenous and re-expressed SKAP55). Staining with an anti-β-actin antibody served as a loading control. The suppression of endogenous SKAP55 and re-expression of FLAG-tagged wild-type SKAP55 and mutants were quantified using the Kodak Image Station 2000R (Kodak ID Image software). One representative experiment out of two is shown. **(C)** Cells were analyzed for surface expression of TCR and CD18 (LFA-1) by flow cytometry. The gray, filled curves represent the shC-transfected control cells and the bold, black lines are the cells transfected with the construct of interest (shSK, RE-SK55$_{WT}$ or RE-SK55$_{mutants}$). The negative control (cells stained with secondary antibody only) is represented as a thin, black line. One out of two independent experiments is shown.

Compared to shC-transfected cells, the downregulation of endogenous SKAP55 in shSK transfectants impaired adhesion to ICAM-1 (**Figure 2.2.7A**, as already published by our group[95]). Re-expression of shRNA-resistant RE-SK55$_{WT}$ fully rescued adhesion (**Figure 2.2.7A**). TCR-induced adherence to ICAM-1 was moderately reduced in Jurkat T cells re-expressing RE-SK55$_{R131M}$ (in line with[124]), while RE-SK55$_{K116M}$-expressing Jurkat T cells behaved comparable to RE-SK55$_{WT}$ transfectants (**Figure 2.2.7A**). By contrast, in Jurkat T cells re-expressing RE-SK55$_{K152E}$, adherence to ICAM-1-coated plates was as strongly impaired as for shSK transfectants (**Figure 2.2.7A**). The functional effects observed for the

individual SKAP55 mutants were not due to insufficient re-expression or altered surface levels of TCR or LFA-1 (CD18) (**Figure 2.2.6B,C**).

As compared to shC transfectants, downregulation of endogenous SKAP55 reduced interactions of shSK-transfected Jurkat T cells with superantigen-loaded Raji B cells. These findings confirm other studies describing the importance of SKAP55 for T-APC contacts.[134,136,176] Re-expression of RE-SK55$_{WT}$ completely restored conjugate formation (**Figure 2.2.7B**). However, conjugate formation of RE-SK55$_{K152E}$ transfectants was strongly reduced and comparable to shSK-transfected cells (**Figure 2.2.7B**). By contrast, RE-SK55$_{K116M}$ and RE-SK55$_{R131M}$ re-expression hardly affected T-APC interactions at all (**Figure 2.2.7B**).

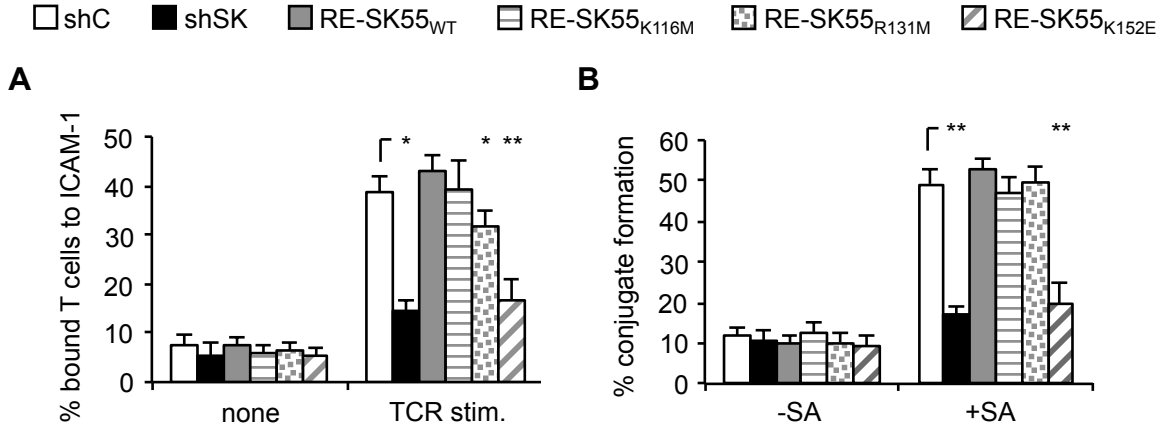

Figure 2.2.7: Lysine 152 (K152) of SKAP55 regulates adhesion and T-APC interaction. (A,B) Jurkat T cells were transfected with constructs shown in **Figure 2.2.6A** and incubated for 48h. **(A)** Cells were left untreated (none) or were stimulated for 30min with OKT3 (TCR stim.). Cells were analyzed for adhesion to ICAM-1-coated 96 well plates. Bound cells were counted and calculated as % input ($2x10^5$ cells). **(B)** Cells were incubated with unloaded (-SA) and superantigen-loaded (+SA) DDAO-SE (red)-stained Raji B cells for 30min. Pair formation was analyzed by flow cytometry. The percentage of conjugates was defined as the number of double-positive events (GFP-positive T cell and DDAO-SE-positive B cells). Error bars represent mean ± SD of at least three independent experiments (*$p \leq 0.05$; **$p \leq 0.01$).

In conclusion, these data suggest that lysine 152 located in the PH domain of full-length SKAP55 is crucial for T cell adhesion and the interaction of T cells with APCs.

We next explored whether the impact that the individual K*R mutations had on the ability of full-length SKAP55 to activate integrins is due to either inaccurate cellular localization (like for the isolated PH$_{SK55}$ mutants; see **Figure 2.2.5**) or the failure of these mutants to bind their interaction partners (impaired LFA-1-activating complex formation; complexes shown in **Figure 1.6**). To answer the question of whether full-length SKAP55 mutants still translocated to the PM upon T cell stimulation, suppression/re-expression vector-transfected Jurkat T cells were left non-stimulated or TCR-activated and PM fractions were prepared. **Figure 2.2.8A** shows that RE-SK55$_{WT}$ and its K*R mutants localized at the PM

upon T cell stimulation. The same was observed for other constitutive (ADAP, RapL and RIAM) and inducible (Rap1 and Talin) components of the LFA-1-activating complexes as well as SLP-76 (**Figure 2.2.8A**).

According to this, none of the three K*R-mutants of SKAP55 – including K152E – had an impact on TCR-triggered recruitment of SKAP55 and its associated molecules to the PM.

To test whether mutations within the PH domain of full-length SKAP55 would interfere with the interaction of the ADAP/SKAP55 module with actin, Talin and/or LFA-1, I prepared SKAP55 immunoprecipitates from non-stimulated or TCR-triggered Jurkat T cells re-expressing either wild-type or mutated (K116M, R131M or K152E) FLAG-tagged SKAP55. As shown in **Figure 2.2.8B**, ADAP, RIAM and RapL constitutively interact with SKAP55 wild-type (previously reported by us[129] and Raab et al.[124]) and all three mutants. In contrast and as already reported,[65,124,129,177] Rap1 and SLP-76 only associated with the ADAP/SKAP55 module upon TCR stimulation. Compared to RE-SK55$_{WT}$, RE-SK55$_{K116M}$ and RE-SK55$_{R131M}$; mutation of K152E strongly reduced the ability of SKAP55 to interact with Talin, LFA-1 and actin (**Figure 2.2.8B**). Control-immunoprecipitation of LFA-1 (CD11a) showed comparable results, where mutation of Lysine 152 (K152E) prohibited the interaction of the ADAP/SKAP55 module with LFA-1, Talin and actin (**Figure 2.2.8C**).

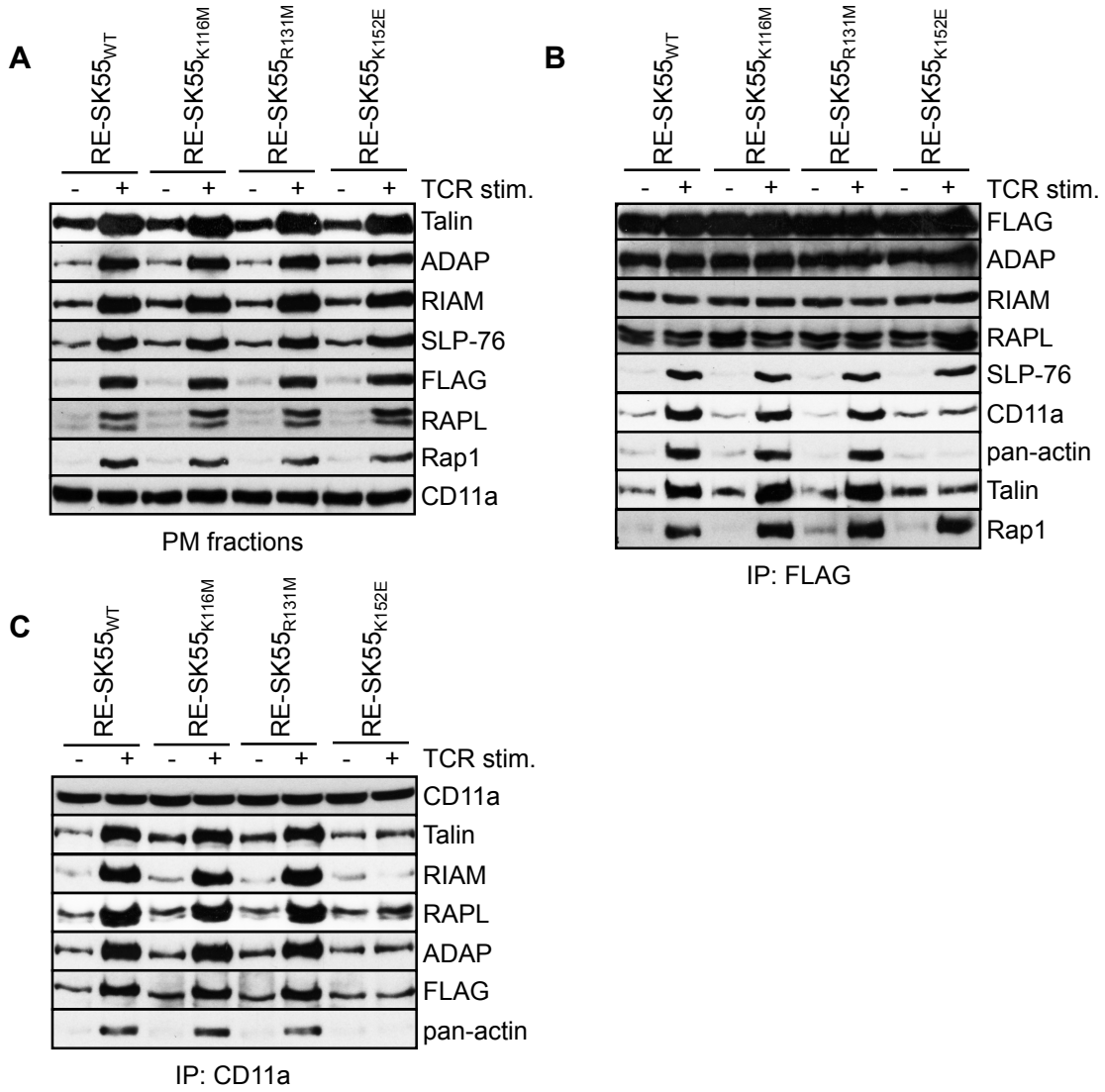

Figure 2.2.8: Lysine 152 (K152) of SKAP55 mediates the interaction with Talin, LFA-1 and actin. (A-C) Jurkat T cells were transfected with the suppression/re-expression constructs shown in **Figure 2.2.6A** that suppressed endogenous SKAP55 and re-expressed FLAG-tagged shRNA-resistant SKAP55 wild-type (RE-SK55$_{WT}$) or its mutants (RE-SK55$_{K116M}$, RE-SK55$_{R131M}$ and RE-SK55$_{K152E}$). After 48h, cells were left untreated or stimulated with OKT3 (TCR stim.). (**A**) PM fractions were isolated, separated by SDS-PAGE, transferred and analyzed by immunoblotting using the indicated antibodies. (**B,C**) Transfected Jurkat T cells were left untreated or stimulated with OKT3 (TCR stim.). Lysates were subjected to immunoprecipitation of SKAP55 using anti-FLAG antibody (IP:FLAG (FLAG-tagged SKAP55)) **(B)** or to immunoprecipitation of LFA-1 using anti-CD11a antibody (IP:CD11a) **(C)**. Precipitates were separated by SDS-PAGE, transferred and immunoblotted using the indicated antibodies. One representative experiment out of two is shown.

These data indicate that expression of the K152E mutant of SKAP55 inhibits the inducible interaction of the ADAP/SKAP55 module with LFA-1, Talin and actin. This inability is the basis for the impaired adhesion and conjugate formation induced by the K152E mutant of SKAP55.

2.2.4. Aspartic acid 120 (D120) prevents TCR-independent plasma membrane targeting of SKAP55

In contrast to the isolated PH domain of SKAP55, full-length GFP-tagged SKAP55 (G-SK55$_{WT}$) protein mainly localizes in the cytoplasm of non-stimulated Jurkat T cells (**Figure 2.2.9,** for quantification see **Figure 2.2.11A**). G-SK55$_{WT}$ only translocates to the PM upon TCR stimulation (**Figure 2.2.9**, for quantification see **2.2.11A**).

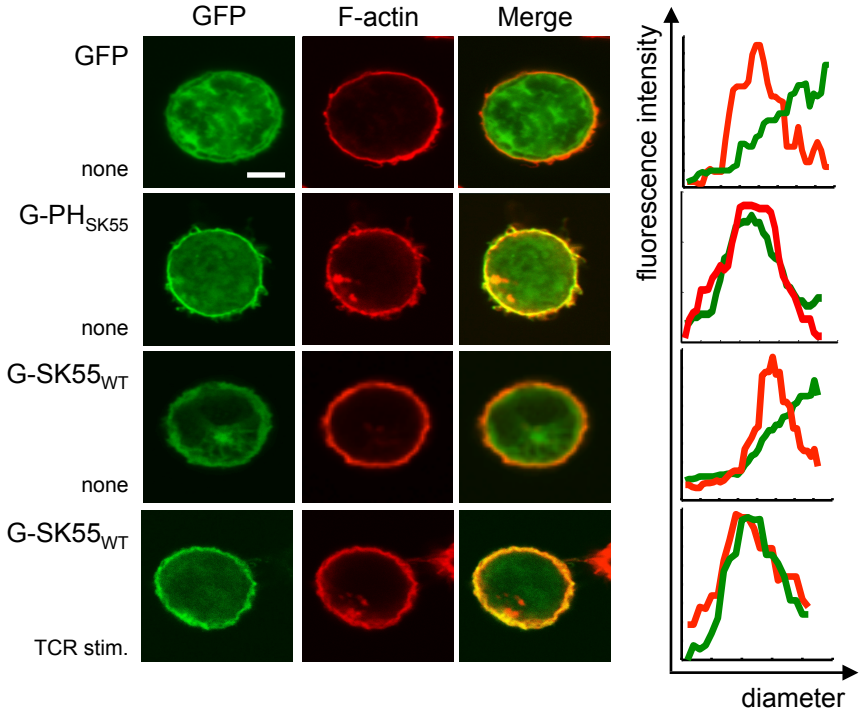

Figure 2.2.9: Full-length SKAP55 primarily localizes in the cytoplasm of non-stimulated Jurkat T cells but translocates to the plasma membrane upon TCR stimulation. Jurkat T cells were transiently transfected with constructs encoding either GFP alone or the GFP-tagged isolated PH domain of SKAP55 (G-PH$_{SK55}$) or GFP-tagged wild-type full-length SKAP55 (G-SK55$_{WT}$). Transfected cells were left untreated (none) or stimulated with OKT3 (TCR stim.), fixed, permeabilized and stained with phalloidin-TRITC (F-actin). CLSM was performed and the fluorescence intensity of GFP/GFP-tagged protein and phalloidin-TRITC was measured using the DisplayOverlay04 software. White bar at the lower right corner: 5µm.

A study by Swanson and colleagues has shown that PM targeting of the SKAP55 homolog SKAP-HOM is controlled by an auto-inhibitory interaction of the N-terminal DM domain (DM$_{SK-HOM}$) with the PH domain (PH$_{SK-HOM}$). The formation of a small interface between these two domains keeps SKAP-HOM in a closed/auto-inhibited conformation and thereby abrogates SKAP-HOM membrane ruffle targeting (see **Figure 1.9**).[125] Swanson et al. additionally identified that in SKAP-HOM the auto-inhibitory interaction of DM and PH domain is mediated by aspartic acid 129 (D129, localized in PH$_{SK-HOM}$, see **Figure 1.8**).[125] A comparison of the amino acid sequence of SKAP-HOM with SKAP55 revealed an equivalent aspartic acid (D120) in PH$_{SK55}$ (**Figure 2.2.10**).

If SKAP55 is regulated by the same mechanism as SKAP-HOM, one would expect chemical shift changes in the PI-binding pocket when comparing the isolated PH_{SK55} with a construct containing DM_{SK55} linked to PH_{SK55} (DM_PH_{SK55}; residues 7-222 of SKAP55). In fact, we observed these chemical shifts in our NMR analysis. NMR analysis revealed potential differences between the conformation of the isolated PH_{SK55} and the PH domain in the context of the DM_PH_{SK55} construct. Additionally, we could show that the interface between the PH and the DM domain is localized in the vicinity of K152 and D120.[161]

```
SKAP-HOM   105-QFPPIAAQDLPFVIKAGYLEKRRKDHSFLGFEWQKRWCALSKTVFYYYGS
                          ||| |||||. |||||.| |||||||..|. .|||| .
SKAP55               106-GSVIKQGYLEKKSKDHSFFGSEWQKRWCVVSRGLFYYYAN
SKAP-HOM   155-DKDKQQKGEFAIDGYDVRMNNTLRKDGKKDCCFEICAPDKRIYQFTAASP
              .| || || |.| || |||   ||.| ||. |||..  |.| | ||| ||
SKAP55     146-EKSKQPKGTFLIKGYSVRMAPHLRRDSKKESCFELTSQDRRTYEFTATSP
SKAP-HOM   205-KDAEEWVQQLKFILQ
               .| .|| |. |.|
SKAP55     196-AEARDWVDQISFLLKDLS
```

Figure 2.2.10: Comparison of the amino acid sequences of the PH domains of human SKAP55 and SKAP-HOM. Shown are the sequence and structural composition based on published crystal structures of PH_{SK-HOM} (residues 105-220; Research Collaboratory for Structural Bioinformatics Protein Data Bank (RCSB PDB): 1U5G) and PH_{SK55} (residues 106-213; (RSCB PDB): 1U5D). Helical structures (α and 3_{10} helix) are shown in green and β strands in red. Additionally, in blue is shown aspartic acid 129 (D129) of PH_{SK-HOM}, which mediates the auto-inhibitory interaction with the N-terminal DM domain[125] and its equivalent aspartic acid (D120) within PH_{SK55}.

To investigate whether D120 regulates to PM targeting of SKAP55, a vector encoding a GFP-tagged SKAP55 mutant was generated where D at position 120 was replaced by lysine ($G\text{-}SK55_{D120K}$). Expression of $G\text{-}SK55_{D120K}$ in Jurkat T cells revealed its constitutive membrane localization (in non-stimulated and TCR-activated T cells), which was comparable to the isolated PH_{SK55} (**Figure 2.2.11A**). To study the role of K152 for the constitutive PM localization of the D120K mutant, I generated the double (D120K/K152E (D/K)) mutant. As shown in **Figure 2.2.11A**, the constitutive membrane localization was abrogated by mutating both sites within SKAP55 ($G\text{-}SK55_{D/K}$). This double mutant showed cytoplasmic localization in non-stimulated Jurkat T cells and – like $G\text{-}SK55_{WT}$ – only localized to the PM upon TCR stimulation.

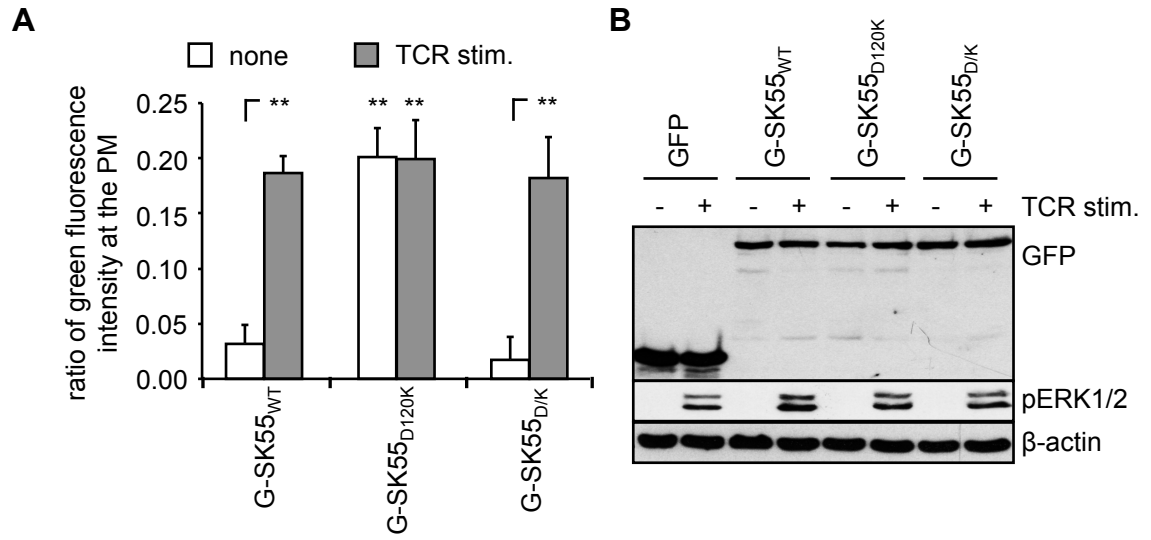

Figure 2.2.11: Mutation of aspartic acid 120 (D120K) leads to constitutive plasma membrane localization of SKAP55. (A) Jurkat T cells were transiently transfected with constructs encoding either GFP alone, GFP-tagged isolated PH domain of SKAP55 (G-PH_{SK55}) or vectors encoding the GFP-tagged wild-type (G-$SK55_{WT}$), D120K-mutated (G-$SK55_{D120K}$) or D120K/K152E-mutated full-length SKAP55 (G-$SK55_{D/K}$). 24h after transfection, cells were left untreated (none) or stimulated with OKT3 (TCR stim.), cells were fixed, permeabilized and stained with phalloidin-TRITC (F-actin) and imaged by CLSM. A histogram tool (DisplayOverlay04) was used to determine the fluorescence intensity of GFP/GFP-tagged protein and phalloidin-TRITC at the PM of individual cells. The ratio of green fluorescence intensity at the PM after subtractions of GFP-background levels was calculated (see chapter 4.2.14.3.1.; n=3-4; mean ± SD; $^{**}p \leq 0.01$). **(B)** Cells from (A) were lysed and lysates were separated by SDS-PAGE, transferred and analyzed by immunoblotting with anti-GFP (GFP/GFP-tagged SKAP55), anti-pERK1/2 (to monitor stimulation) and anti-β-actin (served as a loading control) antibodies.

These data indicate that D120 acts as a critical regulator of PM recruitment of SKAP55. Additionally, my data show that an intact K152 is essential for constitutive PM targeting of the D120K mutant.

2.2.5. Aspartic acid 120 (D120) of SKAP55 negatively regulates adhesion, T-APC interactions and LFA-1 activation

Previous data by us and others showed that constitutive PM targeting of SKAP55 (due to fusion of SKAP55 to a LAT- or a myristoylation (myr-) tag) induces T cells adhesion in the absence of TCR stimulation.[95,124] To address the functional relevance of the D120K mutation of SKAP55 for LFA-1 activation, the suppression/re-expression system was used again (see **Figure 2.2.12A**).

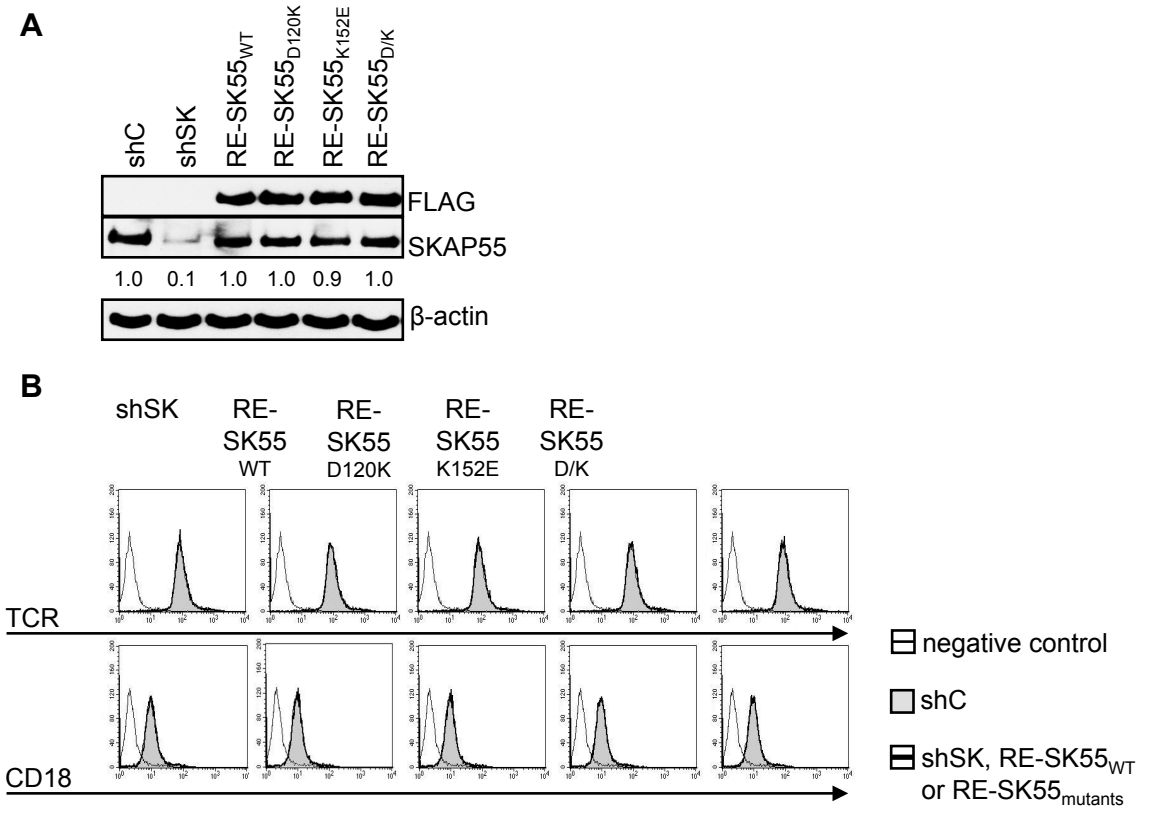

Figure 2.2.12: Suppression/re-expression vectors of aspartic acid 120 (D120K) mutants of SKAP55. (A+B) Jurkat T cells were transiently transfected with the following vectors: shC: control vector encoding GFP (G); shSK: vector encoding shRNA against SKAP55 (shSK) and GFP (G); RE-SK55$_{WT}$: vector encoding shRNA against SKAP55 (shSK), shRNA-resistant FLAG-tagged (F) wild-type SKAP55 (SKwt) and GFP (G); RE-SK55$_{mutants}$: vector encoding shRNA against SKAP55 (shSK), shRNA-resistant FLAG-tagged (F) mutated SKAP55 (SKm; the used mutants are D120K, K152E and D120K/K152E (D/K)) and GFP (G). The transfected cells were incubated for 48h. **(A)** Whole lysates were harvested, separated by SDS-PAGE, transferred and immunoblotted for FLAG (re-expressed FLAG-tagged SKAP55), SKAP55 (endogenous and re-expressed SKAP55) and β-actin (loading control). The suppression of SKAP55, re-expression of FLAG-tagged WT and mutant SKAP55 were quantified using the Kodak Image Station 2000R (Kodak ID Image software). One representative experiment out of two is shown. **(B)** Surface expression of TCR and CD18 (LFA-1) was assessed by flow cytometry gating on the GFP-positive cells. The negative control (cells only stained with secondary antibody) is represented as a thin, black line. One representative experiment out of two is shown.

Expression of RE-SK55$_{D120K}$ enhanced not only stimulation-induced but also basal adhesion to ICAM-1 (**Figure 2.2.13A**). The additional mutation of K152E (RE-SK55$_{D/K}$) overrode the positive effect of the D120K mutant on basal adhesion (**Figure 2.2.13A**). Indeed, RE-SK55$_{D/K}$ transfectants showed impaired adhesion to ICAM-1 comparable to SKAP55 knockdown (shSK) or RE-SK55$_{K152E}$ re-expressing cells. The observed effects were not due to differences in re-expression of the mutants or altered TCR or LFA-1 (CD18) surface expression (**Figure 2.2.12A,B**).
Suppression of endogenous SKAP55 in Jurkat T cells abrogated conjugation with superantigen-loaded Raji B cells. Similar to adhesion, conjugation was rescued by expressing RE-SK55$_{WT}$ (**Figure 2.2.13B**). Importantly, the expression of RE-SK55$_{D120K}$ enhanced basal conjugate formation (**Figure 2.2.13B**). Again, the

effect of the D120K mutation on conjugate formation was completely reversed by combining it with the K152E mutation. Conjugate formation of Jurkat T cells expressing the SKAP55 double mutant was reduced to levels observed for shSK55 and RE-SK55$_{K152E}$ (**Figure 2.2.13B**).

The fact that the re-expression of RE-SK55$_{D120K}$ in non-stimulated cells lead to increased adhesion and interaction with non-superantigen-loaded APCs indicates that this mutant might induce LFA-1 activation independent of an extracellular stimulus. An integrin accomplishes better ligand binding following conformational changes within the integrin (affinity regulation) and the formation of integrin clusters (avidity regulation, see **Figure 1.5**).[36,37] To investigate whether the D120K mutant affects the affinity state of LFA-1, I took advantage of the conformation-specific antibody mAb24. This antibody specifically binds only the high affinity conformation of LFA-1.[178] Jurkat transfectants (for suppression/re-expression vectors see **Figure 2.2.12**) were left untreated (+ICAM-1) or stimulated with OKT3 (+ICAM-1/TCR stim.) in the presence of the ligand ICAM-1, stained with fluorescently labeled mAb24 antibody and analyzed by flow cytometry. Jurkat T cells expressing RE-SK55$_{D120K}$ showed a significantly increased mAb24 binding on non-stimulated T cells and thus exhibit more integrins in their high affinity conformation. The activating effect of the D120K mutant was completely reversed by introducing the K152E mutation (RE-SK55$_{D/K}$; comparable to RE-SK55$_{K152E}$ and shSK; **Figure 2.2.13C**).

Next to SKAP55-dependent LFA-1 affinity regulation, we were interested in investigating whether the D120K mutant also interferes with LFA-1 avidity regulation. To monitor LFA-1 avidity, Jurkat transfectants were left untreated or stimulated with OKT3, incubated with DyLight650-conjugated anti-CD11a antibodies and analyzed by CLSM. As shown in **Figure 2.2.13D**, knockdown of SKAP55 reduced LFA-1 clustering in non-stimulated and stimulated Jurkat T cells (in line with data generated with SKAP55 ko T cells[135]). Clustering was rescued by expression of RE-SK55$_{WT}$. The spontaneous adhesion and conjugate formation of non-stimulated T cells was reflected by an increased LFA-1 avidity on RE-SK55$_{D120K}$ transfectants (see **Figure 2.2.13D**). The increase in LFA-1 avidity was again completely diminished in cells expressing RE-SK55$_{D/K}$. Here, LFA-1 clustering was comparable to RE-SK55$_{K152E}$ and shSK transfectants (**Figure 2.2.13D**).

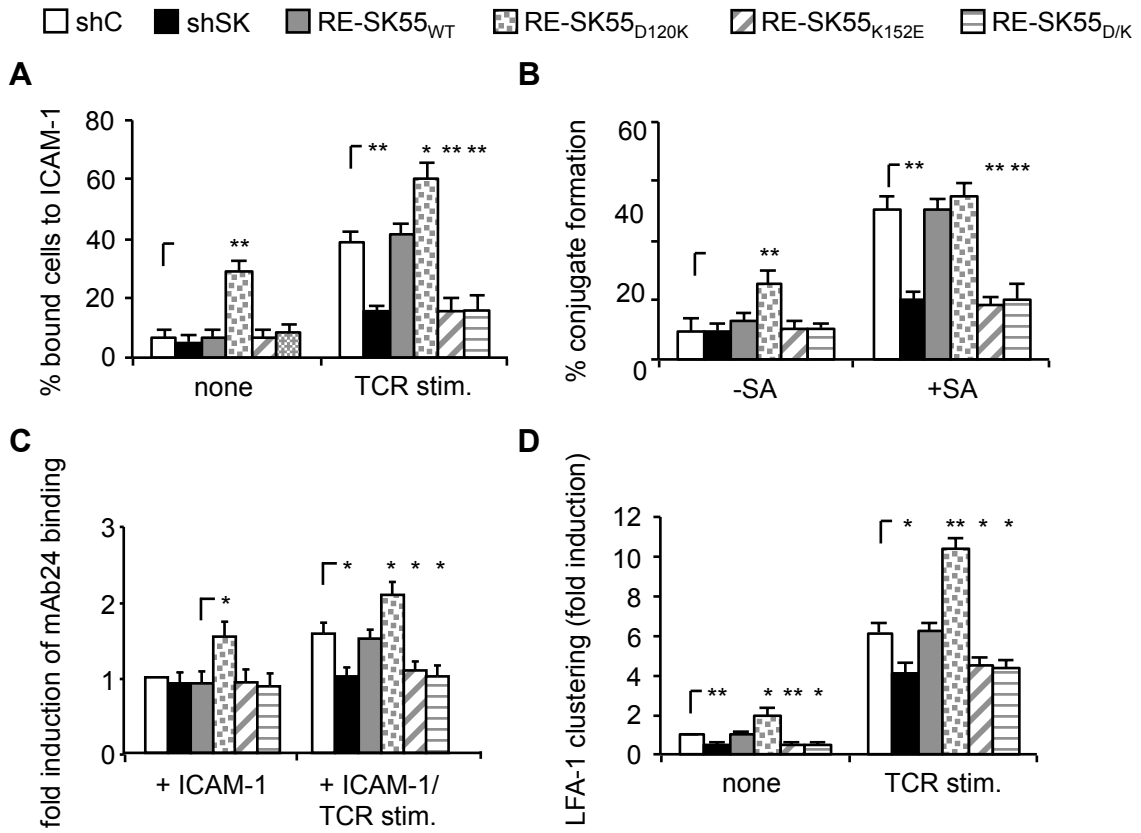

Figure 2.2.13: Mutation of aspartic acid 120 (D120K) induces constitutive adhesion, interaction with APCs and LFA-1 activation. (A-D) Jurkat T cells were transfected with constructs described in **Figure 2.2.12** and incubated for 48 h. **(A)** Cells were left untreated (none) or were stimulated for 30min with OKT3 (TCR stim.). Cells were analyzed for adhesion to ICAM-1-coated 96-well plates. Bound cells were counted and calculated as % input ($2x10^5$ cells). **(B)** Cells were incubated with unloaded (-SA) or superantigen-loaded (+SA) DDAO-SE (red)-stained Raji B cells for 30min. Pair formation was analyzed by flow cytometry. The percentage of conjugates was defined as the number of double-positive events (GFP-positive T cell and DDAO-SE-positive B cell). **(C)** Cells were left untreated (+ICAM-1) or OKT3-stimulated (+ ICAM-1/TCR stim.) and stained with the anti-active LFA-1 antibody mAb24. mAb24 accessibility was measured by flow cytometry within the GFP-positive cells. The mean fluorescence intensity of the untreated (+ICAM-1) shC transfectants was set to 1 and fold induction was calculated (n=3). **(D)** Cells were left untreated (none) or stimulated with OKT3 (TCR stim.) and subsequently with anti-mouse IgG. Cells were fixed, permeabilized and stained with DyLight650-tagged CD11a (LFA-1) antibody. CLSM was performed and the percentage of GFP-positive cells with LFA-1 clusters was calculated. 450 cells from three independent experiments were analyzed. Error bars represent mean ± SD (*$p \leq 0.05$; **$p \leq 0.01$).

These data indicate that D120 – similar to D129 in SKAP-HOM – is a negative regulator of T cell adhesion, conjugation with APCs and LFA-1 activation (affinity and avidity). Additionally, my data reveal a dominant effect of the K152E mutation over the gain-of-function phenotype induced by D120K. This indicates that the positive effect of the D120K mutation depends on the integrity of K152.

Next, I was interested in the mechanism that enables the D120K mutant of SKAP55 to induce integrin activation in non-stimulated Jurkat T cells (**Figure 2.2.13C,D**). As shown in **Figure 2.2.14A**, PM fractions of suppression/re-expression vector-transfected Jurkat T cell (non-stimulated or TCR-stimulated) support the microscopic findings that in contrast to RE-SK55$_{WT}$,

RE-SK55$_{D120K}$ is constitutively at the PM (see **Figure 2.2.11A**). The same was true for the constitutive interaction partners ADAP, RIAM and RapL and surprisingly for Talin in RE-SK55$_{D120K}$ transfectants (**Figure 2.2.14A**). The inducible associates of the ADAP/SKAP55 module (Rap1 and SLP-76) were not detectable in PM fractions of non-stimulated Jurkat T cells. They only translocated to the PM upon TCR stimulation (**Figure 2.2.14A**). The RE-SK55$_{K152E}$ single mutant as well as the RE-SK55$_{D/K}$ double mutant behaved like RE-SK55$_{WT}$. In non-stimulated cells, they localized in the cytoplasm, whereas upon stimulation they translocated to the PM. The same was observed for ADAP, RapL, RIAM, Rap1, Talin as well as SLP-76 (**Figure 2.2.14A**).

To investigate the composition of SKAP55-containing complexes that are formed upon TCR stimulation, I prepared SKAP55 immunoprecipitates from non-stimulated or TCR-triggered Jurkat T cells re-expressing either wild-type or mutated (D120K, K152E or D/K) FLAG-tagged SKAP55. Interestingly, **Figure 2.2.14B** shows that RE-SK55$_{D120K}$ constitutively interacts with ADAP, RIAM, RapL, Talin, LFA-1 and actin. In contrast, the association of RE-SK55$_{D120K}$ with Rap1 and SLP-76 only occurred upon TCR stimulation. RE-SK55$_{K152E}$ and RE-SK55$_{D/K}$ both showed normal association with ADAP, RIAM, RapL, Rap1 and SLP-76 but strongly reduced binding to Talin, LFA-1 and actin (**Figure 2.2.14B**). Control-immunoprecipitation of LFA-1 (CD11a) showed comparable results. The D120K mutation induced constitutive interaction of ADAP/SKAP55 module with LFA-1, Talin and actin. By contrast, additional mutation of K152 (RE-SK55$_{D/K}$) impaired the interaction of the ADAP/SKAP55 module with LFA-1, Talin and actin (**Figure 2.2.14C**).

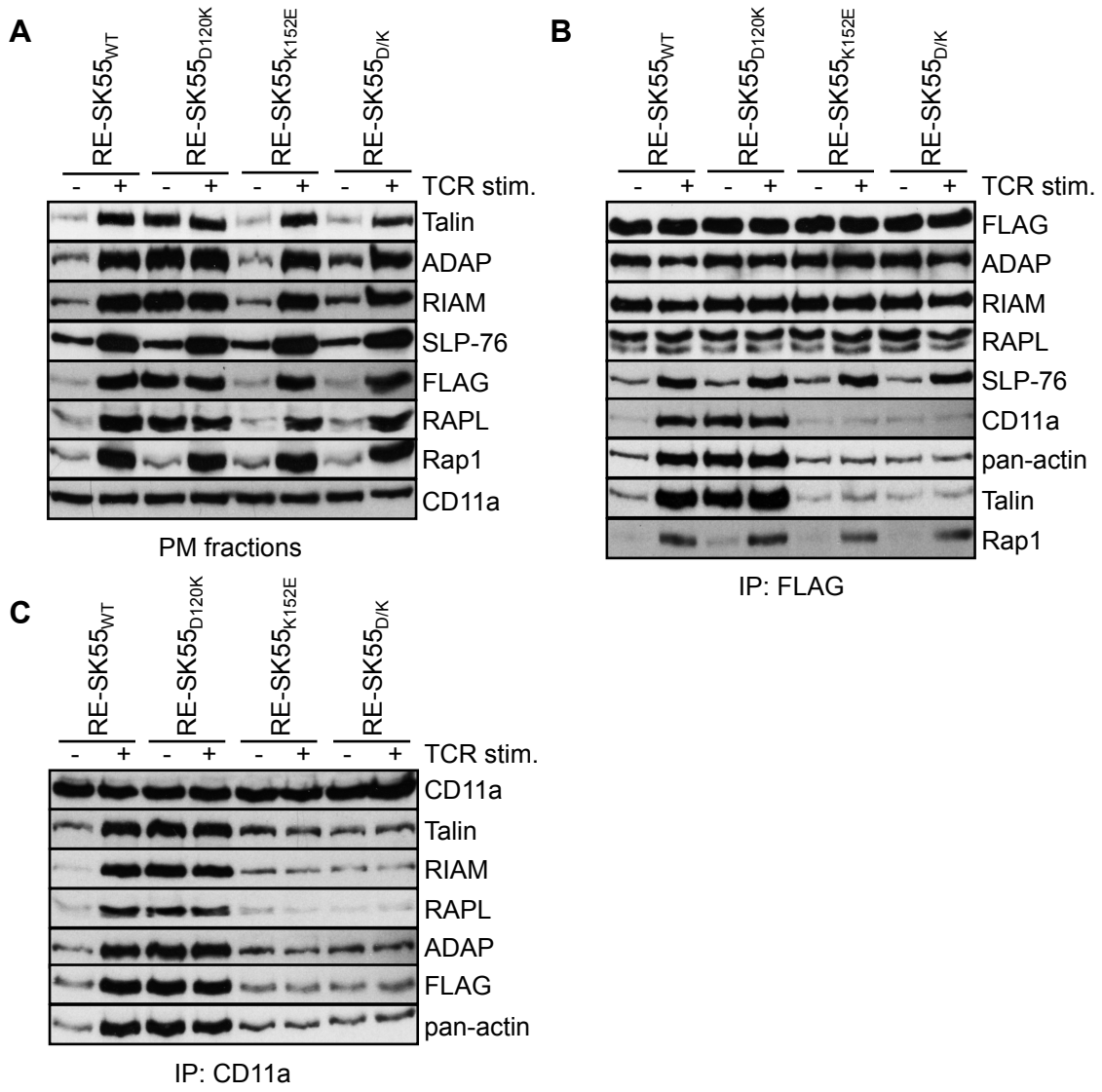

Figure 2.2.14: The lysine 152 (K152E) mutation interferes with the constitutive association of the D120K mutant of SKAP55 with Talin, LFA-1 and actin. (A-C) Jurkat T cells were transfected with the suppression/re-expression constructs that suppressed endogenous SKAP55 and re-expressed FLAG-tagged shRNA-resistant SKAP55 wild-type (RE-SK55$_{WT}$) or its mutants (RE-SK55$_{D120K}$, RE-SK55$_{K152E}$ and RE-SK55$_{D/K}$). After 48h, cells were left untreated or stimulated with OKT3 (TCR stim.). **(A)** PM fractions were isolated, separated by SDS-PAGE, transferred and analyzed by immunoblotting with the indicated antibodies. **(B,C)** Transfected Jurkat T cells were left untreated or stimulated with OKT3 (TCR stim.). Lysates were used for immunoprecipitation of SKAP55 using anti-FLAG antibody (IP:FLAG) **(B)** or of LFA-1 using anti-CD11a antibody (IP:CD11a) **(C)**. Precipitates were separated by SDS-PAGE, transferred and immunoblotted using the indicated antibodies. One representative experiment out of two is shown.

These intriguing data suggest that D120K mutation of SKAP55 induces a constitutive PM localization of the SKAP55 molecule itself and its constitutive interaction partners as well as Talin. These complexes are not only constitutively at the PM but also in association with LFA-1, allowing its activation under non-stimulated conditions. K152E mutation interfered with the gain-of-function effect of the D120K mutation by preventing the complex formation of LFA-1 via SKAP55 with Talin and actin.

In non-stimulated T cells, Rap1 is expressed in its inactive form but becomes activated upon TCR or chemokine receptor stimulation to trigger the adhesive function of integrins.[179,180] Only the active guanosine triphosphate (GTP)-bound form of Rap1 is supposed to bind via RIAM or RapL to the LFA-1-activating complexes.[132,181] The interaction of Rap1 with RapL/SKAP55 or RIAM/SKAP55 is crucial for the association of active Rap1 with integrins and thus integrin activation.[128,129,132,181] Surprisingly, the data shown in **Figure 2.2.14** indicate that although the ADAP/SKAP55$_{D120K}$ module is constitutively at the PM and despite the fact that LFA-1 is constitutively active in RE-SK55$_{D120K}$ transfectants, Rap1 was not found at the PM (**Figure 2.2.14A**) or co-precipitated with SKAP55 in non-stimulated RE-SK55$_{D120K}$ re-expressing Jurkat T cells (**Figure 2.2.14B**). Instead, even in RE-SK55$_{D120K}$ re-expressing T cells, PM recruitment of Rap1 and its interaction with the ADAP/SKAP55 module strictly depended on TCR triggering. This suggests that RE-SK55$_{D120K}$ is able to activate LFA-1 in a Rap1-independent manner. To investigate this further, I transfected Jurkat T cells with RE-SK55$_{WT}$ or RE-SK55$_{D120K}$ in combination with a small interfering RNA (siRNA) against Rap1 (siRap1). Transfectants were left untreated or stimulated with OKT3 and binding to ICAM-1-coated plates was studied. Surprisingly and as shown in Figure **2.2.15A**, knockdown of Rap1 strongly impaired TCR-induced adhesion of RE-SK55$_{WT}$ as well as RE-SK55$_{D120K}$-expressing cells but had no effect on basal adhesion induced by RE-SK55$_{D120K}$. This is in contrast to two studies that reported that either homozygous Rap1 knockout[55] or Rap1 inhibition (by overexpressing a Rap1-specific GTPase-activating protein)[182] both decrease basal adhesion. Therefore, the mechanism how the D120K mutant of SKAP55 induces Rap1-independent adhesion needed further investigation.

Talin is a FERM (four-point-one/ezrin/radixin/moesin) domain-containing protein that forms a direct link between integrins and the actin cytoskeleton.[37] Indeed, loss of Talin leads to an almost complete block of integrin activation (monitored by adhesion, migration, T-APC interaction and conformation-specific antibodies).[46–49] The prevailing view is that PM targeting of Talin requires Rap1. Here, RIAM acts as a scaffold that connects the membrane-targeting sequences within Rap1 to Talin.[183] Additionally, Yang et al. showed that the interaction of RIAM with the N-terminal head of Talin is sufficient to activate Talin, hence triggering integrin activation.[133] Therefore, I asked myself if constitutively PM localized (due to RE-SKAP55$_{D120K}$) and RIAM-associated/activated Talin could induce adhesion in unstimulated RE-SK55$_{D120K}$ transfectants. Therefore, we conducted a Talin knockdown (siTalin) in RE-SK55$_{WT}$ and RE-SK55$_{D120K}$ transfectants, respectively. Data indicate that in our system Talin, in contrast to

Rap1, is essential for both spontaneous as well as TCR-induced adhesion (**Figure 2.2.15C)**. Additionally, these data implicates that the spontaneous adhesion induced by the D120K mutant of SKAP55 depends on Talin.

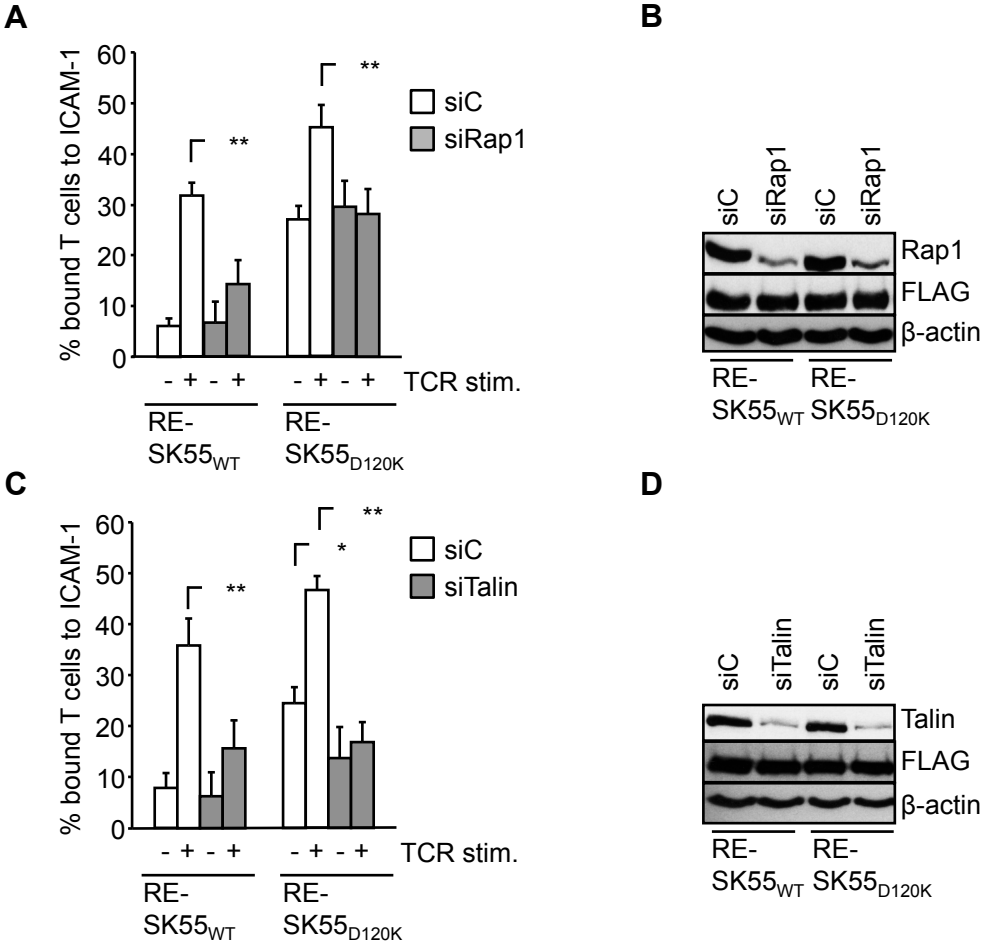

Figure 2.2.15: TCR-independent adhesion triggered by the D120K mutant of SKAP55 depends on Talin but not Rap1. Jurkat T cells were transfected with the suppression/re-expression constructs suppressing endogenous SKAP55 and re-expressing FLAG-tagged shRNA-resistant wild-type (RE-SK55$_{WT}$) or D120K-mutated SKAP55 (RE-SK55$_{D120K}$). **(A)** In addition, cells were co-transfected with either control siRNA (siC) or siRNA against Rap1 (siRap1). 48h after transfection, cells were left untreated or were stimulated with OKT3 (TCR stim.). Cells were analyzed for adhesion to ICAM-1-coated 96-well plates. Bound cells were counted and calculated as % input (2x10^5 cells). Error bars represent mean ± SD of at least three independent experiments (**p≤0.01). **(B)** Whole lysates of transfected cells from (A) were prepared, separated by SDS-PAGE, transferred and immunoblotted for Rap1, FLAG (re-expressed FLAG-tagged SKAP55) and β-actin (loading control). **(C)** In addition to the suppression/re-expression constructs, cells were co-transfected with either control siRNA (siC) or siRNA against Talin (siTalin). 48h after transfection, cells were left untreated or were stimulated with OKT3 (TCR stim.). Cells were analyzed for adhesion to ICAM-1-coated 96-well plates. Bound cells were counted and calculated as % input (2x10^5 cells). Error bars represent mean ± SD of at least three independent experiments (*p≤0.05; **p≤0.01). **(D)** Whole lysates of transfected cells from (C) were prepared, separated by SDS-PAGE, transferred and immunoblotted for Talin, FLAG (re-expressed FLAG-tagged SKAP55) and β-actin (loading control).

In conclusion, our data suggest that two critical amino acid residues within the PH domain of SKAP55 regulate PM targeting of the ADAP/SKAP55 module and TCR-mediated activation of LFA-1. D120 exhibits a negative regulatory role, probably by binding to positively charged amino acids in the DM domain, thereby

holding SKAP55 in an inactive conformation and keeping it in the cytoplasm. K152 is mandatory for the adapter function of SKAP55 in LFA-1 activation by (i) mediating PM recruitment presumably through PI/actin binding and (ii) enabling complex formation of LFA-1 with actin and Talin via SKAP55.

❊ ❊ ❊

3. DISCUSSION AND OUTLOOK

3.1. DISCUSSION

It is mandatory for an adaptive immune response that naïve T cells home to secondary lymphoid organs to get into contact with APCs. The interaction with an APC presenting a cognate peptide induces the activation, differentiation and proliferation of T cells. T cell homing (including firm adhesion and migration) and T-APC interactions are mediated by the integrin LFA-1.[5,37,64] Several studies have shown that the adapter proteins ADAP and SKAP55 are critically involved in chemokine receptor- and TCR-mediated LFA-1 activation (monitored by adhesion, migration and T-APC conjugate formation).[62,95,105,106,135,136,176]

In the first part of my study, we verified the syk kinase ZAP70 as an interaction partner of ADAP upon triggering of the chemokine receptor CXCR4 or the TCR. We showed that this interaction is mediated by pY571 of ADAP and N-pYBP of the tandem SH2 domains of ZAP70 ($tSH2_{ZAP70}$). Phosphorylation of $ADAP_{Y571}$ is required for a signaling pathway that regulates F-actin-induced but LFA-1-independent migration.

In the second part of my work, I focused on the importance of PH_{SK55} for SKAP55 PM targeting and LFA-1 activation in T cells. I found that independent of PI3K activity, the isolated PH_{SK55} constitutively localizes at the PM of T cells. I identified two residues within PH_{SK55} as being essential for PM recruitment of SKAP55 and hence LFA-1 activation, namely K152 and D120. D120 is a negative regulatory residue that prevents PM targeting of SKAP55 in non-stimulated T cells, probably by mediating an auto-inhibitory interaction where the N-terminal DM domain blocks the PH domain. K152 within the PH domain is a positive regulatory residue that enables SKAP55 PM recruitment and subsequently LFA-1 activation after TCR stimulation by mediating the interaction of LFA-1 with Talin and actin.

3.1.1. Y571 of ADAP interacts with ZAP70 and regulates CXCR4-induced migration

ADAP – one of the two adapter proteins that form the backbone of LFA-1-activating complexes shown in **Figure 1.6** – is strongly tyrosine-phosphorylated upon the activation of T cells.[65,66,77,80,88,90] ADAP serves as a central hub for SH2 domain-containing proteins like SLP-76,[65–67,76,77] Nck[75,78,79] and Fyn.[66,80] The best-characterized tyrosine-based signaling motives (Y595, Y625 and Y651) within ADAP are localized in the unstructured region between its two hSH3 domains, whereas tyrosine 571 – which is studied here – is localized at the rim of $N\text{-}hSH3_{ADAP}$ (**Figure 1.7**). In this study, we identified tyrosine 571 as a unique

phospho-tyrosine that is solely required for the regulation of CXCR4-induced integrin-independent but actin-dependent migration.

ZAP70 interacts with the phosphorylated tyrosine 571 of ADAP *in vitro* and *in vivo*

Using the Y571-phosphorylated isolated N-hSH3$_{ADAP}$ as bait, ZAP70 was identified as a predominant and robust binding partner of ADAP (k_D= 2.3µM) *in vitro*.[146] The association of ZAP70 with ADAP is supported by a publication of Okabe and co-workers.[184] They performed immunoprecipitation studies in which they identified a complex that is inducibly formed in T cells upon CXCR4 stimulation and among others contains ADAP and ZAP70.[184] However, in this study they did not investigate which domains/structures within the proteins enable complex formation.

The cytoplasmic protein tyrosine kinase ZAP70 is mandatory for T cell development and function.[147–149] Stimulation-induced PM recruitment and activation of ZAP70 in T cells depends on tSH2$_{ZAP70}$.[147,148] In non-stimulated T cells, ZAP70 is found in its closed/auto-inhibited conformation and bears no catalytic activity in this state.[185] Upon TCR triggering, Lck is recruited to the TCR complex (via the CD4/8 co-receptors) and phosphorylates the ITAMs (Yxx(I/L)x$^{6-8}$Yxx(I/L)) in the CD3ξ chains.[20–22] Doubly-phosphorylated CD3ξ ITAMs (2pY-ITAM) are bound by tSH2$_{ZAP70}$. ITAM binding initiates a conformational change within ZAP70 that releases its auto-inhibitory conformation and allows (auto)phosphorylation of regulatory tyrosines (Y319 and Y493) within ZAP70 by Lck or ZAP70.[147–149] Phosphorylation of ZAP70 at Y319 is mandatory given that it induces structural changes that release the kinase from its inhibitory conformation, so that Y493 can be phosphorylated.[156,157] Phosphorylation of both tyrosines leads to its full enzymatic activity[185] and initiates the formation of signaling platforms through the phosphorylation of several adaptor proteins.[21,22,147,148] The consequences of these early signaling events are T cell activation, proliferation and differentiation.[147–149]

Binding of the 2pY-ITAM by tSH2$_{ZAP70}$ is thought to occur in sequence, whereby each phospho-tyrosine of the 2pY-ITAM engages one SH2 domain of ZAP70 (**Figure 3.1.1A**). 2pY-ITAM binding takes place in a head-to-tail fashion, where the C-terminal phospho-tyrosine binding pocket (C-pYBP$_{ZAP70}$) binds to the N-terminal phospho-tyrosine (pYNEL) and vice versa. The C-pYBP$_{ZAP70}$ is already preformed and only comprises residues from the C-terminal SH2 domain of ZAP70 (C-SH2$_{ZAP70}$). By contrast, N-pYBP$_{ZAP70}$ is built up by residues from both SH2 domains and is only formed due to conformational changes within the tSH2$_{ZAP70}$ that are induced upon the engagemant of C-pYBP$_{ZAP70}$. Only then is the

N-pYBP$_{ZAP70}$ able to bind to the C-terminal phospho-tyrosine (pYDVL) of the 2pY-ITAM.[186] These findings suggest that N-pYBP$_{ZAP70}$ cannot bind to phospho-tyrosines independent of prior engagement of C-pYBP$_{ZAP70}$.

NMR studies show that the interaction with ADAP$_{pY571}$ is realized by N-pYBP$_{ZAP70}$.[146] Given the aforementioned model of sequential binding, it is unlikely that one phospho-tyrosine of ADAP alone is able to bind to N-pYBP$_{ZAP70}$. There are two possible scenarios regarding how pY571 engagement with N-pYBP$_{ZAP70}$ might occur (see **Figure 3.1.1B,C**).
First, there is a potential ITAM localized in N-hSH3$_{ADAP}$ (Y^{559}GYIx$_8$Y^{571}DSL; **Figure 3.1.1B**). If pY559 binds to C-pYBP$_{ZAP70}$ first, this would allow the formation of N-pYBP$_{ZAP70}$ and subsequently pY571 binding. The ITAM scenario is attractive since Sylvester et al. showed that mutation of Y559 to phenylalanine (Y559F) induces a phenotype in Jurkat T cells comparable to that observed in this study. Y595F-transfectants exhibit normal TCR-mediated adhesion but significantly reduced migration upon CXCR4 triggering.[75] Additionally, binding of tSH2$_{ZAP70}$ to a motiv rather that one phospho-tyrosine within N-hSH3$_{ADAP}$ was supported by pull-down experiments showing that tSH2$_{ZAP70}$ did not bind to a pY571-containing peptide (residues 566-579 of ADAP) but rather to pY571 in the context of the whole N-hSH3$_{ADAP}$ domain.[146] Unfortunately, this ITAM is localized in the structured N-hSH3$_{ADAP}$, in contrast to ITAMs of the CD3 chains, which are known to localize in unstructured regions.[187] Although it has already been described that Y559 is phosphorylated, these data were obtained after enrichment of phosphoproteins.[75] In our current study, without enrichment, no Y559 phosphorylation was observed. Mass spectroscopic analysis revealed a phosphorylation degree of 70% for Y571, in contrast to only 2% for the other tyrosines in N-hSH3$_{ADAP}$.[146] Structural analysis further demonstrated that Y559 is largely buried in its neighboring structures and only marginally available for an incoming kinase (and consequently for C-pYBP$_{ZAP70}$ binding) unless a major structural rearrangement is taking place (personal communication with Prof. C. Freund).
Second, since NMR analysis of the tSH2$_{ZAP70}$ in the presence of N-hSH3$_{ADAP}$ demonstrated that upon binding of N-hSH3$_{ADAP}$ to tSH2$_{ZAP70}$ residues in both SH2 domains of ZAP70 showed intensity losses[146], this might indicate that two NhSH3$_{ADAP}$ molecules interact with one tSH2$_{ZAP70}$. First, one N-hSH3$_{ADAP}$ molecule binds to C-pYBP$_{ZAP70}$, which subsequently allows binding of a second N-hSH3$_{ADAP}$ molecule to N-pYBP$_{ZAP70}$. Therefore, another possibility could be that *in vivo* two pY571 residues of an ADAP dimer interact with C-pYBP$_{ZAP70}$ and

N-pYBP$_{ZAP70}$, respectively (**Figure 3.1.1C**). ADAP dimer formation has been shown before.[131] In this study the author additionally predicts a region (residues 465-503) upstream of N-hSH3$_{ADAP}$ that might be involved in the formation of coiled-coils[131] and these structural motif are known to mediate protein oligomerization.[188] It is possible that the association mediated by the coiled-coil allows proper arrangement of both molecules to enable parallel binding of both pY571 residues to tSH2$_{ZAP70}$.

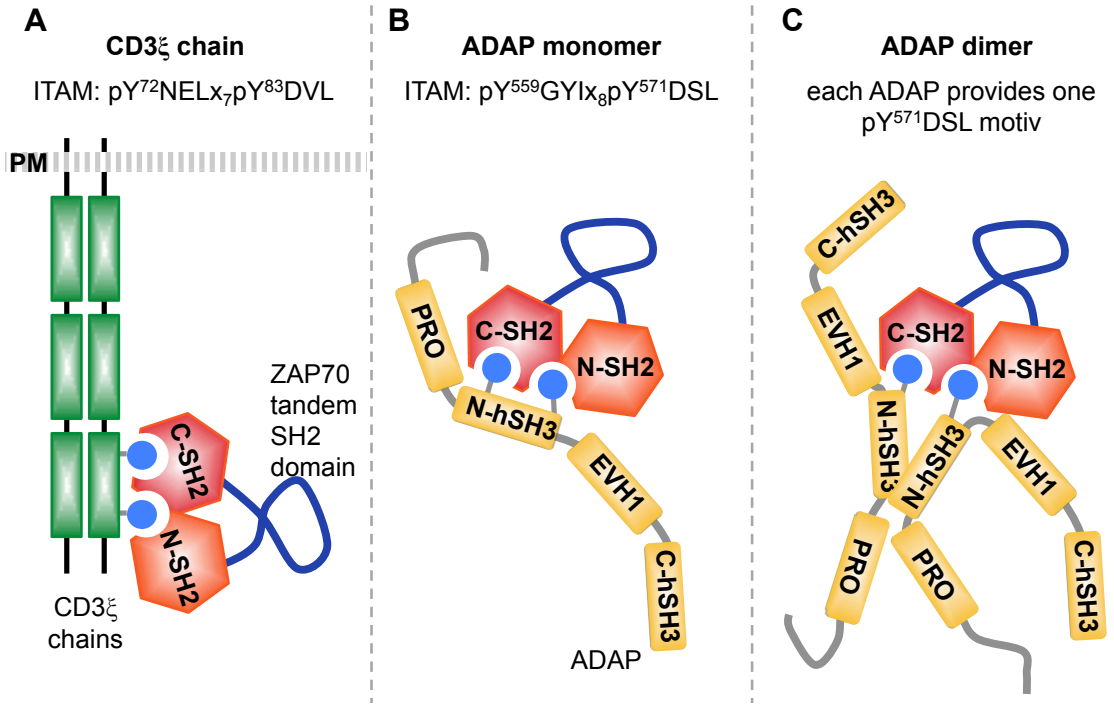

Figure 3.1.1: Model of ZAP70 tandem SH2 domain engagement with doubly-phosphorylated ITAMs of the CD3ξ chains or tyrosine 571-phosphorylated ADAP. Shown is the Y-shaped tSH2$_{ZAP70}$ consisting of a C-SH2$_{ZAP70}$ (red) and an N-terminal SH2 domain (N-SH2$_{ZAP70}$, orange) connected by the interdomain A (dark blue). tSH2$_{ZAP70}$ is associated with phospho-tyrosines (depicted as light blue circles) provided by a 2pY-ITAM of the CD3ξ chains (green) or ADAP (yellow). tSH2$_{ZAP70}$ modified from[148] **(A)** ZAP70 binds the two phospho-tyrosines of the CD3ξ ITAM in sequence. First, binds the binding pocket of the C-SH2$_{ZAP0}$ to the pYNEL motiv. This interaction induces a conformational change that leads to the formation of the second binding pocket (built up by residues of the C-SH2$_{ZAP70}$ and N-SH2$_{ZAP70}$). Subsequently, the pYDVL motif binds to the second binding pocket in the N-SH2$_{ZAP70}$ domain of ZAP70.[186] **(B)** ADAP (yellow) contains one potential ITAM sequence (Y^{559}GYIx$_8$Y^{571}DSL) within its N-hSH3$_{ADAP}$. After binding of pY559 to the C-pYBP$_{ZAP70}$, conformational changes within ZAP70 induce the formation of N-pYBP$_{ZAP70}$. This allows engagement of pY571 with N-pYBP$_{ZAP70}$. **(C)** ADAP molecules probably dimerize via a coiled-coil structure (mediated by residues 465-503; predicted by [131]) localized in front of N-hSH3$_{ADAP}$. One ADAP dimer interacts with tSH2$_{ZAP70}$ by binding of their pY571s. Binding occurs in sequence, first to C-pYBP$_{ZAP70}$ then to N-pYBP$_{ZAP70}$.

For the tSH2$_{ZAP70}$-binding scenario of ADAP (**Figure 3.1.1C**), further studies are needed. First, we have to clarify whether sequential binding of the ADAP homodimer to tSH2$_{ZAP70}$ is possible and what the trimeric complex would look like. Second, it would be interesting to ascertain the binding affinities for ADAP$_{pY571}$/ADAP$_{pY571}$ to tSH2$_{ZAP70}$. It has been shown that binding of tSH2$_{ZAP70}$ to single-phosphorylated ITAMs (58.8±11.6µM and 44.5±14.9µM[189]) occurs with weaker affinity compared to 2pY-ITAM binding (k_D=2±0.5nM to 31±1.1nM[190,191]).

Therefore, it might be possible that in the context of two dimerizing full-length ADAP molecules binding to $tSH2_{ZAP70}$ occurs with higher affinities compared to binding of two isolated N-$hSH3_{ADAP}$.

Using our suppression/re-expression vector system, I could show that binding of ZAP70 to ADAP is impaired when Y571 is mutated. Upon CXCR4 stimulation, there was no $ADAP_{Y571F}$-bound ZAP70 detectable in the precipitates. In contrast to CXCR4 stimulation, upon TCR stimulation $ADAP_{Y571F}$ co-precipitation was only partial reduced by approx. 30% (see **Figure 2.1.3A**). The remaining 70% of $ADAP_{Y571F}$ that are co-precipitated with ZAP70 are probably part of a large signaling complex that is formed in PM proximity upon TCR but not CXCR4 stimulation and includes signaling molecules like LAT, ZAP70, SLP-76 and ADAP (the so called LAT signalosome).[14] In this signaling complex, ADAP is not directly associated with ZAP70 but binds via SLP-76 to LAT.[21,44,192] LAT as well as SLP-76 are phosphorylated by ZAP70 upon TCR triggering[19,21,44] and association of ADAP with both molecules can thus lead to co-precipitation of ADAP by ZAP70. This interpretation is supported by our precipitation studies that clearly identified ADAP/ZAP70 as members of the LAT signalosome including LAT/PLCγ1/SLP-76.[146] The data shown in **Figure 2.1.3A** indicate that in TCR-activated cell only a minority of ZAP70 is directly associated to $ADAP_{pY571}$ whereas the majority of ZAP70 is indirectly linked to ADAP due to binding of both proteins to the LAT signalosome. A possible reason why only 30% of ZAP70 is directly associated with $ADAP_{pY571}$ might be that under competitive conditions (upon TCR simulation and subsequently in the presence of 2pY-ITAMs), it is likely that ZAP70 would rather bind to the TCR complex (high affinity; k_D=2.0±0.5nM to 31.0±1.1nM[190,191]) than to $ADAP_{pY571}$ (k_D= 2.3μM[146]).

In our immunoprecipitation studies, we identified ZAP70 as interacting with ADAP upon both CXCR4 and TCR stimulation, respectively. The interaction reached its maximum at 5min (TCR) and 1min (CXCR4) of stimulation (**Figure 2.1.1**). Interestingly, Y319 phosphorylation of $ADAP_{pY571}$-bound ZAP70 was only observed upon TCR but not CXCR4 stimulation (**Figure 2.1.1**). Given that phosphorylation of ZAP70 at Y319 is mandatory for ZAP70 kinase activation,[156,157] this clearly points in the direction that $ADAP_{pY571}$-bound ZAP70 in chemokine stimulated cells was in its kinase-inactive form.

As previously mentioned, ZAP70 is phosphorylated and subsequently activated by Lck. Due to its myristoylation at serine 6 of its src homology 4 (SH4) domain after synthesis, Lck is constitutively targeted to the PM.[193] A possible explanation for impaired phosphorylation at Y319 of ZAP70 bound to $ADAP_{pY571}$ might be an

inadequate cellular localization of the ADAP$_{pY571}$/SKAP55/ZAP70 complex upon chemokine stimulation. Additionally, it has been shown that CXCL12 stimulation promotes the incorporation of src kinases in particular PM regions (the so called lipid rafts).[194] If the ADAP$_{pY571}$/SKAP55/ZAP70 complex does not localize to lipid rafts, no ZAP70 phosphorylation/activation by Lck might take place. Hence, the cellular localization of the ADAP$_{pY571}$/SKAP55/ZAP70 complex clearly needs further investigation. Microscopic and biochemical studies of PM fractionation and lipid rafts will reveal whether ZAP70 bound to ADAP co-localizes with Lck or remains in other cellular areas or compartments.

Our findings show that CXCR4-triggering induces the pY571-dependent interaction of ADAP with kinase-inactive ZAP70.

The role of tyrosine 571 of ADAP in CXCR4-induced T cell migration

Using the suppression/re-expression system (for constructs see **Figure 2.1.2**), I also investigated the importance of ADAP$_{pY571}$ for T cell function. This system allows investigating the non-phospho RE-ADAP$_{Y571F}$ mutant with only 40% of endogenous ADAP still present (**Figure 2.1.2B**). Upon TCR stimulation, RE-ADAP$_{Y571F}$ transfectants showed no defects in adhesion to ICAM-1, interaction with superantigen-loaded B cells, F-Actin content and upregulation of the activation marker CD69 (**Figure 2.1.4**). These data indicate that phosphorylation of Y571 is not involved in TCR-triggered T cell functions. As already published by our group, knockdown/knockout of ADAP strongly reduced T cell adhesion upon chemokine stimulation.[62] Re-expression of ADAP$_{Y571F}$ completely rescued the phenotype (**Figure 2.1.5A**). This indicates that LFA-1-mediated adhesion does not require phosphorylation of ADAP$_{Y571}$. In clear contrast, the percentage of ADAP$_{Y571F}$ re-expressing cells that migrated along a chemokine gradient was significantly reduced (**Figure 2.1.5B**). Analysis of the actin content in CXCR4-stimulated ADAP$_{Y571F}$ transfectants revealed that F-actin levels were reduced to a degree comparable to shAD-transfected cells (**Figure 2.1.5C**). This suggests that the observed migratory defect is independent of integrins but dependent on actin dynamics. Integrin-independent migration has been described as playing a role in a three-dimensional context under non-shear flow conditions.[195–197] It has been discussed that this integrin-independent migration might maximize T cell motility in LNs, whereas shear flow in blood vessels induces robust integrin-dependent adhesion to endothelial cells.[196] This is intriguing because in 2012 we published data showing that ADAP ko T cells display a reduced migratory velocity within the paracortical T cell zone of LNs compared with wild-type T cells.[62] This

indicates that ADAP is involved in the motility regulation of T cells in LNs and that this intranodal motility might be regulated by the phosphorylation of ADAP at Y571.

With these findings in mind, two questions remain to be answered:
(i) What is the role of $ADAP_{pY571}$-bound kinase-inactive ZAP70 for actin-dependent migration?
(ii) What is the signaling pathway that involves $ADAP_{pY571}$ in actin-dependent migration?
To address the first question, our data showed that the association of ADAP with ZAP70 was relatively short-lived and already declined after 5min of CXCR4 stimulation (**Figure 2.1.1**). Therefore, what could be the benefit of ZAP70 binding to $ADAP_{pY571}$ for such a short duration? One possible explanation might be that ZAP70 needs the association with the ADAP/SKAP55 module to be targeted to a specific cellular compartment. It has been shown that the isolated $C\text{-}SH2_{ZAP70}$ binds PIs (k_D=340±35nM using PM-mimetic vesicles; preference for PIP_3) and localizes at the PM in a PI-dependent fashion.[198] Still, it might be possible that ZAP70 additionally needs an association with actin, which could be provided by the PH domain of SKAP55 (see part two of my work). Another explanation could be that ZAP70 acts as a placeholder that interferes with binding of an actin-regulatory molecule to $ADAP_{pY571}$ immediately after CXCR4 stimulation. Accordingly, ZAP70 binding to $ADAP_{pY571}$ might be involved in the regulation of a specific time schedule required for adequate initiation of migration upon chemokine stimulation without affecting adhesion.
The importance of ZAP70 for directional T cell migration has previously been reported by two other studies.[154,155] Using piceatannol – a ZAP70 inhibitor – both studies emphasize a role for the catalytic activity of ZAP70 in T cell polarization and/or migration. Importantly and in contrast to my data, they additionally found impaired integrin activation (in ZAP70-deficient cells[155] or upon piceatannol treatment[154]). They hypothesized that kinase-active ZAP70 regulates integrin activity and integrin-dependent migration by a mechanism that involves Talin.[154,155]
Therefore, it is possible that two pools of ZAP70 regulate T cell migration: one pool where ZAP70 is kinase inactive, bound to ADAP and regulates integrin-independent migration (**Figure 3.1.2A**); and a second pool, where ZAP70 is kinase active, ADAP-free and regulates integrin-dependent migration (**Figure 3.1.2B**).

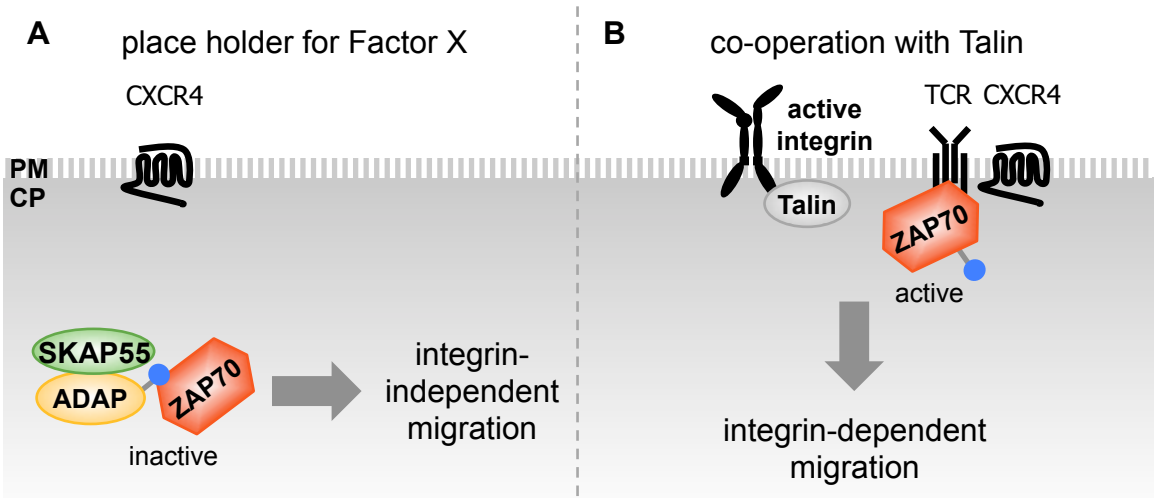

Figure 3.1.2: Two pools of ZAP70 are involved in the regulation of T cell migration. (A) Upon chemokine receptor stimulation ADAP becomes phosphorylated at Y571 (depicted as a light blue circle). The phosphorylated Y571 binds to the N-SH2$_{ZAP70}$. Here, ZAP70 acts as a placeholder to ensure a specific time schedule that is required for adequate initiation of CXCR4-induced integrin-independent migration. After dissociation of ZAP70 from the ADAP/SKAP55 module Factor X can bind. Factor X is involved in the regulation of actin-dependent/integrin-independent migration. **(B)** Data from Kumar et al. indicate that upon ligand binding, CXCR4 associates with the TCR and uses its ITAMs for signal transduction.[13] The src kinase Lck phosphorylates the ITAMs of the TCR. This allows ZAP70 recruitment to the ITAMs and subsequent activation of ZAP70.[9,12] Kinase-active ZAP70 induces the high affinity conformation of the integrin in an Talin-dependent manner.[154,155]

So what is the signaling pathway that involves ADAP$_{pY571}$ in actin-dependent migration? Re-organization of the actin cytoskeleton is a central process in migration[16,158,199] and it is an early cellular response to chemokine stimulation.[158,200] ADAP exhibits three known connections to the cytoskeleton: (1) via Nck/SLP-76/WASp,[78,79,82,201] (2) via Kindlin-3/Talin[62] and (3) via Ena/VASP proteins.[73,201] For all three connections the binding sites within ADAP are known and involve other sites than pY571.[62,73,76,79] Additionally, the first two connections (for Ena/VASP proteins data are only available for fibroblasts[202]) have already been implicated in the regulation of T cell adhesion to ligand-coated surfaces or APCs.[14,46,50,73,79] This is in clear contrast to my findings, where ADAP$_{Y571F}$ transfectants showed normal adhesion and T-APC interaction (**Figure 2.1.4A,B and 2.1.5A**).

Preliminary data from our group indicate a new, yet unknown link of ADAP to the actin cytoskeleton: via cofilin. Cofilin is a critical regulator of actin dynamics by severing actin filaments. Thus, depending on the circumstances, cofilin provides new templates and monomeric actin for further polymerization or leads to actin depolymerization.[16,203,204] Cofilin activity (capacity to bind actin) is regulated by phosphorylation or dephosphorylation of the inhibitory serine 3 of cofilin by LIM domain kinase (LIMK) or slingshot protein phosphatase 1L (SSH1L), respectively.[205–209] Several studies have underlined the importance of cofilin as well as its regulators LIMK and SSH1L for actin re-organization in

CXCL12-directed T cell migration.[209–211] In contrast to migration, to my knowledge none of the three molecules, cofilin, LIMK or SSH1L, have been implicated in the regulation of LFA-1-mediated T cell adhesion. Our first experiments indicated that expression of the RE-AD$_{Y571F}$ mutant in Jurkat T cells led to alterations of the cofilin phosphorylation status and thus its activity (data not shown). This could explain the reduced F-actin content (after 5 and 15min of CXCR4 stimulation) and the attenuated migratory capacity of the RE-AD$_{Y571F}$ expressing cells (**Figure 2.1.5B,C**).

It remains unknown how phosphorylation of Y571 is involved in cofilin activity regulation. We think that after dissociation of ZAP70 from ADAP$_{pY571}$ an unknown interaction partner (Factor X) binds to the ADAP/SKAP55 module. Based on their domain structure, it is unlikely that ADAP$_{pY571}$ directly binds to LIMK or SSH1L. Neither LIMK nor SSH1L contain domains that are known to bind phospho-tyrosines,[212,213] like SH2 domains or phospho-tyrosine binding (PTB) domains.[214]

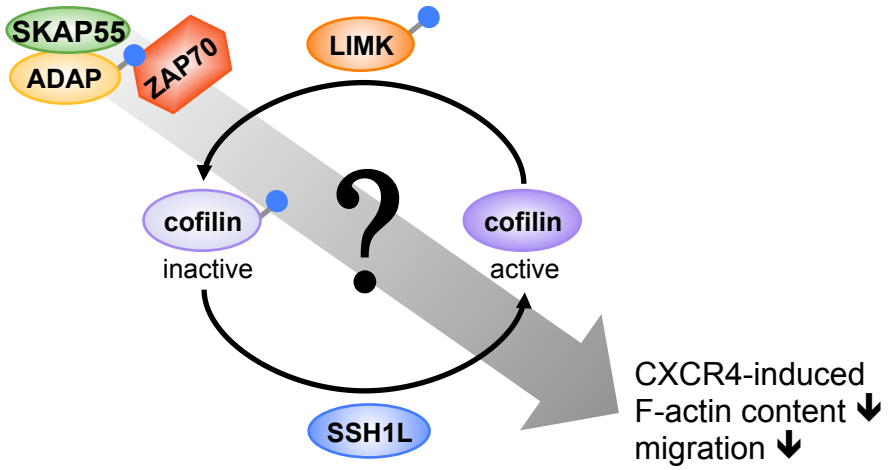

Figure 3.1.3: Model of ADAP phospho-tyrosine 571-mediated F-actin polymerization. Cofilin is an actin-severing protein. The actin-binding capacity of cofilin is regulated by phosphorylation (phosphorylation is depicted as a light blue circle) and dephosphorylation of the inhibitory serine 3. This is realized by LIMK and SSH1L, respectively. Phosphorylation of Y571 of ADAP in a hitherto unknown mechanism is involved in the regulation of cofilin activity. We suggest that ZAP70 bound to ADAP$_{pY571}$ acts as a placeholder to ensure the right timing. After 5min of CXCR4 stimulation, ZAP70 dissociates from the ADAP/SKAP55 module and pY571 enables the interaction with a yet unknown interaction partner that regulates cofilin activity (modified from [215]).

Further experiments are necessary to elucidate the newly-identified link between the ADAP/SKAP55 module and cofilin. Mass spectrometry will help us to identify Factor X that binds to ADAP$_{pY571}$ after ZAP70 has dissociated and regulates cofilin activity. For this purpose, I would suggest comparing the ADAP interactome after one minute of CXCR4 stimulation (ZAP70 still bound to pY571) with the interactome that is bound to ADAP after 5min of CXCR4 stimulation. Factor X should not be present after 1min of CXCR4 stimulation but after 5min.

In addition to identifying the molecular mechanism, it would be quite interesting to further investigate how RE-ADAP$_{Y571F}$ re-expression impairs actin-dependent migration. Before a T cell can migrate, it has to adopt a migratory phenotype characterized by a leading edge at the front and a uropod at the rear (see **Figure 1.4B**).[16,25] It has been shown that LIMK and SSH1L are mandatory for a T cell to adopt this phenotype. While LIMK promotes lamellipodia formation at the leading edge by inhibiting cofilin activity, SSH1L restricts membrane protrusions to one direction by keeping cofilin in its unphosphorylated active state.[209] Since RE-ADAP$_{Y571F}$ re-expression affects the cofilin activity in a hitherto unknown mechanism, it would be helpful to investigate migrating cells using CLSM. Depending on the observed phenotype, one could reason whether RE-ADAP$_{Y571F}$ is involved in LIMK and/or SSH1L activity regulation. To further investigate the consequences of RE-ADAP$_{Y571F}$ re-expression on the actin cytoskeleton, one could use an electron microscope to visualize the actin network or Life-Act (a peptide that stains F-actin[216]) in combination with live cell imaging to investigate actin dynamics upon CXCR4 stimulation.

Nonetheless, with these data I am able to state that phosphorylation of ADAP at Y571 promotes actin-dependent T cell migration in response to CXCR4 signaling. I have identified Y571 in ADAP as a regulatory residue that is solely required for chemokine but not TCR-induced T cell function.

3.1.2. D120 and K152 within the PH domain of SKAP55 regulate plasma membrane localization of SKAP55 and thus LFA-1 activation

SKAP55 is the second adapter protein that – together with ADAP – forms the backbone of the LFA-1-activating complexes, as depicted in **Figure 1.6**.[62] SKAP55 contains a central PH domain (**Figure 1.8**).[69,121,127] This type of domain is best known for its ability to bind PIs thereby mediating PM localization of signaling molecules.[141–145] Until today, it remains controversial whether PH$_{SK55}$ plays a role for TCR-mediated LFA-activation.[95,98,122,124] In this study, we identified two critical residues – D120 and K152 – within the PH domain of SKAP55 that regulate membrane recruitment of the ADAP/SKAP55 module, T cell adhesion, interaction with APCs and LFA-1 affinity/avidity regulation.

PI binding of SKAP55 PH domain *in vitro* versus *in vivo*

Structural modeling of the isolated PH domain of SKAP55 (PH$_{SK55}$; based on the crystal structure published on the Research Collaboratory for Structural Bioinformatics Protein Data Bank (RCSB PDB): 1U5G) revealed that it contains a

classical PI-binding pocket that has been described for many PH domains.[161] It is built up by variable β1-β2-, β3-β4- and β6-β7-loops. SKAP55 contains all amino acids (except serine 118 in the β1 strand; see **Figure 2.2.10**) at homologous positions that have been predicted for PI binding by its homolog SKAP-HOM.[125,161] NMR spectroscopy data revealed that the isolated PH_{SK55} binds PIs with a preference for PIP_3 over PIP_2 (see **Table 3.1**; 8-fold higher affinity for PIP_3 compared to PIP_2).[161] However, in contrast to PH_{SK55}, the isolated PH domain of SKAP-HOM revealed a much stronger binding affinity for PIP_3 (see **Table 3.1**).[125] This difference might be partly due to the different approaches that have been used to determine the k_D values for PIP_3 or PIP_2 binding (fluorescence polarization assay for SKAP-HOM versus NMR titration for SKAP55). On the other hand, it is also possible that the PH domain of SKAP55 possess a non-optimal PI-binding pocket. SKAP-HOM contains an arginine (positive charge) rather than a serine (uncharged) found in SKAP55 at position 118 of the β1 strand (see **Figure 2.2.10**). This residue is in proximity of the PI-binding site and since PI binding is realized by positively charged amino acids this could make a difference in the ability to bind PIs.[161]

Table 3.1: Summary of PI-binding affinities of relevant PH domains.

	PI	affinity (k_D)	method	ref.
PH_{AKT}	$PI(3,4,5)P_3$	23 ± 6nM	Competitive displacement assay	[162]
	$PI(4,5)P_2$	ND		
$PH_{PLC\delta}$	$PI(3,4,5)P_3$	ND	Competitive displacement assay	[162]
	$PI(4,5)P_2$	190 ± 70nM		
PH_{SK-HOM}	$PI(3,4,5)P_3$	8 µM	Fluorescence polarization assay	[125]
	$PI(4,5)P_2$	ND		
PH_{SK55}	$I(1,3,4,5)P_4$	119 ± 59µM	NMR titration	[161]
	$PI(3,4,5)P_3$	74 ± 12µM		
	$I(1,4,5)P_3$	641 ± 276µM		
	$PI(4,5)P_2$	604 ± 202µM		

ND: to weak to be detectable by the used assay/method

However, compared to well-characterized PH domains like PH_{AKT} or $PH_{PLC\delta}$, PI-binding affinities of PH_{SK55} are weak (see **Table 3.1**). PH domains that bind PIs with affinities in the µM-rage are considered as weak/low affinity binders.[217] Due to the higher abundance of $PI(4,5)P_2$ in the PM, it is accepted that the binding affinities for this PI do not need to be as high as for PH domains that bind PI3K products. Nonetheless, for specific $PI(3,4,5)P_3$-binding PH domains (like Btk or general receptor of phosphoinositides 1 (Grp1)) k_D-values of <50nM are expected.

PH domains that bind PIP_2 (like PLCδ or Diacylglycerol kinase-δ (DAGK-δ)) are considered strong binders despite their 4-8 fold lower affinity compared to PIP_3-binding PH domain.[217] In any case, PI-binding affinities of PH_{SK55} is weaker than the affinities measured for the paradigmatic PIP_2 or PIP_3 binding PH domains.

Although NMR studies indicate that the PH_{SK55} preferentially binds to PIP_3 *in vitro* (**Table 3.1**), our *in vivo* studies in Jurkat T cells or human primary T cells showed that the constitutive PM targeting of the isolated GFP-tagged PH domain of SKAP55 was not affected upon inhibition of the PI3K (**Figure 2.2.2A, 2.2.3A**). Hence, my data propose that the isolated PH domain of SKAP55 translocates to the PM independent of PIP_3.

Lysine 152 enables actin-dependent PM recruitment and TCR-mediated LFA-1 activation

Using NMR spectroscopy, three positively charged amino acids have been identified – K116, R131 and K152 – within the lipid-binding pocket that enable PI binding.[161] For localization and functional studies in T cells, I generated non-binding mutants by mutating all three amino acids based on the literature (R131M)[124] or due to their localization within the PH domain. K152 is localized at the surface of PH_{SK55} and was mutated into glutamic acid (K152E). This changes the charge at position 152 from positive to negative. K116 is deeply buried within the encircling amino acids and therefore, we mutated K116 into methionine (K116M; uncharged), which has a longer side chain than glutamic acid (personal communication with Prof. C. Freund).

Mutation of K116 as well as R131 only had a moderate effect on the PM localization of the isolated PH_{SK55} in Jurkat T cells and human primary T cells (**Figure 2.2.5A,B**). To address the functional consequences for LFA-1 activation of these mutants, I generated suppression/re-expression vectors (**Figure 2.2.6A)**. Jurkat T cells re-expressing the K116M mutant of full-length SKAP55 (RE-$SK55_{K116M}$) showed a minor reduction in TCR-mediated adhesion to ICAM-1 and conjugate formation compared to wild-type SKAP55 re-expressing cells, while the R131M mutant (RE-$SK55_{R131M}$) showed an intermediate effect (**Figure 2.2.7**), which is in line with findings by other groups.[98,124] Here, the R131M mutant of SKAP55 was still able to induce a significant increased in adhesion of T cells to ICAM-1 compared to the control cells (Mock).[124] A study by Burbach et al. showed that introduction of the R131M mutation reduces the interaction of T cells with APCs, albeit not as strongly as in the knockout control.[98] Hence, in our

experimental system using suppression/re-expression vectors it appears that K116 and R131 are only of moderate importance for SKAP55 function.

In clear contrast to K116M and R131M, mutation of K152 completely attenuated PM targeting of the isolated PH domain (G- $PH_{SK55*K152E}$ as well as G- $PH_{SK55*K152M}$) **Figure 2.2.5A,B**). Positively charged amino acids within PH domains have been shown to interact with actin as described for the PH domain of Btk.[173] The immunoprecipitation experiments shown in **Figure 2.2.4A** revealed that PH_{SK55} – in contrast to $PH_{PLC\delta}$ – co-precipitated with actin, suggesting that these proteins can interact with each other. In contrast to the wild-type PH domain of SKAP55, introducing the K152E mutation within the isolated PH domain completely blocked the interaction with actin (**Figure 2.2.4C**). This study suggests that the isolated PH_{SK55} is targeted to the PM by a K152-mediated interaction with actin.
Subsequently co-sedimentation and co-precipitation assays using purified G- and F-Actin were performed to assess the question of whether the purified recombinant His-tagged PH domain of SKAP55 directly interacts with actin. The data indicated that this is not the case.[161] Moreover, neither the wild-type PH domain nor the K152E mutant co-sedimented with F-actin. Additionally, the wild-type PH domain of SKAP55 and the K152E mutant both did not sequester G-actin for F-actin polymerization. Finally, anti-His precipitates of the wild-type PH domain did not co-precitipitate either F- or G-actin.[161] Hence, our data indicate: (i) that the isolated PH_{SK55} interacts with actin, (ii) that this interaction is mediated by K152 and (iii) that the interaction between the two proteins is indirect. Therefore, the identification of protein(s) that link the isolated PH_{SK55} to actin requires further investigation. Possible candidates are the three members of the ezrin/radixin/moesin (ERM) family. In non-activated Jurkat T cells, these proteins are located at the PM and additionally are linked to F-actin.[16,218,219]

Re-expression of RE-$SK55_{K152E}$ in Jurkat T cells impaired TCR-induced adhesion to ICAM-1, interaction with APCs and activation of LFA-1 (affinity and avidity) to levels comparable to shSK transfectants (**Figure 2.2.7, 2.2.13C+D**). Surprisingly, biochemical analysis of PM fractions revealed that RE-$SK55_{K152E}$ – in contrast to the K152 mutant of the isolated GFP-tagged PH domain (**Figure 2.2.5**) – is localized at the membrane upon TCR stimulation. The same was observed for other components of LFA-1-activating complexes, such as ADAP, RapL and RIAM, which are constitutively associated with SKAP55 or inducibly linked to the ADAP/SKAP55 module (Rap1 and SLP-76; **Figure 2.2.8A**). These data indicate that there might be an alternative membrane-targeting pathway that guided the

K152E mutant of full-length SKAP55 to the PM. Further biochemically analysis revealed that despite being localized at the PM, mutation of K152E within SKAP55 completely disturbed the association of the ADAP/SKAP55 module with actin, Talin and LFA-1 (**Figure 2.2.8B,C**).
The difference in the localization of the isolated K152E-mutated PH_{SK55} (cytoplasm, **Figure 2.2.5A,B**) versus the K152E mutation within the full-length SKAP55 molecule (PM, **Figure 2.2.8A**) suggests that full-length SKAP55 can use two routes to translocate to the PM. One route involves the K152-mediated association with actin/Talin and the second route is mediated by the TCR-induced binding of ADAP to SLP-76.[65–67,76,77] Upon TCR-triggering, SLP-76 binds via Gads to tyrosine-phosphorylated LAT.[19,21,44] In contrast to TCR-induced signaling, chemokine receptor triggering mediates the PM recruitment of the ADAP/SKAP55 module and LFA-1 activation in the absence of LAT phosphorylation and without an inducible association of ADAP with SLP-76.[14] Thus, it appears that the ADAP/SKAP55 module does not depend on SLP-76/Gads/LAT for PM recruitment to activate LFA-1 and that localization at the PM is not enough to activate LFA-1.

The results discussed here indicate that K152 is a key residue within PH_{SK55}, which regulates actin-mediated PM localization of the ADAP/SKAP55 module. Additionally, in the context of full-length SKAP55 K152 is a positive regulator of LFA-1 activity. K152 mediates the interaction of LFA-1 with Talin and the actin cytoskeleton.

<u>Aspartic acid 120 controls plasma membrane localization of SKAP55 and LFA-1 activation</u>
The fact that RE-$SK55_{D120K}$-induced LFA-1 activation can take place independent of LAT/Gads/SLP-76-mediated PM recruitment prompts the question of how cytoplasmic localization of SKAP55 in non-stimulated T cells is warranted to prevent integrin activation. For the SKAP55 homolog SKAP-HOM, Swanson and co-workers proposed a model in which an intramolecular switch mechanism regulates the cellular localization of SKAP-HOM (see **Figure 1.9**).[125] Here, the protein exists in two conformations: an open/active and a closed/auto-inhibited conformation. This intramolecular switch is probably regulated by PIP_3 binding by PH_{SK-HOM}. While at low PIP_3 levels SKAP-HOM remains in its closed conformation and therefore in the cytoplasm, an increase in local PIP_3 levels induces/stabilizes the open conformation and allows targeting to actin-rich membrane ruffles.[125] Swanson et al. identified aspartic acid 129 (D129) within the PH domain as the

mediator of the auto-inhibitory interaction between the DM and PH domain.[125] Indeed, mutation of D129 within the PH Domain of full-length SKAP-HOM results in constitutive localization of this mutated molecule in macrophages at actin membrane ruffles.[125,137]

Based on these findings, we compared the sequences of PH_{SK55} and $PH_{SK\text{-}HOM}$ and identified aspartic acid 120 (D120) within SKAP55 as the potential equivalent of D129 in SKAP-HOM (**Figure 2.2.10**). Microscopic studies with G-$SK55_{D120K}$ revealed a constitutive PM localization of this SKAP55 mutant (**Figure 2.2.11A**). Moreover, biochemical analysis of PM fractions from Jurkat T cells re-expressing the D120K mutant confirmed the constitutive localization of this molecule at the PM (as well as all its constitutive interaction partners ADAP, RIAM and RapL) (**Figure 2.2.14A**). In line with these findings, Jurkat T cells re-expressing RE-$SK55_{D120K}$ adhered to ICAM-1, interacted with APCs and positively modulated affinity/avidity regulation of LFA-1 in the absence of TCR stimulation (**Figure 2.2.13**). These findings are in line with previous reports showing that forced PM targeting of SKAP55 (induced by fusion to myr-tag or a LAT-tag) bypasses TCR stimulation.[95,124] My results indicate that D120 is a negative regulator of SKAP55, probably by mediating an auto-inhibitory conformation ensuring the cytoplasmic localization of SKAP55 in non-stimulated T cells.

Working with the D120K mutant of SKAP55, I made three important observations. First, activation of LFA-1 in non-stimulated T cells induced by re-expression of the D120K mutant takes place independent of Rap1 (**Figure 2.2.15A**). No localization of Rap1 at the PM or association with the ADAP/SKAP55 module was detectable in non-stimulated cells (**Figure 2.2.14**). The general opinion is that Rap1 is inactive in non-stimulated T cells and that it only becomes activated and recruited to the PM as a component of the LFA-1-activating complexes upon stimulation. At the PM, Rap1 triggers the adhesive function of integrins.[129,132,179,180] Surprisingly, our knockdown studies of Rap1 revealed that this small GTPase was dispensable for basal adhesion triggered by the D120K mutant of SKAP55 (**Figure 2.2.15A**). In contrast, TCR-induced adhesion of either wild-type or D120K-mutated SKAP55 re-expressing T cells was dependent on the presence of Rap1. These data are in contrast to previous published data by Su and colleagues and De Bruyn et al. showing that Rap1 ko or Rap1 inhibition impairs basal as well as TCR-mediated adhesion.[55,182]

Second, in contrast to Rap1, knockdown of Talin impairs basal and stimulation-induced adhesion in cells re-expressing the D120K mutant (**Figure 2.2.15C**). There are two independent LFA-1-activating complexes (see **Figure 1.6**) existing in

T cells that contain either the Rap1-binding protein RapL or RIAM.[95] It has been shown that RIAM inducibly interacts with Talin and that this interaction triggers PM localization of Talin (mediated by Rap1)[183] and the release of Talin from its auto-inhibitory conformation, which allows binding of Talin to the cytoplasmatic domain of the β-chain of integrins.[133] On the other hand, RapL has been shown to interact with the cytoplasmatic domain of the α-chain of LFA-1, although to my knowledge it is unknown whether knockout of RapL impaires affinity modulation of LFA-1.

Third, we found that the effects of the gain-of-function mutation D120K were completely reversed when K152 was additionally mutated. K152E mutation abrogated constitutive PM localization (**Figure 2.2.11A, 2.2.14A**) as well as LFA-1 activation in non-stimulated T cells induced by the D120K mutant (**Figure 2.2.13C,D**). Like the RE-SK55$_{K152E}$, the D/K double mutant was no longer able to interact with Talin, LFA-1 and actin, (**Figure 2.2.14B,C**). These data indicate that the gain-of-function effect of the D120K mutant depends on the integrity of the K152 residue (see **Figure 3.2.1**).

Based on the findings presented in this study, I propose the model shown in **Figure 3.2.1**. In non-stimulated T cells, partially preformed LFA-1-activating complexes remain in the cytoplasm due to a D120-mediated auto-inhibitory interaction of the DM with the PH domain within SKAP55. Stimulation of the TCR induces a conformational change that releases the PH domain from the DM domain by a hitherto unknown trigger. The unshielded K152 now enables the LFA-1-activating complexes to translocate to the PM. In TCR-stimulated T cells, PM recruitment is supported (this association is not mandatory) by the interaction with the LAT signalosome (mediated by ADAP/SLP-76). At the PM, K152 within SKAP55 enables the association of Talin and the actin cytoskeleton with LFA-1. Only then does LFA-1 change into its active conformation to mediate adhesion and interaction with APC.

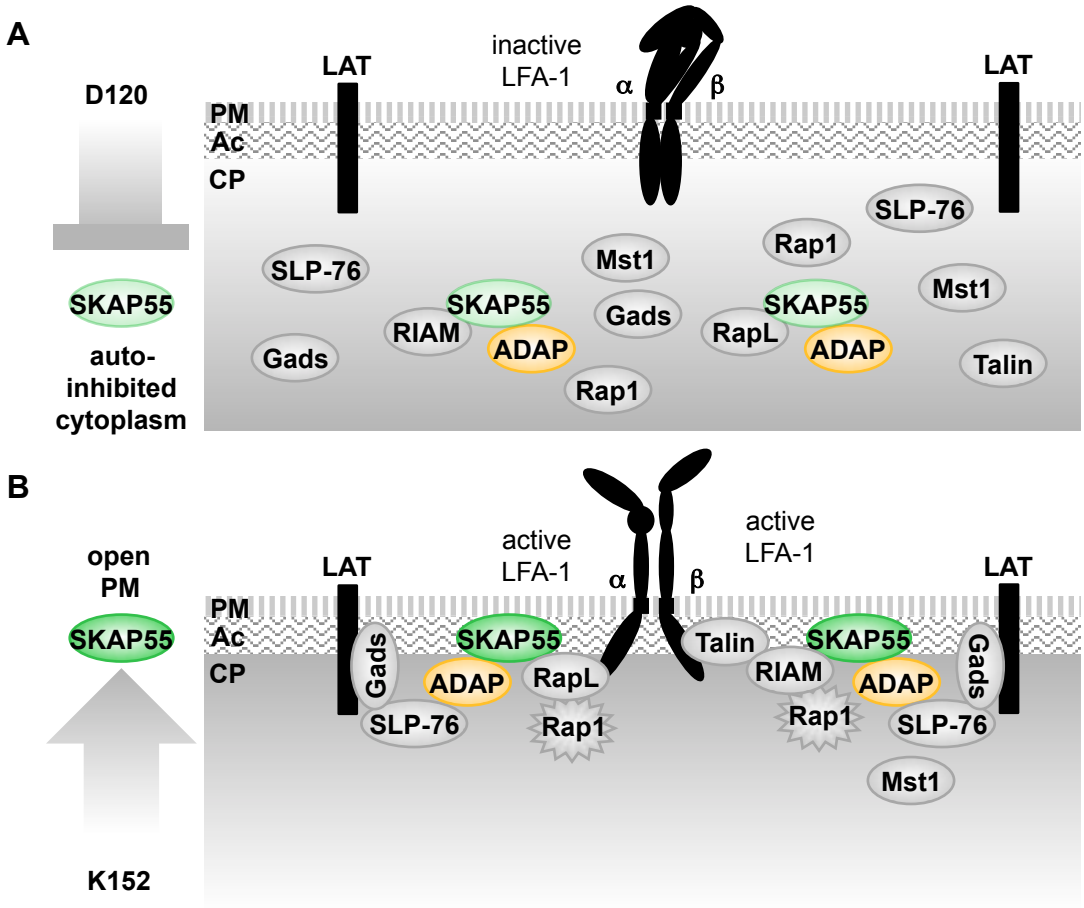

Figure 3.2.1: Model of how SKAP55 auto-inhibition regulates plasma membrane recruitment and LFA-1 activation. (A) In non-stimulated T cells both LFA-1-activating complexes are already partially preformed but remain in the cytoplasm due to the auto-inhibited conformation of SKAP55 mediated by D120. **(B)** Upon TCR stimulation, the interaction of DM and PH domain is released by an unknown mechanism and both LFA-1-avtivating complexes can translocate to the PM by two independent routes. They can associate via ADAP with SLP-76/Gads/LAT or they can bind actin via K152 within the PH domain of SKAP55. At the PM, both complexes can bind to LFA-1 and induce its activation. Ac: actin cytoskeleton, CP: cytoplasm

Further experiments are necessary to prove the auto-inhibitory interaction within SKAP55 and identify the trigger that releases the PH domain from the DM domain to promote recruitment to the PM leading to LFA-1 activation.

To analyze the auto-inhibitory interaction within SKAP55, one could use Förster resonance energy transfer (FRET). This is a method for detecting structural changes within a protein, as previously described for the src kinase Lck.[220,221] I suggest generating a unimolecular FRET sensor consisting of the DM-PH of SKAP55 with cyan fluorescent protein (CFP) mutant (mTurquoise2) at the N-terminus and a yellow fluorescent protein (YFP) mutant (mVenus) at the C-terminus (see **Figure 3.2.2**). The wild-type (DM_PH$_{SK55}$) and the mutated (DM_PH$_{SK55.D120K}$ and DM_PH$_{SK55.D/K}$) constructs could be used to investigate their conformation under non-stimulated and stimulated conditions. I would expect the DM_PH$_{SK55}$ to be closed under non-stimulated conditions (**Figure 3.2.2A**), while the D120K-mutated construct is open and thus shows weaker FRET

signals (**Figure 3.2.2B**) than the wild-type. The double mutant (DM_PH$_{SK55*D/K}$) should be comparable to DM_PH$_{SK55*D120K}$ because the K152E-mutation is supposed to exchange the charge at position 152 to prevent actin binding but not induce structural changes. Under stimulatory conditions, I speculate that only DM_PH$_{SK55}$ changes its conformation from closed to open, showing FRET signals like DM_PH$_{SK55*D120K}$.

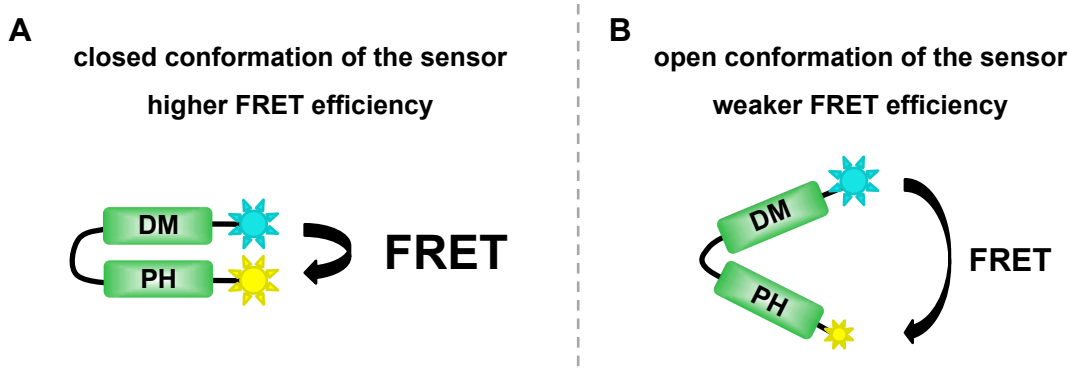

Figure 3.2.2: Model of a unimolecular FRET sensor to visualize the auto-inhibitory regulation of SKAP55. Shown is a FRET construct that contains the first half of SKAP55 including the DM domain, a linker and the PH domain (green). mTurquoise2 (a CFP mutant) is fused to the N-terminus and mVenus (a YFP mutant) is fused to the C-terminus. **(A)** In the closed conformation of the sensor, the two fluorophors are in close proximity of each other. This allows a strong energy transfer from the donor (mTurquoise2) to the acceptor (mVenus) and therefore a high FRET efficiency. **(B)** In the open conformation of the sensor, the distance between the two fluorophors is increased which impaires the energy transfer from the donor to the acceptor resulting in a weaker FRET efficiency.

In addition, the factors releasing the DM_PH-mediated auto-inhibition of SKAP55 following TCR stimulation remain elusive. Dimerization domains are known to be involved in intra- or intermolecular protein-protein interactions, which can be used for the auto-inhibition of functional domains.[222] It has been shown that SKAP55 forms homodimers (and heterodimers with SKAP-HOM)[122,223] and that this dimerization is mediated by DM$_{SK55}$.[122,131] Therefore, I speculate that TCR-induced dimerization (or de-dimerization) of SKAP55 could induce conformational changes within the DM domain that could release the PH domain from auto-inhibition and thus promote PM targeting of SKAP55. Alternative possibilities would be that local production of PIs or the binding of the activated GTPase Rap1 to SKAP55-bound RapL or RIAM upon T cell stimulation shifts the closed towards the open actin/Talin-binding conformation of SKAP55.

In summary, we identified two residues – D120 and K152 – within the PH domain of SKAP55 that regulate the function of this adapter protein: D120 keeps LFA-1-activating complexes in the cytoplasm to prohibit LFA-1 activation in non-stimulated T cells, while K152 enables PM recruitment and LFA-1 activation upon T cell stimulation.

3.2. OUTLOOK

Within recent years, the importance of ADAP and SKAP55 for proper immune function *in vivo* has become increasingly clear. ADAP and/or SKAP55-deficient mice seem to be less susceptible for cancer, EAE and transplant rejection.[108–110,112] By contrast, ADAP-deficiency makes mice much more prone to Influenza infection and autoimmune diabetes.[113] Therefore, it holds strong importance to understand how the ADAP/SKAP55 module regulates immune cell function, whereby we can use them as a therapeutical target to modulate T cell function in the immune system.

To investigate the functional role and consequences of ADAP Y571 phosphorylation and the regulatory role of D120/K152 of SKAP55 for T cell biology *in vivo*, BM chimeras will be used. For example, bone marrow cells of SKAP55- or ADAP-deficient mice could be transduced by retroviruses encoding different mutants of SKAP55 (e.g. D120K, K152E and D120K/K152E) or ADAP (e.g. Y571F). Lethally irradiated mice would be reconstituted with successfully transduced BM cells to investigate the impact of the respective SKAP55 or ADAP mutant on e.g. T cell development, adhesion, migration, etc. under physiological and pathophysiological conditions.

The integrin LFA-1 fulfills a crucial role for T cell function. Loss of function or dysregulation of LFA-1 activity have fundamental consequences on immune function.[224–228] By blocking the interaction of LFA-1 with its ligand, LFA-1 has become a valid therapeutic target in many chronic inflammatory diseases.[63,139] Unfortunately, LFA-1 antagonists have not been clinically successful due to the development of a general immunosuppression, which causes immense side effects. Therefore, proteins that control LFA-1 function in specific immune cell types might holds special interest.[63] SKAP55 is expressed exclusively in T cells[121,126] and thus it might be a useful target for therapy of T cell-dominated diseases.

As mentioned above, expression of $SKAP55_{D120K}$ by T cells induced a constitutive activation of the integrin LFA-1, resulting in adhesion and interaction with APCs of non-stimulated T cells (**Figure 2.2.13**). Constitutive active LFA-1 mutants have been shown to cause major problem for T cells. *Ex vivo* studies of T cells expressing mutant LFA-1 revealed constitutive adhesion and impaired de-adhesion resulting in defective migration on ICAM-1 and transmigration through endothelial cell layers.[227] T cell activation by superantigen-loaded APCs, T cell proliferation in response to allogeneic stimuli, cytotoxic T cell activity and T cell-mediated humoral immune responses (defective TH1/TH2-mediated B-cell activation) were also impaired.[227,228] As a consequence, mice expressing a

constitutive active mutant of LFA-1 displayed prolonged heart allograft survival due to reduced numbers of alloantigen-specific T cells within the allograft.[228] Global loss of LFA-1 leads to impaired cytolytic activity of $CD8^+$ T cells, increased susceptibility to metastasis and increased transplant survival.[224,225] With these facts in mind, it would be quite interesting to investigate the consequences of T cells expressing a potential constitutive open/active (D120K) or constitutive inactive (K152E) SKAP55 mutant in the living animal.

Chemokine receptor-induced directed migration is essential for homing of T cells to and within sites of antigen presentation (secondary lymphoid organs, tumors and sites of inflammation),[7,8] which is essential for the defense against pathogens and tumors.[229–231] Moving T cells exhibit an amoeboid morphology (**Figure 1.4B**) that strongly depends on the actin cytoskeleton.[16,25] In T cells, expression of $ADAP_{Y571F}$ led to reduced amounts of F-actin (**Figure 2.1.5C**). Therefore, it would hold strong interest to investigate whether blockage of tyrosine 571 phosphorylation has consequences for T cell homing and clearance of tumors or pathogens.

❊ ❊ ❊

4. MATERIALS AND METHODS

4.1. MATERIALS

4.1.1. Equipment and software

Equipment	Source
Autoclave Laboklave	SHP Steriltechnik AG
Autoclave Varioklave	Thermo Fisher Scientific
AutoMACS Seperator	Miltenyi Biotec
Centrifuge 5415D	Eppendorf
Centrifuge 5415R	Eppendorf
Culture hood Antares	BIOHIT
Culture hood Safe 2020	Thermo Fisher Scientific
Developing machine Cawomat 2000IR	CAWO
Deware bottle	KGW ISOTHERM
Dishwasher Compact-Desinfector G7783 CD	Miele
Electrophoresis system Mini-PROTEAN® 3 Cell	BIO-RAD
Electrophoresis system Mini-PROTEAN® Tetra Cell	BIO-RAD
ELISA reader MR5000	DYNATECH
ELISA reader Tristar LB941	Berthold Technologies
FACS Calibur flow cytometer	BD Bioscience
Flatbed blotting system Multiphor II	Amersham Bioscience
Freezer comfort (-20 grad celsius (°C))	Liebherr
Freezer Heto Mini Freeze (-70°C)	Thermo Fisher Scientific
Gel documentation station (camera: E.A.S.Y. B-455-F)	Herolab
Gene Pulser II	BIO-RAD
Glass marbles (5mm diameter)	VWR
Heating cabinet Heraeus B15	DJB Labcare
Ice machine AF80	Scotsman
Incubator (cell culture)	BINDER
Incubator (with rotator, bacteria)	EB Edmund Bühler
Incubator (with rotator, bacteria)	GFL
Incubator (bacteria)	Heraeus
Incubator C200 (cell cultur)	Labotect
Intelli Mixer	ELMI laboratory
Kodak Image Station 2000R	Kodak

Leica TCS SP2 confocal scanner	Leica
Leica DM IL inverted fluorescent microscope	Leica
Leica DM IRE2 inverted fluorescent microscope	Leica
Leica HBO lamp	Leica
Magnetic stirrer MR3001	Heidolph
Liquid nitrogen reservoir Apollo	Messer Griesheim GmbH
Liquid nitrogen tank Chronos	Messer Griesheim GmbH
Microscope Axiovert 25	Zeiss
Microwave Severin 700	Severin
Multifuge 1 S-R Centrifuge	Heraeus
Multipette® plus	Eppendorf
Nova Blot	Amersham Bioscience
PCR Gradient cycler	BIO-RAD
potentia Hydrogenii (pH)-Meter	inoLab
Pipettes (0.1-2.5µl, 0.5-10µl, 2-20µl, 10-100µl, 20-200µl, 100-1000µl)	Eppendorf
Pipette boy accu-jet® pro	Brand
Power PAC Basic, 200, 3000	BIO-RAD
Pulser Nucleofector™ II	Amaxa biosystems
Pump AZ02/AZ04	HLC Bio Tech
Quartz cuvette	VWR
Refrigerator AEG Santo	AEG
Refrigerator gastroline	Liebherr
Rocking platform lab shaker Duomax 1030	Heidolph
Scale	Sartarius
Scale SCOUT	OKAUS
Thermomixer compact	Eppendorf
UV/Vis Spectrophotometer Ultraspec 3000	Pharmacia Biotech
Vortexer REAXtop	Heidolph
Water bath W6	Medingen
Milli-Q® Integral Water Purification System	MERCK MILLIPORE
X-Omatic Cassett	Kodak

Software	Source
Adobe Photoshop CS5	Adobe Systems
BioLinx©	BioLinx labsystems
CellQuest™ Pro	BD Bioscience
Chromas lite 2.01	Technelysium

DisplayOverlay04	generated and provided by Lars Philipsen (Otto-von-Guericke University Magdeburg)
Easy Win32	HeroLab
FlowJo 7.6.5	Tree Star
ID image software	Kodak
Microsoft Office 2011	Microsoft
MikroWin	Siemens

4.1.2. Consumables

	Source
6-well cell culture plates	TPP
12-spot slide, precoated with poly-L-Lysine	Marienfeld KG
15ml and 50ml tubes	Greiner Bio-one
96-well cell culture plates	BD Bioscience
96-well cell culture plates (U bottom)	Costar
Blotting paper sheets	Munktell
Butterfly needles (19G x 0.75'' x 12'')	BD Bioscience
Cell scraper	TPP
Combitips (5ml, 10ml)	Eppendorf
Coverslip 24x50mm, for immunofluorescence	Carl Roth
Coverslips, for Neubauer counting chamber	Carl Roth
Culture Flasks Corning® (25cm^2, 75cm^2, 175cm^2)	Corning Incorporated
Cryo Pure Tube 1.6ml	Sarstedt
Eppendorf tupes (1.5ml, 2ml)	Eppendorf
FACS tubes	BD Bioscience
Gaze balls	Fuhrmann
Gloves (latex)	Ansell
Gloves (nitrile)	Kimberly-Clark
Microlace 27G	BD Bioscience
Neubauer counting chamber	Marienfeld KG
Nitrocellulose membrane Amersham Hydrobond™-C Extra	GE Healthcare
Parafilm	Bemis
PCR soft tubes	Biozym
Pipette tips (1ml)	Sorenson
Pipette tips (20µl, 100µl, 200µl)	Eppendorf
Pipette tips (2.5µl, 10µl)	Carl Roth

Plastic cuvettes	Sarstedt
Plastic pipettes (5ml, 10ml, 25ml, 50ml)	Costar
Petri Culture Dish (100mm)	BD Bioscience
Scalpel	Braun
Syringes (2ml, 20ml)	BD Bioscience
Syringe filters (0.22µm)	TPP
Transfection cuvettes	BIO-RAD
Transfection cuvettes	Lonza
Transwell® (6.5mm diameter insert, 5.0µm pore size, tissue culture treated membrane, sterile)	Costar
Tissue Culture Dish (100mm)	BD Bioscience
Tubes BD Falcon™ (14ml)	BD Bioscience
X-ray film Amersham Hyperfilm™ MP	GE Healthcare

4.1.3. Reagents

	Source
2-mercaptoethanol	Sigma-Aldrich
2-propanol	Carl Roth
250bp DNA ladder	Carl Roth
30% Acrylamide/BIS, 29:1	Serva
4-(2-hydroxyethyl)-1-piperazineethanesulfonic acid (HEPES)	Carl Roth
Acetic acid (96% v/v)	Carl Roth
Agar-Agar	Carl Roth
Agarose (Peqgold universal agarose)	PeqLab
Ammoniumpersulfat (APS)	Carl Roth
Ampicillin	Carl Roth
BD FACS Flow™ Sheath Fluid	BD Bioscience
BD FACS™ Clean Solution	BD Bioscience
BD FACS™ Rinse Solution	BD Bioscience
Biocoll seperating solution	Biochrom AG
Bovine serum albumin (BSA) fraction V	PAA
Bromophenol blue	Carl Roth
Calciumchloride ($CaCl_2$)	Carl Roth
Calf intestine alkaline phosphatase	NEB
CellTrace™ Far Red DDAO-SE	Thermo Fischer Scientific
CiproBay 200	Bayer Schering Pharma

C-X-C motif chemokine 12 (CXCL12; human, recombinant) carrier-free	BioLegend
Deoxyribonucleoside triphosphate (dNTP) Set	Fermentas
Dimethyl sulfoxide (DMSO)	Carl Roth
Ethanol (99% v/v)	Carl Roth
Ethidium bromide (10mg/ml)	Carl Roth
Ethylenediaminetetraacetic acid (EDTA)	Carl Roth
Fetal Calf Serum (FCS)	Pan Biothech GmbH
Glucose	Sigma-Aldrich
Glycerol	Carl Roth
Glycine	Carl Roth
Hank's balanced salt solution (HBSS)	Biochrom AG
Heparin (5000 units (U)/ml)	Biochrom AG
Horse serum	Biochrom AG
Hydrochloric acid (HCl; 37% v/v)	Carl Roth
ICAM-1 (CD54; human, recombinant) Fc chimera	R&D Systems
Immersion liquid, Type F	Leica
Isopropyl-β-D-thiogalactopyranoside (IPTG; dioxane-free)	Carl Roth
Lauryl maltoside/n-dodecyl-β-D-maltoside (LM)	Calbiochem
Liquid nitrogen	AIR LIQUID Medical GmbH
LY294002	Calbiochem
Manganese chloride ($MnCl_2$)	Sigma-Aldrich
Methanol (99.9%)	Carl Roth
Morpholino-propanesulfonic acid (Na-MOPS, sodium salt)	Carl Roth
Mowiol 4-88	Calbiochem
Nonidet P40 (NP-40; Ipegal CA-630)	Sigma-Aldrich
Pageruler prestained protein ladder	Fermentas
PBS Dulbecco (phosphate-buffered saline, without (w/o) Ca^{2+}, Mg^{2+})	Biochrom AG
PBS Dulbecco (phosphate-buffered saline, w/o Ca^{2+}, Mg^{2+}); powder	Biochrom AG
Paraformaldehyde (PFA)	Merck
Pefabloc®Sc (PEFA-Block)	Carl Roth
Penicillin/Streptomycin (10000U/10000µg/ml)	Biochrom AG
Phalloidin-Alexa Fluor®633	Invitrogen

Phallodin-TRITC (tetramethylrhodamine isothiocyanate)	Sigma-Aldrich
Phenol-Chloroform-Isoamylalcohol (25:24:1)	Carl Roth
Phenylmethylsulfonyl fluoride (PMSF)	Carl Roth
Phorbol-12-myristate-13-acetate (PMA)	Sigma-Aldrich
Ponceau S	Sigma-Aldrich
Potassium chloride (KCl)	Carl Roth
Powdered Milk (Blotting grade)	Carl Roth
Protein A-Agarose immunoprecipitation reagent	Santa Cruz
Protein G PLUS-Agarose immunoprecipitation reagent (beads)	Santa Cruz
RPMI1640 medium	Biochrom
Sodium azide (NaN_3)	Carl Roth
Sodium chloride (NaCl)	Carl Roth
Sodium dodecyl sulfate (SDS)	Carl Roth
Sodium fluoride (NaF)	Sigma-Aldrich
Sodium hydroxide (NaOH)	Carl Roth
Sodium hypochlorite solution (NaClO in H_2O, 12% Cl)	Carl Roth
Sodium orthovanadate (Na_4VO_3)	Sigma-Aldrich
Staphylococcal enterotoxin E (SEE)	Toxin Technology, Inc.
Streptavidin	Dianova
Tertamethylethylenediamine (TEMED)	Carl Roth
Tris (hydroxymethyl)-aminomethan (Tris)	Carl Roth
Triton X-100	Sigma-Aldrich
Trypane Blue Solution (0.4%)	Sigma-Aldrich
Trypsine/EDTA (0.05% v/v, 0.02% v/v)	Biochrom AG
Tryptone/Peptone	Carl Roth
Tween 20	Carl Roth
Wortmannin	Calbiochem
Xylene Cyanol	Carl Roth
Yeast extract	Carl Roth

4.1.4. Kits

	Source
Agfa fixation and developing solution	Röntgen Bender GmbH
Amaxa™ human T cell Ncleofector™ Kit	Lonza
CloneJet™ PCR Cloning Kit	Thermo Fisher Scientific

Myco Alert® Assay Control Set	Lonza
Myco Alert® Mycoplasma Detection Kit	Lonza
Nucleo Bond® Xtra Maxi Plus EF	MACHEREY-NAGEL
Nucleo Spin® Extract II	MACHEREY-NAGEL
Pan T cell isolation kit, human	Miltenyi Biotec
Roti®-Lumin 1+2	Carl Roth
Roti®-Nanoquant	Carl Roth
Quik Change® XL Site-directed Mutagenesis Kit	Stratagene

4.1.5. Antibodies

	Species/Clone	Dilution	Source/Reference
Primary antibodies (Flow cytometry (FC), Immunoprecipitation (IP), Microscopy (M), Stimulation (S), Western Blot (WB))			
anti-β-Actin	mouse monoclonal antibody (Clone: AC-15), unconjugated	1:5000 (WB)	Sigma-Aldrich (#A1978)
anti-ADAP	mouse monoclonal antibody, (Clone: 5/FYB), unconjugated	1:1000 (WB)	BD Bioscience (#610944)
anti-ADAP	sheep antiserum, uncojugated	1:1000 (WB)	kindly provided by G. Koretzky[65]
anti-CD3 (TCR)	mouse monoclonal antibody (Clone: OKT3), unconjugated	5µg/ml or 10µg/ml (S)	eBioscience (#16-0037-81)
anti-CD3 (TCR)	mouse monoclonal antibody (Clone: OKT3), Biotin-conjugated	5µg/ml (S)	eBioscience (#13-0037-82)
anti-CD11a (LFA-1)	mouse monoclonal antibody (Clone: 38), unconjugated	10µg/ml (IP)	Calbiochem (#217640)
anti-CD11a (LFA-1)	mouse monoclonal antibody (Clone: 38), DyLight® 650-conjugated	1:20 (M)	Leinco Technologies, Inc. (#C1714)
anti-CD18 (LFA-1)	mouse monoclonal antibody (Clone: mAb24), unconjugated	10µg/ml (FC)	provided by N. Hogg[232]
anti-CD18 (LFA-1)	mouse monoclonal antibody (Clone: MEM-48), unconjugated	1:100 (WB)	provided by V. Horejsi[233]
anti-CD28	mouse monoclonal antibody (Clone: CD28.2), Biotin-conjugated	5µg/ml (S)	eBioscience (#13-0289-82)

anti-CD69	mouse monoclonal antibody (Clone: FN50), allophycocyanin (APC)-conjugated	1:100 (FC)	BioLegend (#310910)
anti-CD184 (CXCR4)	mouse monoclonal antibody, (Clone: 12G5), unconjugated	1:100 (FC)	BD Bioscience (#555972)
anti-FLAG	mouse monoclonal antibody (Clone: M2), unconjugated	1:5000 (WB), 10µg/ml (IP)	Sigma-Aldrich (#F3165)
anti-GFP	mouse monoclonal antibody (Clone: B-2), unconjugated	1:1000 (WB)	Santa Cruz (#sc-9996)
anti-GFP	rabbit polyclonal antibody; unconjugated	1:2000 (WB), 10µg/ml (IP)	Santa Cruz (#sc-8334)
anti-GFP	rabbit antibody (FL), agarose-conjugated 500 µg/ml, 25% agarose	30µl (pro IP)	Santa Cruz (#sc9996 AC)
anti-pAKT (S473)	rabbit monoclonal antibody (Clone: D9E), unconjugated	1:1000 (WB)	Cell Signaling (#4060)
anti-pan-actin	mouse monoclonal antibody (Clone: AC-40), unconjugated	1:1000 (WB)	antikoerper-online (#ABIN1105234)
anti-pErk1/2 (T202/Y204)	rabbit monoclonal antibody (Clone: 20G11), unconjugated	1:1000 (WB)	Cell Signaling (#4376)
anti-pZAP70 (Tyr319)	mouse monoclonal antibody (Clone: 17A/PZAP70), unconjugated	1:1000 (WB)	BD Transduction Laboratories (#612575)
anti-RIAM	rat monoclonal antibody (Clone: 15B7E8), unconjugated	1:5 (WB)	generated in our lab[14]
anti-Rap1	mouse monoclonal antibody (Clone: 3), unconjugated	1:1000 (WB)	BD Bioscience (#610195)
anti-RapL	rat monoclonal antibody (Clone: 104B4G12), unconjugated	1:5 (WB)	generated in our lab[62]
anti-SKAP55	rat monoclonal antibody (Clone: 13B6F2), unconjuagted	1:5 (WB)	generated in our lab[95]
anti-SLP-76	mouse antibody (Clone: F-7), unconjugated	1:1000 (WB)	Santa Cruz (#sc-13151)
anti-Talin	mouse monoclonal antibody (Clone: 8D4), unconjugated	1:1000 (WB)	Sigma-Aldrich (#T3287)

anti-ZAP70	mouse monoclonal antibody (Clone: 29/ZAP70), unconjugated	1:5000 (WB), 10µg/ml (IP)	BD Transduction Laboratories (#610240)
anti-ZAP70	rabbit monoclonal antibody (Clone: 99F2), unconjugated	1:1000 (WB)	Cell Signaling (#2705)
Secondary antibodies (Flow cytometry (FC), Stimulation (S), Western Blot (WB))			
anti-mouse IgG1	goat polyclonal antibody, APC-conjugated	1:100 (FC)	Dianova (#115-135-205)
anti-mouse IgG	donkey antibody, Alexa Fluor®647-conjugated	1:100 (FC)	Dianova (#715-605-151)
anti-mouse IgG	goat antibody, HRP-conjugated	1:10000 (WB)	Dianova (#115-035-062)
anti-mouse IgG	goat antibody, unconjugated	5µg/ml (S)	Dianova (#115-005-062)
anti-rabbit IgG	goat antibody, HRP-conjugated	1:10000 (WB)	Dianova (#111-035-144)
anti-rat IgG	goat antibody, HRP-conjugated	1:10000 (WB)	Dianova (#112-035-167)

4.1.6. Enzymes and their appropriate buffers

	Source
Ligation	
T4 DNA ligase	New England Biolabs (NEB)
10 x T4 DNA ligase buffer	NEB
PCR	
Pfu DNA Polymerase	Fermentas
10 x *Pfu* DNA Polymerase buffer	Fermentas
Restriction	
BglII (10U/µl)	NEB
HindIII (20U/µl)	NEB
MluI (10U/µl)	NEB
NotI (10U/µl)	NEB
Diluent Buffer-A	NEB
Diluent Buffer-B	NEB
Diluent Buffer-C	NEB
SuRE/Cut Buffer B	Roche
SuRE/Cut Buffer H	Roche

4.1.7. Oligonucleotides

Oligonucleotides purchased from biomers.net

***in vitro* Mutagenesis**

ADAP sh-res_for
5′-CCCATCAACTTGCCCAAAGAgGAcTCaAAgCCcACcTTTCCCTGGCCTCCT-3′
ADAP sh-res_rev
5′-CAGGAGGCCAGGGAAAgGTgGGcTTtGAgTCcTCTTTGGGCAAGTTGATGGG-3′
Y571F ADAP_for
5'-GCTGTAGAGATTGACTtTGATTCTTTGAAACTG-3′
Y571 ADAP_rev
5'-CAGTTTCAAAGAATCAaAGTCAATCTCTACAGC-3'
SKAP55 sh-res_for
5′-CGAAGAGATTCCAAGAAgGAgTCgTGtTTcGAgCTGAACTCCCAGGATAGG-3′
SKAP55 sh-res_rev
5′-CCTATCCTGGGAGGTCAGcTCgAAaCAcGAcTCcTTCTTGGAATCTCTTCG-3′
K116M SKAP55-for
5′-ATCAAGCAAGGATACTTGGAGAtGAAAAGCAAAGATCATAGTTTC-3′
K116M SKAP55-rev
5′-GAAACTATGATCTTTGCTTTTCaTCTCCAAGTATCCTTGCTTGAT-3′
D120K SKAP55_for
5′-TACTTGGAGAAGAAAAGCAAAaAaCATAGTTTCTTTGGATCGGAGTGG-3′
D120K SKAP55-rev
5′-CCACTCCGATCCAAAGAAACTATGtTtTTTGCTTTTCTTCTCCAAGTA-3′
R131M SKAP55_for
5′-TGGATCGGAGTGGCAGAAGatgTGGTGTGTTGTCAGCAGAGG-3′
R131M SKAP55_rev
5′-CCTCTGCTGACAACACACCAcatCTTCTGCCACTCCGATCCA-3′
K152E SKAP55_for
5′-GAGAAGAGCAAGCAGCCCgAgGGGACCTTCCTCATTAAG-3′
K152E SKAP55_rev
5′-CTTAATGAGGAAGGTCCCcTcGGGCTGCTTGCTCTTCTC-3′
K152M SKAP55-for
5′-GAGAAGAGCAAGCAGCCCAtgGGGACCTTCCTCATTAAG-3′
K152M SKAP55-rev
5′-CTTAATGAGGAAGGTCCCcaTGGGCTGCTTGCTCTTCTC-3′

Polymerase chain reaction (PCR)

Mlu ADAP for
5'-CCCACGCGTATGGCGAAATATACCACGGGG-3′

Not ADAP rev
5'-CCCGCGGCCGCCTAGTCATTGTCATAGAT-3'
Mlu SKAP55 for
5'-CCCACGCGTATGCAGGCCGCCGCCCTC-3'
Not SKAP55 rev
5'-CCCGCGGCCGCTCATCTTTCTTCCACTTC-3'

shRNA (small hairpin RNA)

shADAP_for
5'- GATCCCCGAAGATTCCAAACCTACATTTCAAGAGAATGTAGGTTTGGAATC TTCTTTTTGGAAA-3'
shADAP_rev
5'-AGCTTTTCCAAAAAGAAGATTCCAAACCTACATTCTCTTGAAATGTAGGTTTGG AATCTTCGGG-3'
shSKAP55_for
5'-GATCCCCGAAAGAATCCTGCTTTGAATTCAAGAGATTCAAAGCAGGATTCTTTC TTTTTGGAAA-3'
shSKAP55_rev
5'-AGCTTTTCCAAAAAGAAAGAATCCTGCTTTGAATCTCTTGAATTCAAAGCAGGA TTCTTTCGG G-3'

Lowercase letters indicate the changed nucleotide (site-directed mutagenesis, see **4.2.21.2**) and underlined are the introduced restriction sites (PCR, see **4.2.21.1**).

Oligonucleotides purchased from Santa Cruz
small interfering RNA (siRNAs)
control siRNA (siC), siRNA against Rap1 (siRap1) and siRNA against Talin (siTalin)

4.1.8. Constructs

4.1.8.1. Vectors and provided constructs

	Source
pCMS4	Daniel Billadeau[234]
pEF Bos FLAG ADAP	Gary Koretzky[65]
pEF Bos FLAG SKAP55	Burkhart Schraven[70]
pEGFP C1 PH_{AKT}, murine	Doreen Cantrell[235]
pEGFP N1	Clonetech
pEGFP C1 $PH_{PLC\delta}$	Jacob Rullo[236]
pEGFP N1 SKAP55	Christian Freund
pEGFP N1 PH_{SK55}	Stefanie Kliche[95]
pJet1.2 (CloneJet™ PCR Cloning Kit)	Thermo Fisher Scientific
RE $ADAP_{Y571F}$ vector	generated by Natalie Waldt

4.1.8.2. Generated constructs

The pEGFP N1 SKAP55 and pEGFP N1 PH_{SK55} vectors were used for *in vitro* mutagenesis (see **4.2.22.2.**).

Suppression/re-expression constructs (depicted in **Figure 4.1**) were generated using the pCMS4 and introducing an shRNA against ADAP or SKAP55 into the vector by restriction with BglII and HindIII. Ligation of the shRNA into the vector destroyed the BglII restriction site, allowing the detection of clones that contained the shRNA. Prior to cloning into the pCMS4 vector, MluI- and NotI-flanked ADAP (template: pEF Bos F ADAP) or SKAP55 (template: pEF Bos F SKAP55) were silently mutated by site-directed *in vitro* mutagenesis (**4.2.22.2.**) to prevent that the shRNA binds to the mRNA and subsequent mRNA degradation (for primer sequence see **4.1.7.**). The suppression/re-expression constructs were tested first in HEK293T cells that do not express ADAP or SKAP55. Therefore, exogenous GFP-tagged ADAP or SKAP55 were transfected together with the suppression/re-expression constructs in a ratio of 1:5. Using Western Blotting, the efficiency of GFP-tagged ADAP/SKAP55 downregulation and re-expression of FLAG-tagged shRNA-resistant ADAP/SKAP55 wild-type or mutants (RE-AD/$SK55_{WT}$ and RE-AD/$SK55_{mutants}$) was tested (exemplified in **Figure 4.1B**). In a second step, the constructs were tested in Jurkat T cells (exemplified in **Figure 4.1C**). RE-AD/$SK55_{mutant}$ clones were selected if they showed a high efficiency in downregulating the GFP-tagged protein and re-expression of the shRNA-resistant mutant at comparable levels as RE-AD/$SK55_{WT}$ (exemplified in **Figure 4.1B,C**).

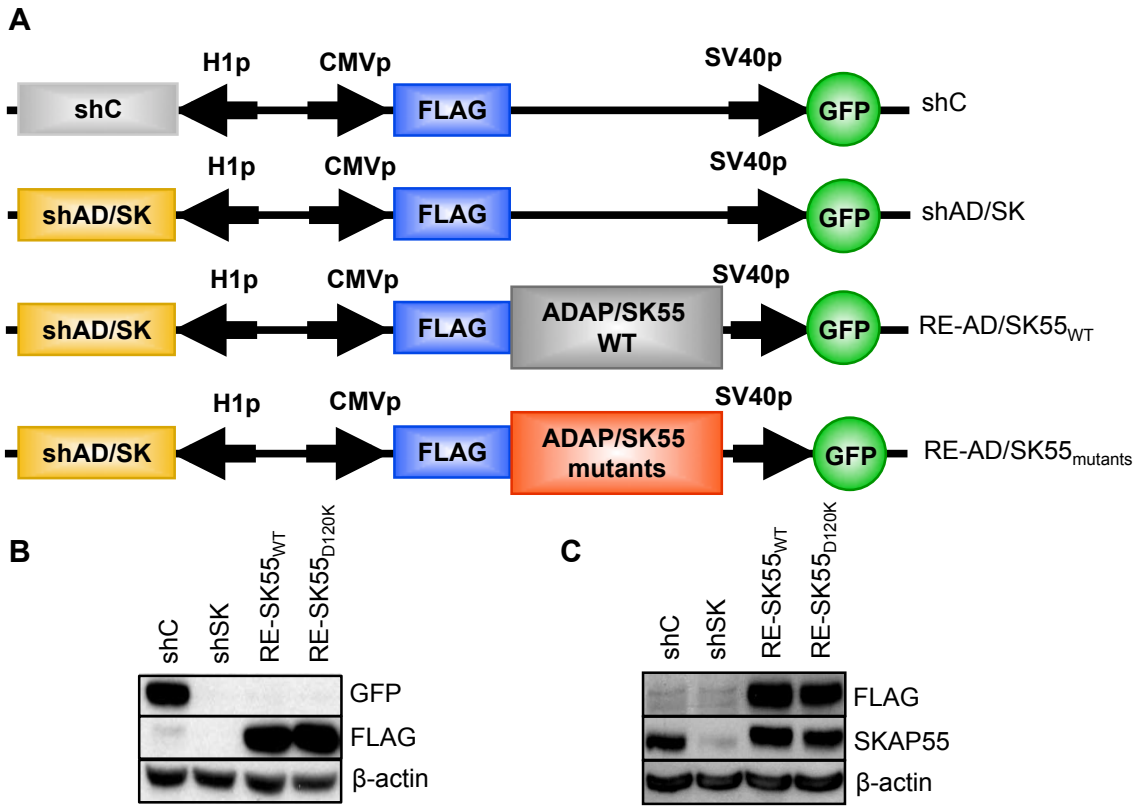

Figure 4.1: Model of the ADAP and SKAP55 suppression/re-expression vectors. (A) The suppression/re-expression vectors contain three promotors (H1 promoter (H1p), *Cytomegalovirus* promoter (CMVp) and simian virus 40 promoter (SV40p)) that allow simultaneous: (i) shRNA (shAD/SK)-mediated downregulation of the endogenous protein, (ii) re-expression of a FLAG-tagged shRNA-resistant wild-type (RE-AD/SK55$_{WT}$) or mutant (RE-AD/SK55$_{mutants}$) ADAP/SKAP55, and (iii) expression of a GFP reporter. **(B,C)** To ensure efficient suppression of the endogenous protein and re-expression of the shRNA-resistant FLAG-tagged mutant at levels comparable to the wild-type construct (RE-SK55$_{WT}$), all RE-SK55$_{mutants}$ were tested first in HEK293T cells **(B)** and second in Jurkat E6 T cells **(C)**. **(B)** In the example shown here, HEK293T cells were transfected with GFP-tagged SKAP55 and suppression/re-expression constructs (shC, shSK, RE-SK55$_{WT}$ or RE-SK55$_{D120K}$) in a ratio of 1:5. Whole lysates were prepared, separated by SDS-PAGE, transferred and immunoblotted with anti-GFP (exogenous GFP-tagged SKAP55, sensitive for shRNA), anti-FLAG (shRNA-resistant re-expressed RE-SK55$_{WT}$ or RE-SK55$_{D120K}$), and anti-β-actin (served as a loading control). **(C)** After the first test in HEK293T cells, constructs were tested in T cells. Therefore, Jurkat T cells were transfected with suppression/re-expression constructs (shC, shSK, RE-SK55$_{WT}$ or RE-SK55$_{D120K}$) incubated for 48h, whole lysates were prepared, separated by SDS-PAGE, transferred and analyzed by immunoblotting with anti-FLAG (shRNA-resistant re-expressed RE-SK55$_{WT}$ or RE-SK55$_{D120K}$), anti-SKAP55 (endogenous and re-expressed SKAP55), and anti-β-actin (served as a loading control).

4.1.9. Cells

	Source
Escherichia coli (E. coli) DH10B	Promega
Jurkat E6.1 T cells	ATCC
Raji B cells	ATCC

4.2. METHODS

Cell-based methods

4.2.1. Isolation and cultivation of primary human T cells ($CD3^+$)

Kit: pan T cell isolation kit, human

Biocoll seperating solution

Primary human T cell culture medium: RPMI1640 with 10% (volume/volume (v/v)) FCS, 0.1% (v/v) Ciprobay 200

Peripheral blood mononuclear cells were isolated by Ficoll gradient centrifugation of heparinized blood from healthy donors. Human T cells (TCR/$CD3^+$ T cells) were purified by negative selection (depletion of non-T cells) using the pan T cell isolation kit and AutoMACS Seperator. The purity of T cells, determined by flow cytometry, was usually more than 96%. After isolation, T cells were cultured for 24h at 37°C and 5% CO_2 in primary human T cell culture medium at a concentration of 1 x 10^6 cells/ml.

Isolation of primary human T cells from healthy donors was approved by the Ethic Committee of the Medical Faculty at the Otto-von-Guericke University, Magdeburg, Germany (89/13). Informed consent was obtained in writing in accordance with the Declaration of Helsinki.

4.2.2. Cultivation of Jurkat E6.1 and Raji B cells

Trypane blue: Trypane Blue Solution 1:2 diluted in PBS

Culture cell medium: RPMI1640 with 10% (v/v) FCS

Jurkat T cells and Raji B cells (ATCC) were maintained at 37°C and 5% CO_2 in culture cell medium. Cells were passaged every 48-72h to keep them at a density of 0.12-0.25 x 10^6 cells/ml. Cells were counted using a Neubauer chamber. Trypane Blue (mix of equal volume of cell suspension and Trypane Blue) was used to differ between dead and viable cells.

4.2.3. Mycoplasma test

Kits: Myco Alert® Assay Control Set (positive control)

Myco Alert® Mycoplasma Detection Kit (assay buffer, reagent and substrate)

Jurkat T cells and Raji B cells were tested on a regular basis (every 4 weeks) for contamination with Mycoplasma. Testing was done according to manufacture's instructions. 72h after the last passage, supernatants were taken and centrifuged for 2min at room temperature (RT) at 3,300*g*. 25µl of assay buffer (negative control), supernatants and positive control were incubated with 25µl of reagent at RT for 5min and luminescence was measured (ELISA reader TriStar LB941) for the first time to define the background signal (1°). 25µl of the substrate were added

and samples were incubated for 10min at RT. Second measurement (2°) was taken and ratio of second and first measurement (2°/1°) was determined. A ratio < 1 was considered negative for mycoplasma.

4.2.4. Cryoconservation of Jurkat E6.1 T cells and Raji B cells

Cryo medium: FCS with 10% (v/v) DMSO

Mycoplasma-free Jurkat T cells and Raji B cells were centrifuged at 301*g* for 4min at RT. Supernatant was removed and cell pellet was resuspended in cryo medium (2 x 10^6/ml). Aliquoted cells (1ml, Cryo Pure Tube) were frozen for 1-2h at -20°C, 1-2 days at -70°C and finally stored in liquid nitrogen.

4.2.5. Electroporation of Jurkat E6.1 and primary human T cells

Kit: Amaxa™ Human T Cell Nucleofector™ Kit (Amaxa solution and cuvettes)

Electroporation was done according to manufacture's instructions. Primary human T cells (5-8 x 10^6/sample) were centrifuged at 470*g* for 10min at RT, washed once with culture cell medium and resuspended in 100µl Amaxa solution. Cells were transferred into cuvettes, 5µg DNA was added and cells were pulsed with the Pulser Nucleofector™ II (Nucleofector®Program U-014 for high viability). Cells were cultured in 5ml of primary T cell culture medium for 24h at 37°C and 5% CO_2.

Jurkat T cells were diluted with culture cell medium to 0.12 x 10^6 cells/ml the day before usage. 2 x 10^7 cells were washed with culture cell medium resuspended in 350µl culture cell medium and transferred in transfection cuvettes. Finally, 30µg DNA were added and the cells were electroporated using the Gene Pulser II (230V, 950µF). Depending on the DNA, cells were incubated for 24-48h in culture cell medium at 37°C and 5% CO_2 until used for further experiments.

4.2.6. Stimulation and Wortmannin/LY294002 treatment

For stimulation, Jurkat E6 T cells were centrifuged (4min, 301*g*, RT), washed once with culture cell medium, resuspended in cell culture medium (1 x 10^7 cells/ml) containing OKT3 (TCR stimulation; 5 or 10µg/ml) or CXCL12 (CXCR4 stimulation; 100ng/ml). Cells were incubated at 37°C and 230rpm for the indicated time points. Stimulation was stopped with ice-cold PBS, cells were centrifuged (4 min, 301*g*, RT) and lysed (see **2.2.8.**).

For LFA-1 clustering transfected Jurkat T cells were incubated with OKT3 (5µg/ml in RPMI1640) for 30min at 4°C. Cells were washed once with RPMI1640 and stimulated with anti-mouse IgG antibody (unconjugated, 10µg/ml in RPMI1640) for 30min at 37°C. Stimulation was stopped with ice-cold PBS, cells were centrifuged (4min, 301*g*, RT) and used for CLSM (see **4.2.14**.).

4 x 10^6 primary human T cells were washed with culture cell medium, incubated with anti-TCR-Biotin and anti-CD28-Biotin (OKT3 and CD28.2; 5µg/ml in RPMI1640) for 30min at 4°C. Cells were washed two times with culture cell medium. Finally, cells were incubated with streptavidin (40µg/ml in RPMI1640) for the indicated time points at 37°C. Stimulation was stopped with ice-cold PBS, cells were centrifuged (4min, 3,300*g*, 4°C) and lysed (see **4.2.8**) or used for CLSM (see **4.2.14.**).

For inhibition of the PI3K, Jurkat T cells were incubated with Wortmannin (0.5µM) or LY294002 (100µM) for 1h at 37°C. Primary human T cells were treated with 100µM Wortmannin for 1h at 37°C. Wortmannin/LY294002 concentrations have been tested to ensure that they downregulate PI3K activity (readout: pS473 AKT) but do not impair viability of cells. Untreated cells were incubated with DMSO.

Biochemical methods

4.2.7. Plasma membrane fractionation

Hypotonic lysis buffer: 10mM HEPES pH7.4, 10mM KCl, 10mM $MgCl_2$, 0.5mM EDTA, 1mM PMSF in UPW (ultra pure water; Milli-Q® Integral Water Purification System)

NP-40-hypotonic lysis buffer: 10mM HEPES pH7.4, 10mM KCl, 10mM $MgCl_2$, 0.5mM EDTA, 1mM PMSF, 150mM NaCl, 1% (v/v) NP-40 in UPW

To isolate PM fractions, 2-5 x 10^7 Jurkat T cells (non-stimulated or OKT3 stimulated) were washed with ice cold PBS and resuspended in a hypotonic lysis buffer (on ice). Cells were sheared 15-20 times with a syringe (2ml, microlance: 27G) and incubated for 10min on ice. Nuclei/intact cells were removed by centrifugation (10min, 100*g*, 4°C). Supernatant was re-centrifuged (10min, 16,000*g*, 4°C). The newly formed supernatant (cytosolic fraction) was removed and the remaining pellet was washed with hypotonic lysis buffer (shear 10 times with 2ml syringe, microlance: 27G). The pellet was dissolved in NP-40-hypotonic lysis buffer and incubated on ice for 30min. The supernatant (membrane fraction) was harvested after another centrifugation step for 10min at 16,000*g* and at 4°C.

4.2.8. Cell lysis

Cell lysis buffer: 1% (v/v) LM, 1% (v/v) NP-40, 1mM Na-monovanadate, 1mM PMSF, 10mM NaF, 10µg/ml PEFA-Block, 10mM EDTA, 0.15M NaCl, 50mM Tris-HCl (pH 7.4) in UPW

1 x 10^6 Jurkat T cells or 3 x 10^6 primary human T cells were lysed in 30µl lysis buffer for 30min at 4°C. Lysates were centrifuged for 10min at 16,000*g* and at 4°C to remove cell debris and supernatant was harvested.

4.2.9. Protein concentration

Kit: Roti®-Nanoquant (diluted 1:5 in UPW)
BSA standard: 0-100µg/ml in UPW

Protein concentration was measured using a Bradford protein assay.[237] Supernatants were diluted 1:100 with UPW, 50µl were transferred to a 96-well plate and incubated with 200µl 1 x Roti®-Nanoquant. Absorption was measured at 570nm (ELISA reader MR5000, DYNATECH). Protein concentration was calculated on the basis of a concentration curve of BSA standard.

4.2.10. Immunoprecipitation

BSA blocking solution: 10mg/ml in UPW
Washing buffer: 0.1% (v/v) LM, 0.1% (v/v) NP-40, 1mM PMSF, 10nM NaF, 0.15M NaCl, 50mM Tris-HCl pH 7.8 in UPW
1 x reducing sample buffer: 10% (weight/volume (w/v)) glycerol, 100mM Tris, pH 6.8, 5% (w/v) SDS, 1% (w/v) bromophenol blue, 10% (v/v) 2-mercaptoethanol in UPW

Lysates (500µg total protein) of untreated or stimulated (OKT3, OKT3/CD28.2 or CXCL12; see **4.2.6.**) Jurkat T cells were used for co-precipitation studies. Lysates were filled up to a volume of 500µl with lysis buffer, antibodies (concentrations see **4.1.5.**), 15µl BSA blocking solution and 30µl Protein A/G PLUS-Agarose beads were added. The samples were incubated on an Intelli mixer for two hours at 4°C. After three times washing with 1ml ice cold washing buffer and complete removal of the supernatant, beads were incubated with 1 x reducing loading buffer at 99°C for 10min and used for SDS-PAGE (**4.2.11.**).

4.2.11. SDS-PAGE

Marker: pageruler prestained protein ladder
Separating gel buffer: 150mM Tris-HCl, pH 8.8, 0.4% (w/v) SDS in UPW
Stacking gel buffer: 500mM Tris-HCl, pH 6.8, 0.4% (w/v) SDS in UPW
SDS-PAGE running buffer (1 x): 25mM Tris, 250mM glycine, 0.1% (w/v) SDS in UPW
5 x reducing sample buffer: 50% (w/v) glycerol, 100mM Tris, pH 6.8, 5% SDS, 1% (w/v) bromophenol blue, 10% (v/v) 2-mercaptoethanol in UPW

SDS-PAGE[238] gels were prepared following the scheme in **Table 4.1**. The mixtures were enough for one separating and two stacking gels.

Table 4.1: Pipetting scheme for SDS-PAGE gels.

	separating gel (10%)	separating gel (12.5%)	stacking gel
UPW	3.75ml	3ml	5.15ml
seperating gel buffer	2.25ml	2.25ml	-
stacking gel buffer	-	-	2.1ml
30% Acrylamide/BIS, 37.5:1	3ml	3ml	1.13ml
10% APS	60µl	60µl	60µl
TEMED	12.5µl	12.5µl	17.5µl

Cell lysates (50µg total protein), 1 x reducing sample buffer and 5 x reducing sample buffer were mixed and boiled at 99°C for 5min. Samples (cell lysates and immunoprecipitates) and protein marker (5µl supplemented with 20µl 1 x reducing sample buffer) were loaded and resolved on 10 or 12.5% SDS-PAGE gel. Electrophoresis was done with BIO-RAD Protein system at 120V for about 80min.

4.2.12. Immunoblotting

Kit: Roti®-Lumin 1+2

Protein transfer buffer (1x): 39mM glycine, 48mM Tris, 0.037% (w/v) SDS, 20% (v/v) methanol in UPW

TBS: 0.01M Tris, 0.15M NaCl in UPW

Blocking buffer: 5% (w/v) milk powder in washing buffer

Washing buffer: 0.1% (v/v) Tween 20 in PBS, pH 8.6

Ponceau S solution: 2% (w/v) Ponceau S in 5% (v/v) acetic acid

Stripping buffer: 1% (w/v) NaN_3 in TBS

Proteins separated by SDS-PAGE (see **4.2.11.**) were subsequently transferred to a nitrocellulose membrane and were detected using antibodies specific for the target proteins (see **4.1.5.**). Protein transfer from the gel to the membrane was controlled by staining the membrane for 2min with Ponceau S solution. Ponceau S staining was removed with washing buffer. Unspecific antibody binding was prevented by incubation of the membrane for 1h at RT with blocking buffer. Antibodies were used diluted in blocking buffer (see **4.1.5.**) and incubated for 1h at RT and low rocking. After incubation with the primary antibodies, the membranes were washed three times for 5min with washing buffer and incubated with the appropriate horseradish peroxidase (HRP)-conjugated secondary antibodies (diluted 1:10000 in blocking buffer). Finally, the membranes were again washed three times for 5min with washing buffer and incubated for 1min with Roti®-Lumin 1+2 according to the manufactor's instructions. The HRP-signals were detected using Amersham Hyperfilms and the developing machine Cawomat 2000IR. For quantification, the intensity of the detected bands was calculated using

the Kodak Image station 2000R (soft ware: ID image software). Membranes were reprobed after deactivation of the HRP by incubating for 45min at RT and low rocking with stripping buffer.

4.2.13. Cell biology assays

4.2.13.1. Flow cytometry-based methods

4.2.13.1.1. Surface staining

1% PFA: 1% (w/v) PFA in PBS

To analyze the cell surface expression on Jurkat T cells, 0.2 x 10^6 cells were incubated with anti-CD18 (LFA-1), anti-CD184 (CXCR4) or OKT3 (1:100 in PBS) antibodies for 30min at 4°C. After washing with ice-cold PBS, cells were stained with the APC-conjugated goat anti-mouse IgG (1:100 in PBS) for 30min at 4°C in dark, fixed with 1% PFA in PBS, measured by flow cytometry (device: FACSCalibur, software: CellQuest™ Pro) and analyzed with the FlowJo 7.6.5 software. Cells stained with the secondary antibody only were used as a reference (negative control).

4.2.13.1.2. TCR-induced CD69 upregulation

For TCR-induced CD69 expression, 48 well plates were left untreated or precoated for 18h with OKT3 (0.5µg/ml) at 4°C. On the next day, wells were washed and 0.5x10^5 cells were cultured in untreated wells containing culture cell medium (negative control), culture cell medium with 50ng/ml PMA (positive control) or in wells pre-coated with OKT3. After 12h, cells were stained with an APC-conjugated anti-CD69 antibody and CD69 surface expression was analyzed by flow cytometry (device: FACSCalibur, software: CellQuest™ Pro).

4.2.13.1.3. Determination of the F-actin content

4% PFA: 4% (w/v) PFA in PBS

To assess F-actin content, T cells were left untreated or stimulated with OKT3 (TCR stimulation, 10µg/ml) or CXCL12 (CXCR4 stimulation, 1µg/ml) for the indicated time points. Stimulation was stopped by adding PBS containing 4% PFA, 2µg/ml phalloidin-Alexa Fluor®633 and 0.2% Triton X-100. After 15min, cells were washed with 1% PFA in PBS and analyzed by flow cytometry (device: FACSCalibur, software: CellQuest™ Pro).

4.2.13.2. Integrin-based methods

4.2.13.2.1. mAb24-binding assay

Transfected Jurkat T cells were left non-stimulated or were stimulated for 30min with plate-bound OKT3 (1µg/ml) in the presence of plate-bound human Fc-tagged ICAM-1 (10µg/ml). Cells were harvested and incubated for 30min with mAb24 antibody (10µg/ml) on ice. After a washing step with ice-cold PBS, cells

were incubated with anti-mouse IgG1 conjugated with APC for 30min on ice. Cells were washed, fixed with 1% PFA and analyzed by flow cytometry (device: FACSCalibur, software: CellQuest™ Pro).

4.2.13.2.2. Adhesion assay

96-well plates were pre-coated with 0.5µg ICAM-1/well. After washing with PBS, wells were blocked with BSA (1µg/ml) overnight at 4°C. Transfected cells were left untreated or stimulated with anti-TCR antibody (OKT3, 5µg/ml), CXCL12 (100ng/ml), PMA (50ng/ml) or Manganese ($MnCl_2$, 1mM) for 30min at 37°C. Subsequently, cells were allowed to adhere for 30min at 37°C. Unbound cells were carefully washed off with Hanks balanced salt solution (HBSS). Bound cells were counted and calculated as % input (2×10^5 cells) in triplicates.

To ensure normal integrin activation potential after transfection of Jurkat T cells with the suppression/re-expression constructs that encode either an shRNA against ADAP or SKAP55 (see **Figure 4.1A**), cells were treated with PMA or Mn^{2+}. Mn^{2+} directly activates LFA-1 by binding to its ectodomain,[239] while PMA acts as a DAG analogue triggering PKC activation.[240] Both molecules can therefore be used to measure integrin activation independent of inside-out signaling events.[64]

4.2.13.2.3. Conjugation assay

Raji B cells (ATCC) were left untreated or were loaded with staphylococcal enterotoxin E (SEE; 20µg/ml) for 2h at 37°C. Cells were washed and incubated for 5min at RT with 0.5µM DDAO-SE (red dye). Raji B cells were washed and incubated with an equal number of transfected Jurkat T cells (GFP-positive) for 30min at 37°C. Nonspecific aggregates were disrupted by short vortexing, cells were fixed with 1% PFA (15min, 4°C) and then analyzed by flow cytometry (device: FACSCalibur; software: CellQuest™ Pro). The percentage of conjugates was defined as the number of double-positive (red and green signal) events.

4.2.13.2.4. Transwell migration assay

Assay medium: RPMI1640 with 10mM HEPES (pH 7.4), 0.1% BSA in UPW

Stopping solution: 0.1M EDTA (pH7.3) in UPW

Chemotaxis assays were performed using Transwells coated with ICAM-1 (10µg/ml) for 1h at 37°C and washed two times with PBS. Transfected Jurkat T cells were washed two times in RPMI1640 and resuspended in assay medium (1×10^6 cells/ml). 0.5×10^6 cells per well were incubated for 2h at 37°C in the presence or absence of human CXCL12 (200ng/ml; lower chamber). Stopping solution was added to each well and incubated for 10min at RT and low rocking. The number of cells migrated into the lower chamber was counted and calculated as % input (of 0.5×10^6 cells).

Fluorescence imaging-based methods

4.2.14. Confocal laser scanning microscopy (CLSM)

4.2.14.1. Slide preparation

12-spot slide (precoated with poly-$_L$-Lysine)
3.5% PFA: 3.5% (w/v) PFA in PBS
Permeabilization solution: 0.1% (v/v) Triton X-100 in PBS
Blocking solution: 5% (w/v) horse serum in PBS
Mounting medium: 2.4g Mowiol 4-88, 6g glycerol dissolved in 12ml 0.2 M Tris, pH 8.5

Transfected T cells were left untreated or incubated with Wortmannin/LY294002 and/or stimulated with OKT3 or OKT3/CD28.2 antibodies (see **4.2.6.**). Cells were diluted to 5 x 10^6 cells/ml in PBS and 20µl were dropped on each spot of a 12-spot slide. The slide was incubated for 15min at 4°C, washed once with ice-cold PBS to remove the unattached cells and the attached cells were fixed with 3.5% PFA for 15min at 4°C. After 5min of washing with PBS, cells were permeabilized (permeabilization solution) for 10min at RT, washed three times for 5min with PBS and unspecific binding of the antibodies was blocked by incubation with blocking solution for 15min at RT. Cells were stained either with DyLight®650-conjugated anti-CD11a (1:20 in blocking solution, for LFA-1 clustering studies (**4.2.14.3.2.**)) or phalloidin-TRITC (1:100 in blocking solution, for PM localization studies (**4.2.14.3.1.**)) for 1h at RT in the dark. After three washing steps the cells were embedded in mounting medium and the coverslip was fixed with nail polish.

4.2.14.2. Microscopy

The cells were imaged using a Leica DM IRE2 inverted fluorescent microscope equipped with a Leica TCS SP2 confocal scanner. Technical specifications and microscopic settings are summarized below.

Technical specifications of the microscope:

Lasers:	argon/krypton
	green helium/neon
	helium/neon
Excitation Filter:	AOTF (Acousto Optical Tunable Filter)
Detectors:	PMT (photomultiplier tubes)

Microscopic settings for imaging:

Lens:	63x/1.32 oil
laser line (in nm):	488
	543
	633
Adjusted emission bandwidth (in nm):	500-535 (488)
	555-620 (543)
	641-745 (633)
Airy unit:	1.0
Average frame:	12
Resolution (in Bit):	8
Scan solution:	512 x 512 pixels
Frame size:	19.82 x 19.82 µm (Jurkat T cells)
	11.92 x 11.92 µm (primary human T cells)
PMT detector output:	8 Bit

4.2.14.3. Image evaluation

4.2.14.3.1. Plasma membrane localization studies

Image analysis for PM localization of GFP-tagged proteins (PH domains or SKAP55 mutants) was done with Adobe Photoshop CS5. Therefore, the fluorescence signals near the PM were calculated and a curve (fluorescence intensity versus length of the measured area (µm), **Figure 4.2B**) was generated using the DisplayOverlay04 software. The fluorescence signals were measured at four different positions (at position 3, 6, 9 and 12 o'clock; see **Figure 4.2A**) of each cell (a total of 25 cells from 3-4 independent experiments). The generated curves were analyzed by determining the middle of the F-actin curve (red) and dropping a perpendicular that divides the green curve (GFP/GFP-tagged proteins) in two halves (**Figure 4.2B,C**). The areas M (at the PM) and Y (cytoplasm) were determined using Adobe Photoshop CS5.

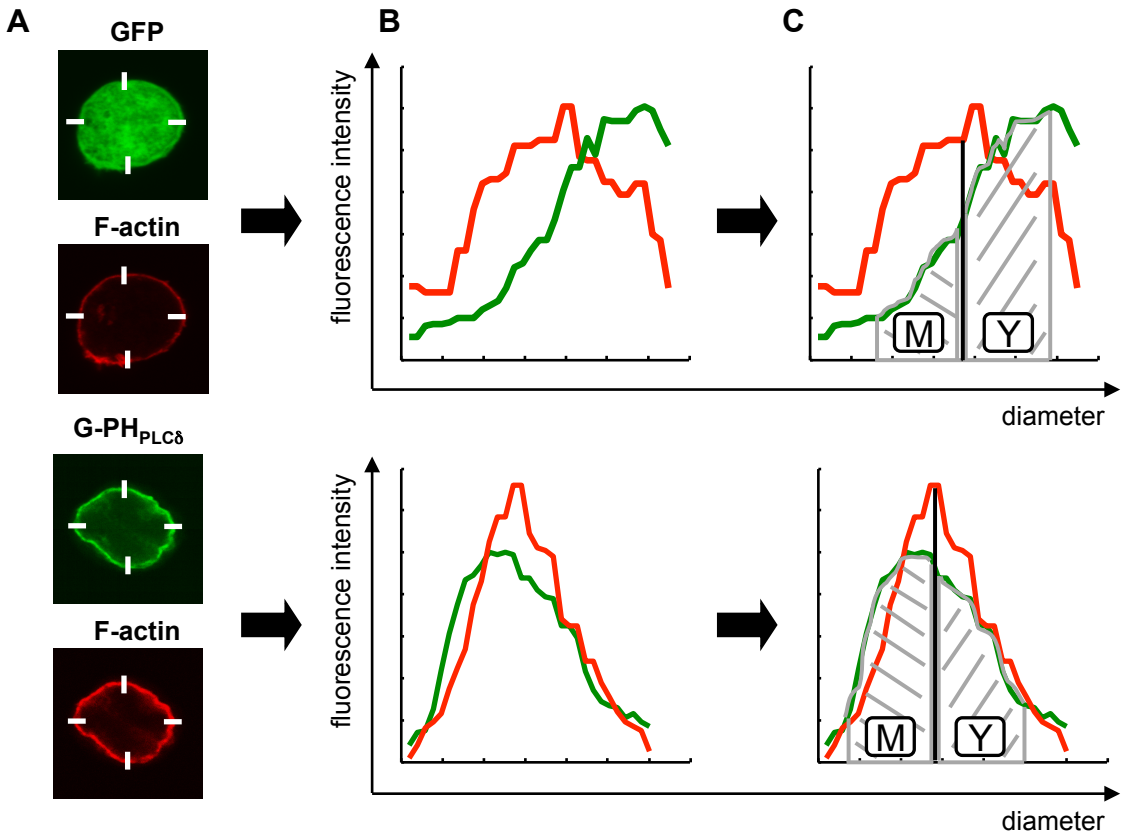

Figure 4.2: Analysis of plasma membrane localization of GFP and the GFP-tagged isolated PH domain of PLCδ in Jurkat T cells. T cells were transfected with constructs encoding GFP or the GFP-tagged PH domain of PLCδ (G-PH$_{PLC\delta}$). After 24h, cells were fixed, stained with phalloidin-TRITC (F-actin) and CLSM was performed. From each cell the fluorescence intensity of GFP/GFP-tagged protein and the cortical actin (stained with phalloidin-TRITC) was measured at four positions (at position 3, 6, 9, and 12 o'clock **(A)**) close to the PM using the DisplayOverlay04 software. The obtained curves **(B)** were analyzed by determining the middle of the F-actin curve (red) and dropping a perpendicular that divides the green curve (GFP/GFP-tagged proteins) in half. Using Adobe Photoshop CS5, the area M (at the PM) and Y (cytoplasm) were calculated **(C)**.

The obtained values for M and Y were used to calculate the ratio of fluorescence intensity at the PM. GFP was used as a negative control (cytoplasmic localization) and its mean fluorescence intensity signal was subtracted from the fluorescent intensity signal of the proteins of interest.

Calculation for GFP was done as follows: (1.) calculation of the ratio: (M)/(M+Y) for each curve, (2.) mean of all four positions within one cell and (3.) mean of calculated values of all 25 cells.

Example (GFP):

(1.) Position 1 (cell 1): p_1= (M)/(M+Y)= 5099/(5099+12677)=5099/17776=0.29

(2.) Mean of cell 1: c_1= (p_1+p_2+p_3+p_4)/4= ((0.29)+(0.32)+(0.33)+(0.31))/4=0.31

(3.) Mean of all 25 cells: X_{GFP}= (c_1+…+c_{25})/25=0.32

Calculation for GFP-tagged proteins of interest (PH domains or SKAP55 proteins/mutants) was done as follows: (1.) calculation of the ratio: (M)/(M+Y) for each curve, (2.) mean of all four positions within one cell, (3.) mean of each cell

subtracted by the mean of GFP (X_{GFP}), (4.) mean of the calculated values for each experiment and (5.) mean of all experiments.

Example (G-$PH_{PLC\delta}$):

(1.) Position 1 (cell 1): p_1= (M)/(M+Y)= 3236/(3236+3756)=3236/6992=0.46

(2.) Mean of cell 1: $c_1= (p_1+p_2+p_3+p_4)/4= ((0.46)+(0.53)+(0.62)+(0.38))/4=0.50$

(3.) Mean of each cell minus mean of GFP (X_{GFP}): $x_1=(c_1-X_{GFP})= (0.50-0.32)=0.18$ … $x_{25}=(c_{25}-X_{GFP})= (0.51-0.32)=0.19$

(3.) Mean of each experiment: $E_1= (x_1+\ldots+x_{10})/10=0.18$

$E_2= (x_{11}+\ldots+x_{20})/10=0.19$

$E_3= (x_{21}+\ldots+x_{25})/5=0.17$

(5.) Mean of all experiments: $X_{PLC}= (E_1+E_2+E_3)/3=0.18$

4.2.14.3.2. LFA-1 clustering studies

For determining LFA-1 clustering, generated pictures were analyzed by calculating the percentage of GFP-positive cells with LFA-1 caps. 450 cells from three independent experiments were examined. Non-stimulated control cells (shC) were set 1 and fold induction was calculated.

4.2.15. Statistical analysis

Statistical significances were determined using a paired or unpaired (student`s) *t* test. As indicated * $p\leq0.05$; ** $p\leq0.01$; *** $p\leq0.001$.

Molecular biology methods

4.2.16. Generation of competent *E. coli* DH10B

TYM medium: 0.5% (w/v) yeast extract, 2% (w/v) Tryptone/Peptone, 0.1M NaCl, 10mM $MgSO_4*7H_2O$ in UPW

TFB1: 30mM $C_2H_3KO_2$, 50mM $MNCl_2$, 100mM KCl, 10mM $CaCl_2$, 15% (w/v) glycerol in UPW

TFB2: 10mM Na-MOPS, pH 7.0, 75mM $CaCl_2$, 10mM KCl, 15% (w/v) glycerol in UPW

Liquid LB medium: 0.5% (w/v) yeast extract, 1% (w/v) Tryptone-Peptone, 85mM NaCl in UPW

Solid LB medium (Petri Culture Dishes): 1.5% (w/v) agar-agar in liquid LB medium

E. coli DH10B (Promega) were plated on solid LB medium (w/o antibiotics) and cultured 18h at 37°C. A swab was used to infect 5ml of liquid medium (w/o antibiotics), incubated for 18h at 37°C and 1ml was used to inocculate 35ml of TYM medium. The bacteria were cultured until they reached an optical density (OD; measured at 600nm) of 0.2-0.8. 25ml of this culture were used to inocculate 100ml of fresh TYM medium. The bacteria grew again at 37°C till the bacterial culture reached an OD between 0.2-0.8, 500ml TYM medium was added, and the bacteria were cultured until they reached an OD of 0.6. The bacteria suspension was cooled while shaking at 4°C and centrifuged for 20min at 3,866*g* and 4°C. Supernatant was removed and the bacteria were resuspended in 100ml ice-cold TFB1. Again, the suspension was centrifuged (8min, 3,866*g*, 4°C), the supernatant

was removed and the pellet was resuspended in 20ml ice-cold TFB2. 400µl aliquots were immediately frozen in liquid nitrogen and stored at -80°C. Bacteria with a competence between $1x10^6$ to $1x10^7$ cfu/ml/µg DNA were used.

4.2.17. Culture of *E. coli* DH10B

E. coli DH10B were cultured in liquid or solid LB medium. To select for the bacteria that contain vectors, the media were supplemented with antibiotics (Ampicillin: 200µg/ml or Kanamycin: 30µg/ml). After chemical transformation, bacteria were plated on solid LB medium (in Petri Culture Dishes) and cultured for 18h at 37°C. For MINI-DNA preparation 5ml of liquid LB medium was inoculated with one colony of transformed bacteria. While for MAXI-DNA preparation 1ml of MINI-DNA culture was used to inocculate 200ml of liquid LB medium. Both cultures were incubated for 18h at 37°C with the liquid culture shaking at 220rpm .

4.2.18. Chemical transformation

$CaCl_2$ solution: 50mM $CalCl_2$ in UPW

IPTG solution: 100mM IPTG in UPW

SOC medium: 0.5% (w/v) yeast extract, 2% (w/v) Tryptone/Peptone, 10mM NaCl, 2.5mM KCl, 10mM $MgSO_4*7H_2O$, 20mM glucose in UPW

Chemical transformation was used to introduce vector DNA into competent E. coli DH10B.

For transformation the following template was used:

Table 4.2: Pipetting scheme for chemical transformation.

	MAXI-DNA	after ligation	after *in vitro* mutagenesis
DNA	1µl	10-20µl *	10-40µl #
$CaCl_2$ (50 mM)	99µl	80-90µl	60-90µl
competent E. coli DH10B	40µl	100µl	100µl

* depending on the ligation (pJet or another vector, see **2.2.26.**)
\# first 10µl, if this did not work the remaining 40µl were used

The DNA was filled up to 100µl with $CaCL_2$, bacteria were added and the sample was incubated at 4°C for 10min. Afterwards, the sample was incubated for 1min at 42°C, 5min at 4°C and for 1h at 37°C and 600rpm. For the last incubation time 800µl SOC medium was added which allowed the bacteria to multiply. The bacteria (400 and 600µl) were plated on solid LB agar and incubated for 18h at 37°C. The pJET1.2 vector was used according to manufacture's instructions. 50µl IPTG was spread over the plate prior to use, incubated for 10min and only 200 and

400µl of the bacteria suspension was used. At the following day, single colonies were picked.

4.2.19. DNA preparation

4.2.19.1. MAXI-DNA preparation

Kit: Nucleo Bond® Xtra Maxi Plus EF

MAXI-DNA preparation was done to isolated large amounts of RNA- and endotoxin-free DNA from bacteria (E. coli DH10B). The preparation was done according to manufacture's instructions. Briefly, 200ml-cultures of bacteria were centrifuged for 20min at 3,866*g* and RT. The pellet was resuspended in 12ml of buffer RES-EF, 12ml LYS-EF buffer were added and incubated for 5min at RT (alkaline lysis). Next, 12ml NEU-EF were added, mixed and incubated for additional 5min on ice. The now renaturated vector DNA was isolated with a silica-based anion exchange column, followed by three washing steps (10ml FIL-EF, 90ml ENDO-EF and 45ml WASH-EF) and elution (15ml ELU-EF). The vector DNA was further purified by washing steps with 10.5ml 2-propanol and 3ml 70% ethanol. The DNA pellet was solved in TE-EF buffer (volume depends on the size of the DNA pellet) over night at 4°C. The DNA was stored at 4°C.

The quality of the DNA preparation was verified by agarose gel electrophoresis (**2.2.21.**) and the ratio of OD_{260}/OD_{280} (see **2.2.20.**). The OD_{260}/OD_{280} ratio reflects the contamination with proteins, while the agarose gel shows the contamination with transfer RNA (tRNA) or genomic DNA that was fragmented during the first steps of isolation.

4.2.19.2. MINI-DNA preparation

Kit: Nucleo Bond® Xtra Maxi Plus EF (buffer: RES-EF, LYS-EF and NEU-EF)

MINI-DNA preparation was used to isolate vector DNA from many clones in a short period of time. The obtained DNA contains RNA and endotoxins and could not be used for transfection of eukaryotic cells but was pure enough to be used for restriction digest (see **2.2.24.**) or sequencing (see **4.2.27.**).

One milliliter of bacterial culture was centrifuged for 5min at 16,100*g* at RT. The pellet was resuspended in 100µl RES-EF buffer and incubated for 10min at 37°C and 300rpm. Additional 100µl LYS-EF buffer were added, mixed and incubated for 5min at RT (alkaline lysis). To renaturate the vector DNA, 100µl NEU-EF were added and incubated for 5min on ice. After a centrifugation step (13,100*g*, 10min, 4°C), the supernatant was mixed with 300µl phenol-chloroform-isoamylalcohol, centrifuged again (9,300*g*, 1min, RT) and the aqueous phase was used for following isolation steps. To further purify the vector DNA, washing steps with 250µl 2-propanol and 500µl 70% ethanol followed. The DNA pellet was dried and resolved with 50µl UPW at 37°C and 300rpm. The DNA was stored at -20°C.

The quality of the DNA preparation was verified as described in **2.2.19.1.** and the DNA was used for further analysis by restriction digest (**4.2.24.**) or sequencing (see **2.2.27.**).

4.2.20. DNA concentration

DNA concentration was measured with the UV/Vis Spectrophotometer Ultraspec 3000. DNA was diluted 1:20, 1:100 and 1:200 (after gel elution in UPW, MAXI-DNA in TE-EF buffer, MINI-DNA in UPW) and OD was measured at 260nm. Additionally, the OD at 280nm was measured to verify the contamination with proteins. OD260/OD280 ratios between 1.8 and 2.0 were considered as pure (no protein contamination).

The Lambert-Beer law was used to calculate the DNA concentration in the samples.

Lambert-Beer law: $A=\varepsilon*c*d$

A: absorption
ε: absorption coefficient
c: concentration of the material
d: diameter of the cuvette

The double-strand DNA concentration was calculated with the following formula:

$c\ (\mu g/ml)= OD_{260}*V*F$

F: multiplication factor (for DNA: F=50)
V: dilution factor

4.2.21. Agarose gel electrophoresis

Marker: 250bp DNA ladder
1 x TAE buffer: 40mM Tris, pH7.6, 20mM acetic acid, 1mM EDTA, pH 8.0 in UPW
Agarose gel: 1% (w/v) agarose, 0.01% (v/v) ethidium bromide (10mg/ml) in TAE buffer
5 x loading buffer: 50% (w/v) glycerol, 0.25% (w/v) bromophenol blue, 0.25% (w/v) xylencyanol in TAE buffer

DNAs were analyzed after DNA preparation (see **2.2.19.**; quality control of the isolated DNA) or after restriction digest (see **4.2.24.**; to verify ligation of an insert or generated restriction sites by PCR). Samples were supplemented with 2µl of 5 x loading buffer. Electrophoresis was done with BIO-RAD Mini DNA system in TAE buffer at constant electric tension (at 80 to 120V, depending on the size of the gel) and for 15 to 30min (depending on the size of the DNA/DNA fragment of interest). The DNA was visualized and recorded under UV light at the gel documentation station. Marker (5µl) was used to estimate the size of the generated DNA-fragments after digestion.

4.2.22. PCR

4.2.22.1. PCR for the generation of DNA fragments

PCR was used to generate restriction sites that flanked the cDNA of interest. The oligonucleotides that were used for the PCR are listed in **2.1.7.** They were solved in UPW (concentration: 1µg/µl) at 37°C and 300rpm and further diluted to 0.1µg/µl for PCR reaction. The pipetting scheme is listed in **Table 4.3**.

Table 4.3: Pipetting scheme for PCR.

	volume (in µl)
UPW	36
10 x Pfu DNA polymerase buffer	5
dNTPs (2mM)	5
forward oligonucleotide (0.1µg/µl)	1
reverse oligonucleotide (0.1µg/µl)	1
template DNA (0.1µg/µl)	1
Pfu DNA polymerase	1

The samples were incubated as follows in a gradient cycler:

Table 4.4: PCR program.

segment	cycles	temperature (in °C)	time (in min)
1	1	95	2
2	30	95	1
		*	1
		72	#
3	1	72	10
4	1	4	∞

The annealing temperature of the oligonucleotide (*) depended on their melting temperature and was determined by subtracting 5°C from the lowest melting temperature of the used oligonucleotides. The elongation time (#) depended on the length of the synthesized DNA fragment and was calculated with 1min/kb.

The PCR product was controlled with agarose gel electrophoresis together with a DNA marker to calculate the size of the generated PCR product. The PCR product was stored at -20°C.

4.2.22.2 *In vitro* Mutagenesis

Kit: QuikChange II-XL Site-directed Mutagenesis Kit

QuikChange II-XL Site-directed Mutagenesis Kit was used to generate specific mutations within cDNAs. Mutagenesis was done according to manufacture's instructions. The pipetting scheme is shown in **Table 4.5**.

Table 4.5: Pipetting scheme for site-directed *in vitro* mutagenesis.

component	10ng template DNS	20ng template DNA
UPW	36.5µl	34.5µl
10 x reaction buffer	5µl	5µl
dNTP mix	1µl	1µl
forward primer (0.1µg/µl)	1.25µl	1.25µl
reverse primer (0.1µg/µl)	1.25µl	1.25µl
template DNA (5ng/µl)	2µl	4µl
Quik solution reagent	3µl	3µl
Pfu Ultra HF DNA polymerase	1µl	1µl

The samples were incubated as follows in a gradient cycler:

Table 4.6: *In vitro* mutagenesis programm.

segment	cycles	temperature (in °C)	time
1	1	95	1min
2	18	95	50s
		60	1min
		68	*
3	1	68	10min
4	1	4	∞

*The elongation time depended on the length of the mutated vector and was calculated with 1min/kb.

After mutagenesis the template DNA was destroyed by incubating the samples with 1µl Dpn I restriction enzyme for 1h at 37°C. Dpn I cuts only the methylated template DNA not the newly generated unmethylated DNA. The samples were frozen for 1-2h before transformation into E. coli DH10B cells. MINI-DNAs were sequenced to select the clones that contained the wanted mutation.

4.2.23. Annealing of oligonucleotides

Annealing buffer: 100mM NaCl, 50mM HEPES, pH 7.4 in UPW

To clone the shRNA-oligonucleotides (see **4.1.7.**) that are directed against ADAP or SKAP55 into the pCMS4 vector, the oligonucleotides were dissolved in UPW (3µg/µl) and 1µl of both single strand Oligonucleotides were added to 48µl annealing buffer. **Table 4.7** shows the program that allowed the attachment of both single strands to form double strand DNA that was integrated into the vector.

Table 4.7: Scheme of the shRNA oligonucleotide annealing.

temperature (in °C)	80	70	60	50	40	30	20	15	10	4
duration (in min)	5	5	10	5	5	5	5	5	10	∞

4.2.24. Restriction digest

To cut DNA at specific positions, restriction enzymes are used that recognize and cut specific palindromic sequences. This method was used to test DNA for their newly generated restriction sites or inserts by PCR (**4.2.22.**). Two types of restriction are distinguished: the analytical and the preparative restriction.

Table 4.8: Pipetting scheme for restriction.

	Analytic restriction digest	Preparative restriction digest
DNA	5-10µl * (MINI-DNA undiluted, MAXI-DNA (0.1µg/µl))	5-10µl * (MAXI-DNA undiluted)
10x reaction buffer	2µl	5µl
restriction enzymes	1µl (of each enzyme; diluted to 1U/µl)	1µl (of each enzyme; undiluted)
UPW	fill up to 20µl	fill up to 50µl

The amount of DNA (*) used for restriction depends on the size of the fragment of interest. If the fragment is smaller then 500bp, 10µl of DNA were used. The appropriate reaction buffer for each restriction enzyme can be found in manufacture's instructions. If two enzymes were used for one restriction digest, one reaction buffer was used that worked best for both enzymes. The restrictions were incubated for 18h at 37°C and 300rpm. Afterwards, the restriction was analyzed by agarose gel electrophoresis (**4.2.21.**). The preparative restricted DNA was further used for DNA extraction (**4.2.25.**).

4.2.25. DNA extraction after restriction digest

Kit: NucleoSpin® Extract II

Calve intestine phosphatase

For ligation of a vector with an insert only one of them has to be phosphorylated at its overhang. Therefore, normally all restricted vectors that were supposed to be used for ligation were incubated with calve intestine phosphatase for 2h at 37°C. Agarose gel electrophoresis was used to separate the DNA fragments. The DNA fragment of interest was cut out and isolated with the NucleoSpin® Extract II Kit (according to manufacture's instructions). First, the agarose gel fragment was solved by incubation with NT buffer at 50°C and 600rpm. In a second step, the DNA was isolated using a silica-based anion exchange column. After a washing

step, DNA was eluted from the column with 20µl UPW. The concentration was measured and agarose gel electrophoresis (see **4.2.21.**) was used to control the extraction (size and purity of the isolated fragment).

4.2.26. Ligation

Kit: CloneJet™ PCR Cloning Kit

Blunt-ended DNA fragments generated by PCR were ligated into the pJet1.2 vector using the CloneJet™ PCR Cloning Kit. This kit contains the already restricted/blunted pJet1.2 vector. Since the pJet1.2 vector cannot be used for transfection of eukaryotic cells, it was only used as an intermediate vector for ligation (see **4.2.26.**) and sequencing (see **4.2.27.**) of blunt-ended PCR products. Afterwards, the pJet1.2 constructs were restricted again, the inserts (now with sticky ends) were isolated (see **4.2.25.**) and ligated into eukaryotic expression vectors. The pipetting scheme for ligation is depicted in **Table 4.9**.

Table 4.9: Pipetting scheme for ligation.

	ligation into pJet1.2 vector	ligation into other vectors
H_2O nuclease free	6µl	5µl
vector	1µl	1µl (50ng)
PCR product/insert	2µl	X
T4 ligase buffer	10µl	1µl
T4 ligase	1µl	1µl
incubation temperature	RT	RT
incubation time	5min	18h

Ligation into other vectors then the pJet1.2 was done with 50ng of vector DNA and an amount of insert that has been calculated with the following formula:

$$X = (bp\ (insert) * 50ng\ (vector)) / bp\ (vector)$$

The reaction mixtures (**Table 4.9**) were incubated at RT for 5min or 18h. After the incubation time they were transformed into competent E. coli DH10B (see **4.2.18.**).

4.2.27. Sequencing

For sequencing, MINI-DNA samples were diluted with UPW to 0.1µg/µl and 20µl were send to GATC *Biotech*. Sequencing primers which were not provided by GATC *Biotech* were diluted to 10pmol/µl. GATC uses a nonradioactive Sanger method-based approach for sequencing.[241,242] The received sequences of DNAs

were screened for the inserted mutations, no additional mutations and for the correctness of generated restriction sites.

❊ ❊ ❊

5. REFERENCES

1. Murphy, K. 2012, *Janeway's immunobiology* 8th ed. Garland Science, Taylor & Francis Group, LLC.
2. Germain, R. N. 2002, T-cell development and the CD4-CD8 lineage decision. *Nat. Rev. Immunol.*, **2**, 309–22.
3. Starr, T. K., Jameson, S. C., and Hogquist, K. A. 2003, Positive and negative selection of T cells. *Annu. Rev. Immunol.*, **21**, 139–76.
4. von Andrian, U. H., and Mempel, T. R. 2003, Homing and cellular traffic in lymph nodes. *Nat. Rev. Immunol.*, **3**, 867–78.
5. Denucci, C. C., Mitchell, J. S., and Shimizu, Y. 2009, Integrin function in T-cell homing to lymphoid and nonlymphoid sites: getting there and staying there. *Crit. Rev. Immunol.*, **29**, 87–109.
6. Comerford, I., Harata-Lee, Y., Bunting, M. D., Gregor, C., Kara, E. E., and McColl, S. R. 2013, A myriad of functions and complex regulation of the CCR7/CCL19/CCL21 chemokine axis in the adaptive immune system. *Cytokine Growth Factor Rev.*, **24**, 269–83.
7. Girard, J.-P., Moussion, C., and Förster, R. 2012, HEVs, lymphatics and homeostatic immune cell trafficking in lymph nodes. *Nat. Rev. Immunol.*, **12**, 762–73.
8. Griffith, J. W., Sokol, C. L., and Luster, A. D. 2014, Chemokines and chemokine receptors: positioning cells for host defense and immunity. *Annu. Rev. Immunol.*, **32**, 659–702.
9. Pozzobon, T., Goldoni, G., Viola, A., and Molon, B. 2016, CXCR4 signaling in health and disease. *Immunol. Lett.*, **177**, 6–15.
10. Ebert, L. M., Schaerli, P., and Moser, B. 2005, Chemokine-mediated control of T cell traffic in lymphoid and peripheral tissues. *Mol. Immunol.*, **42**, 799–809.
11. Hauser, M. A., and Legler, D. F. 2016, Common and biased signaling pathways of the chemokine receptor CCR7 elicited by its ligands CCL19 and CCL21 in leukocytes. *J. Leukoc. Biol.*, **99**, 1–14.
12. Patrussi, L., and Baldari, C. T. 2008, Intracellular mediators of CXCR4-dependent signaling in T cells. *Immunol. Lett.*, **115**, 75–82.
13. Kumar, A., Humphreys, T. D., Kremer, K. N., et al. 2006, CXCR4 physically associates with the T cell receptor to signal in T cells. *Immunity*, **25**, 213–24.
14. Horn, J., Wang, X., Reichardt, P., et al. 2009, Src homology 2-domain containing leukocyte-specific phosphoprotein of 76 kDa is mandatory for TCR-mediated inside-out signaling, but dispensable for CXCR4-mediated LFA-1 activation, adhesion, and migration of T cells. *J. Immunol.*, **183**, 5756–67.
15. Mempel, T. R., Henrickson, S. E., and Von Andrian, U. H. 2004, T-cell priming by dendritic cells in lymph nodes occurs in three distinct phases. *Nature*, **427**, 154–9.
16. Dupré, L., Houmadi, R., Tang, C., and Rey-Barroso, J. 2015, T Lymphocyte Migration: An Action Movie Starring the Actin and Associated Actors. *Front. Immunol.*, **6**, 586.
17. Dustin, M. L. 2014, The immunological synapse. *Cancer Immunol. Res.*, **2**, 1023–33.
18. Le Floc'h, A., and Huse, M. 2015, Molecular mechanisms and functional implications of polarized actin remodeling at the T cell immunological synapse. *Cell. Mol. Life Sci.*, **72**, 537–56.
19. Acuto, O., Di Bartolo, V., and Michel, F. 2008, Tailoring T-cell receptor signals by proximal negative feedback mechanisms. *Nat. Rev. Immunol.*, **8**, 699–712.
20. Chakraborty, A. K., and Weiss, A. 2014, Insights into the initiation of TCR signaling. *Nat. Immunol.*, **15**, 798–807.
21. Ménasché, G., Kliche, S., Bezman, N., and Schraven, B. 2007, Regulation of T-cell antigen receptor-mediated inside-out signaling by cytosolic adapter proteins and Rap1 effector molecules. *Immunol. Rev.*, **218**, 82–91.
22. Bartelt, R. R., and Houtman, J. C. D. 2013, The adaptor protein LAT serves as an integration node for signaling pathways that drive T cell activation. *Wiley Interdiscip. Rev. Syst. Biol. Med.*, **5**, 101–10.

23. Billadeau, D. D., Nolz, J. C., and Gomez, T. S. 2007, Regulation of T-cell activation by the cytoskeleton. *Nat. Rev. Immunol.*, **7**, 131–43.
24. Cotta-de-Almeida, V., Dupré, L., Guipouy, D., and Vasconcelos, Z. 2015, Signal integration during T lymphocyte activation and function: Lessons from the Wiskott-Aldrich syndrome. *Front. Immunol.*, **6**, 1–11.
25. Samstag, Y., Eibert, S. M., Klemke, M., and Wabnitz, G. H. 2003, Actin cytoskeletal dynamics in T lymphocyte activation and migration. *J. Leukoc. Biol.*, **73**, 30–48.
26. Babich, A., and Burkhardt, J. K. 2013, Coordinate control of cytoskeletal remodeling and calcium mobilization during T-cell activation. *Immunol. Rev.*, **256**, 80–94.
27. Majstoravich, S., Zhang, J., Nicholson-Dykstra, S., et al. 2004, Lymphocyte microvilli are dynamic, actin-dependent structures that do not require Wiskott-Aldrich syndrome protein (WASp) for their morphology. *Blood*, **104**, 1396–403.
28. Berlin, C., Bargatze, R. ., Campbell, J. ., et al. 1995, α4 integrins mediate lymphocyte attachment and rolling under physiologic flow. *Cell*, **80**, 413–22.
29. Bruehl, R. E., Springer, T. A., and Bainton, D. F. 1996, Quantitation of L-selectin distribution on human leukocyte microvilli by immunogold labeling and electron microscopy. *J. Histochem. Cytochem.*, **44**, 835–44.
30. von Andrian, U. H., Hasslen, S. R., Nelson, R. D., Erlandsen, S. L., and Butcher, E. C. 1995, A central role for microvillous receptor presentation in leukocyte adhesion under flow. *Cell*, **82**, 989–99.
31. Brown, M. J., Nijhara, R., Hallam, J. A., et al. 2003, Chemokine stimulation of human peripheral blood T lymphocytes induces rapid dephosphorylation of ERM proteins, which facilitates loss of microvilli and polarization. *Blood*, **102**, 3890–9.
32. Lub, M., van Kooyk, Y., van Vliet, S. J., and Figdor, C. G. 1997, Dual role of the actin cytoskeleton in regulating cell adhesion mediated by the integrin lymphocyte function-associated molecule-1. *Mol. Biol. Cell*, **8**, 341–51.
33. Blanchoin, L., Boujemaa-Paterski, R., Sykes, C., and Plastino, J. 2014, Actin dynamics, architecture, and mechanics in cell motility. *Physiol. Rev.*, **94**, 235–63.
34. Taylor, M. P., Koyuncu, O. O., and Enquist, L. W. 2011, Subversion of the actin cytoskeleton during viral infection. *Nat. Rev. Microbiol.*, **9**, 427–39.
35. Comrie, W. A., and Burkhardt, J. K. 2016, Action and traction: Cytoskeletal control of receptor triggering at the immunological synapse. *Front. Immunol.*, **7**, 1–25.
36. Zhang, Y., and Wang, H. 2012, Integrin signalling and function in immune cells. *Immunology*, **135**, 268–75.
37. Hogg, N., Patzak, I., and Willenbrock, F. 2011, The insider's guide to leukocyte integrin signalling and function. *Nat. Rev. Immunol.*, **11**, 416–26.
38. Niu, G., and Chen, X. 2011, Why integrin as a primary target for imaging and therapy. *Theranostics*, **1**, 30–47.
39. Lagarrigue, F., Kim, C., and Ginsberg, M. H. 2016, The Rap1-RIAM-talin axis of integrin activation and blood cell function. *Blood*.
40. Luo, B.-H., Carman, C. V, and Springer, T. a. 2007, Structural basis of integrin regulation and signaling. *Annu. Rev. Immunol.*, **25**, 619–47.
41. Yang, G. X., and Hagmann, W. K. 2003, VLA-4 antagonists: potent inhibitors of lymphocyte migration. *Med. Res. Rev.*, **23**, 369–92.
42. Shimaoka, M., Lu, C., Palframan, R. T., et al. 2001, Reversibly locking a protein fold in an active conformation with a disulfide bond: integrin alphaL I domains with high affinity and antagonist activity in vivo. *Proc. Natl. Acad. Sci. U. S. A.*, **98**, 6009–14.
43. Etzioni, A. 2007, Leukocyte adhesion deficiencies: molecular basis, clinical findings, and therapeutic options. *Adv. Exp. Med. Biol.*, **601**, 51–60.
44. Witte, A. 2013, Emerging Roles of ADAP, SKAP55, and SKAP-HOM for Integrin and NF-κB Signaling in T cells. *J. Clin. Cell. Immunol.*, **1**.
45. Manevich, E., Grabovsky, V., Feigelson, S. W., and Alon, R. 2007, Talin 1 and paxillin facilitate distinct steps in rapid VLA-4-mediated adhesion strengthening to vascular cell adhesion molecule 1. *J. Biol. Chem.*, **282**, 25338–48.
46. Simonson, W. T. N., Franco, S. J., and Huttenlocher, A. 2006, Talin1 regulates TCR-mediated LFA-1 function. *J. Immunol.*, **177**, 7707–14.

47. Ebisuno, Y., Katagiri, K., Katakai, T., et al. 2010, Rap1 controls lymphocyte adhesion cascade and interstitial migration within lymph nodes in RAPL-dependent and -independent manners. *Blood*, **115**, 804–14.
48. Klapproth, S., Sperandio, M., Pinheiro, E. M., et al. 2015, Loss of the Rap1 effector RIAM results in leukocyte adhesion deficiency due to impaired β2 integrin function in mice. *Blood*, **126**, 2704–12.
49. Wernimont, S. A., Wiemer, A. J., Bennin, D. A., et al. 2011, Contact-dependent T cell activation and T cell stopping require talin1. *J. Immunol.*, **187**, 6256–67.
50. Moser, M., Bauer, M., Schmid, S., et al. 2009, Kindlin-3 is required for beta2 integrin-mediated leukocyte adhesion to endothelial cells. *Nat. Med.*, **15**, 300–5.
51. Manevich-Mendelson, E., Feigelson, S. W., Pasvolsky, R., et al. 2009, Loss of Kindlin-3 in LAD-III eliminates LFA-1 but not VLA-4 adhesiveness developed under shear flow conditions. *Blood*, **114**, 2344–53.
52. Svensson, L., Howarth, K., McDowall, A., et al. 2009, Leukocyte adhesion deficiency-III is caused by mutations in KINDLIN3 affecting integrin activation. *Nat. Med.*, **15**, 306–12.
53. Ishihara, S., Nishikimi, A., Umemoto, E., Miyasaka, M., Saegusa, M., and Katagiri, K. 2015, Dual functions of Rap1 are crucial for T-cell homeostasis and prevention of spontaneous colitis. *Nat. Commun.*, **6**, 8982.
54. Duchniewicz, M., Zemojtel, T., Kolanczyk, M., Grossmann, S., Scheele, J. S., and Zwartkruis, F. J. T. 2006, Rap1A-deficient T and B cells show impaired integrin-mediated cell adhesion. *Mol. Cell. Biol.*, **26**, 643–53.
55. Su, W., Wynne, J., Pinheiro, E. M., et al. 2015, Rap1 and its effector RIAM are required for lymphocyte trafficking. *Blood*, **126**, 2695–703.
56. Katagiri, K., Ohnishi, N., Kabashima, K., et al. 2004, Crucial functions of the Rap1 effector molecule RAPL in lymphocyte and dendritic cell trafficking. *Nat. Immunol.*, **5**, 1045–51.
57. Katagiri, K., Katakai, T., Ebisuno, Y., Ueda, Y., Okada, T., and Kinashi, T. 2009, Mst1 controls lymphocyte trafficking and interstitial motility within lymph nodes. *EMBO J.*, **28**, 1319–31.
58. Katagiri, K., Imamura, M., and Kinashi, T. 2006, Spatiotemporal regulation of the kinase Mst1 by binding protein RAPL is critical for lymphocyte polarity and adhesion. *Nat. Immunol.*, **7**, 919–28.
59. Nehme, N. T., Pachlopnik Schmid, J., Debeurme, F., et al. 2012, MST1 mutations in autosomal recessive primary immunodeficiency characterized by defective naive T-cell survival. *Blood*, **119**, 3458–68.
60. Simeoni, L., Kliche, S., Lindquist, J., and Schraven, B. 2004, Adaptors and linkers in T and B cells. *Curr. Opin. Immunol.*, **16**, 304–13.
61. Zou, T., May, R. M., and Koretzky, G. A. 2010, Understanding signal integration through targeted mutations of an adapter protein. *FEBS Lett.*, **584**, 4901–9.
62. Kliche, S., Worbs, T., Wang, X., et al. 2012, CCR7-mediated LFA-1 functions in T cells are regulated by 2 independent ADAP/SKAP55 modules. *Blood*, **119**, 777–85.
63. Verma, N. K., and Kelleher, D. 2014, Adaptor regulation of LFA-1 signaling in T lymphocyte migration: Potential druggable targets for immunotherapies? *Eur. J. Immunol.*, **44**, 3484–99.
64. Abram, C. L., and Lowell, C. a. 2009, The ins and outs of leukocyte integrin signaling. *Annu. Rev. Immunol.*, **27**, 339–62.
65. Musci, M. A., Hendricks-Taylor, L. R., Motto, D. G., et al. 1997, Molecular cloning of SLAP-130, an SLP-76-associated substrate of the T cell antigen receptor-stimulated protein tyrosine kinases. *J. Biol. Chem.*, **272**, 11674–7.
66. da Silva, A. J., Li, Z., de Vera, C., Canto, E., Findell, P., and Rudd, C. E. 1997, Cloning of a novel T-cell protein FYB that binds FYN and SH2-domain-containing leukocyte protein 76 and modulates interleukin 2 production. *Proc. Natl. Acad. Sci. U. S. A.*, **94**, 7493–8.
67. Veale, M., Raab, M., Li, Z., et al. 1999, Novel isoform of lymphoid adaptor FYN-T-binding protein (FYB-130) interacts with SLP-76 and up-regulates interleukin 2 production. *J. Biol. Chem.*, **274**, 28427–35.
68. Thiere, M., Kliche, S., Müller, B., Teuber, J., Nold, I., and Stork, O. 2016, Integrin Activation Through the Hematopoietic Adapter Molecule ADAP Regulates Dendritic Development of Hippocampal Neurons. *Front. Mol. Neurosci.*, **9**, 91.

69. Liu, J., Kang, H., Raab, M., da Silva, a J., Kraeft, S. K., and Rudd, C. E. 1998, FYB (FYN binding protein) serves as a binding partner for lymphoid protein and FYN kinase substrate SKAP55 and a SKAP55-related protein in T cells. *Proc. Natl. Acad. Sci. U. S. A.*, **95**, 8779–84.
70. Marie-Cardine, A., Hendricks-Taylor, L. R., Boerth, N. J., Zhao, H., Schraven, B., and Koretzky, G. A. 1998, Molecular interaction between the Fyn-associated protein SKAP55 and the SLP-76-associated phosphoprotein SLAP-130. *J. Biol. Chem.*, **273**, 25789–95.
71. Heuer, K., Sylvester, M., Kliche, S., et al. 2006, Lipid-binding hSH3 Domains in Immune Cell Adapter Proteins. *J. Mol. Biol.*, **361**, 94–104.
72. Raab, M., Kang, H., Da Silva, A., Zhu, X., and Rudd, C. E. 1999, FYN-T-FYB-SLP-76 interactions define a T-cell receptor ξ/CD3-mediated tyrosine phosphorylation pathway that up-regulates interleukin 2 transcription in T-cells. *J. Biol. Chem.*, **274**, 21170–9.
73. Krause, M., Sechi, A. S., Konradt, M., Monner, D., Gertler, F. B., and Wehland, J. 2000, Fyn-binding protein (Fyb)/SLP-76-associated protein (SLAP), Ena/vasodilator-stimulated phosphoprotein (VASP) proteins and the Arp2/3 complex link T cell receptor (TCR) signaling to the actin cytoskeleton. *J. Cell Biol.*, **149**, 181–94.
74. Heuer, K., Kofler, M., Langdon, G., Thiemke, K., and Freund, C. 2004, Structure of a helically extended SH3 domain of the T cell adapter protein ADAP. *Structure*, **12**, 603–10.
75. Sylvester, M., Kliche, S., Lange, S., et al. 2010, Adhesion and degranulation promoting adapter protein (ADAP) is a central hub for phosphotyrosine-mediated interactions in T cells. *PLoS One*, **5**, e11708.
76. Geng, L., Raab, M., and Rudd, C. E. 1999, Cutting edge: SLP-76 cooperativity with FYB/FYN-T in the Up-regulation of TCR-driven IL-2 transcription requires SLP-76 binding to FYB at Tyr595 and Tyr651. *J. Immunol.*, **163**, 5753–7.
77. Boerth, N. J., Judd, B. A., and Koretzky, G. A. 2000, Functional association between SLAP-130 and SLP-76 in Jurkat T cells. *J. Biol. Chem.*, **275**, 5143–52.
78. Lettau, M., Pieper, J., Gerneth, A., et al. 2010, The adapter protein Nck: role of individual SH3 and SH2 binding modules for protein interactions in T lymphocytes. *Protein Sci.*, **19**, 658–69.
79. Lettau, M., Kliche, S., Kabelitz, D., and Janssen, O. 2014, The adapter proteins ADAP and Nck cooperate in T cell adhesion. *Mol. Immunol.*, **60**, 72–9.
80. da Silva, A. J., Janssen, O., and Rudd, C. E. 1993, T cell receptor ξ/CD3-p59fyn(T)-associated p120/130 binds to the SH2 domain of p59fyn(T). *Jem*, **178**, 2107–13.
81. Motto, D. G., Ross, S. E., Wu, J., Hendricks-Taylor, L. R., and Koretzky, G. A. 1996, Implication of the GRB2-associated phosphoprotein SLP-76 in T cell receptor-mediated interleukin 2 production. *J. Exp. Med.*, **183**, 1937–43.
82. Pauker, M. H., Reicher, B., Fried, S., Perl, O., and Barda-Saad, M. 2011, Functional cooperation between the proteins Nck and ADAP is fundamental for actin reorganization. *Mol. Cell. Biol.*, **31**, 2653–66.
83. Wang, H., McCann, F. E., Gordan, J. D., et al. 2004, ADAP-SLP-76 binding differentially regulates supramolecular activation cluster (SMAC) formation relative to T cell-APC conjugation. *J. Exp. Med.*, **200**, 1063–74.
84. Wang, H., Wei, B., Bismuth, G., and Rudd, C. E. 2009, SLP-76-ADAP adaptor module regulates LFA-1 mediated costimulation and T cell motility. *Proc. Natl. Acad. Sci. U. S. A.*, **106**, 12436–41.
85. Suzuki, J., Yamasaki, S., Wu, J., Koretzky, G. A., and Saito, T. 2007, The actin cloud induced by LFA-1-mediated outside-in signals lowers the threshold for T-cell activation. *Blood*, **109**, 168–75.
86. Kwon, J., Qu, C.-K., Maeng, J.-S., Falahati, R., Lee, C., and Williams, M. S. 2005, Receptor-stimulated oxidation of SHP-2 promotes T-cell adhesion through SLP-76-ADAP. *EMBO J.*, **24**, 2331–41.
87. Lange, S., Sylvester, M., Schümann, M., Freund, C., and Krause, E. 2010, Identification of phosphorylation-dependent interaction partners of the adapter protein ADAP using quantitative mass spectrometry: SILAC vs (18)O-labeling. *J. Proteome Res.*, **9**, 4113–22.
88. Mayya, V., Lundgren, D. H., Hwang, S.-I., et al. 2009, Quantitative phosphoproteomic analysis of T cell receptor signaling reveals system-wide modulation of protein-protein interactions. *Sci. Signal.*, **2**, ra46.

89. Nguyen, V., Cao, L., Lin, J. T., et al. 2009, A new approach for quantitative phosphoproteomic dissection of signaling pathways applied to T cell receptor activation. *Mol. Cell. Proteomics*, **8**, 2418–31.
90. Cao, L., Ding, Y., Hung, N., et al. 2012, Quantitative Phosphoproteomics Reveals SLP-76 Dependent Regulation of PAG and Src Family Kinases in T Cells. *PLoS One*, **7**.
91. Kim, J.-E., and White, F. M. 2006, Quantitative analysis of phosphotyrosine signaling networks triggered by CD3 and CD28 costimulation in Jurkat cells. *J. Immunol.*, **176**, 2833–43.
92. Zimmermann, J., Kühne, R., Sylvester, M., and Freund, C. 2007, Redox-regulated conformational changes in an SH3 domain. *Biochemistry*, **46**, 6971–7.
93. Heuer, K., Arbuzova, A., Strauss, H., Kofler, M., and Freund, C. 2005, The helically extended SH3 domain of the T cell adaptor protein ADAP is a novel lipid interaction domain. *J. Mol. Biol.*, **348**, 1025–35.
94. Edwards, M., Zwolak, A., Schafer, D. A., Sept, D., Dominguez, R., and Cooper, J. A. 2014, Capping protein regulators fine-tune actin assembly dynamics. *Nat. Rev. Mol. Cell Biol.*, **15**, 677–89.
95. Kliche, S., Breitling, D., Togni, M., et al. 2006, The ADAP/SKAP55 signaling module regulates T-cell receptor-mediated integrin activation through plasma membrane targeting of Rap1. *Mol. Cell. Biol.*, **26**, 7130–44.
96. Huang, Y., Norton, D. D., Precht, P., Martindale, J. L., Burkhardt, J. K., and Wange, R. L. 2005, Deficiency of ADAP/Fyb/SLAP-130 destabilizes SKAP55 in Jurkat T cells. *J. Biol. Chem.*, **280**, 23576–83.
97. Burbach, B. J., Srivastava, R., Medeiros, R. B., O'Gorman, W. E., Peterson, E. J., and Shimizu, Y. 2008, Distinct regulation of integrin-dependent T cell conjugate formation and NF-kappa B activation by the adapter protein ADAP. *J. Immunol.*, **181**, 4840–51.
98. Burbach, B. J., Srivastava, R., Ingram, M. A., Mitchell, J. S., and Shimizu, Y. 2011, The pleckstrin homology domain in the SKAP55 adapter protein defines the ability of the adapter protein ADAP to regulate integrin function and NF-kappaB activation. *J. Immunol.*, **186**, 6227–37.
99. Medeiros, R. B., Burbach, B. J., Mueller, K. L., et al. 2007, Regulation of NF-kappaB activation in T cells via association of the adapter proteins ADAP and CARMA1. *Science*, **316**, 754–8.
100. Srivastava, R., Burbach, B. J., and Shimizu, Y. 2010, NF-kappaB activation in T cells requires discrete control of IkappaB kinase alpha/beta (IKKalpha/beta) phosphorylation and IKKgamma ubiquitination by the ADAP adapter protein. *J. Biol. Chem.*, **285**, 11100–5.
101. Thome, M. 2004, CARMA1, BCL-10 and MALT1 in lymphocyte development and activation. *Nat. Rev. Immunol.*, **4**, 348–59.
102. Liu, S., and Chen, Z. J. 2011, Expanding role of ubiquitination in NF-κB signaling. *Cell Res.*, **21**, 6–21.
103. Srivastava, R., Burbach, B. J., Mitchell, J. S., Pagán, A. J., and Shimizu, Y. 2012, ADAP regulates cell cycle progression of T cells via control of cyclin E and Cdk2 expression through two distinct CARMA1-dependent signaling pathways. *Mol. Cell. Biol.*, **32**, 1908–17.
104. Wu, J. N., Gheith, S., Bezman, N. A., et al. 2006, Adhesion- and degranulation-promoting adapter protein is required for efficient thymocyte development and selection. *J. Immunol.*, **176**, 6681–9.
105. Peterson, E. J., Woods, M. L., Dmowski, S. A., et al. 2001, Coupling of the TCR to integrin activation by Slap-130/Fyb. *Science*, **293**, 2263–5.
106. Griffiths, E. K., Krawczyk, C., Kong, Y. Y., et al. 2001, Positive regulation of T cell activation and integrin adhesion by the adapter Fyb/Slap. *Science*, **293**, 2260–3.
107. Mueller, K. L., Thomas, M. S., Burbach, B. J., Peterson, E. J., and Shimizu, Y. 2007, Adhesion and degranulation-promoting adapter protein (ADAP) positively regulates T cell sensitivity to antigen and T cell survival. *J. Immunol.*, **179**, 3559–69.
108. Tian, J., Pabst, O., Römermann, D., et al. 2007, Inactivation of T-cell receptor-mediated integrin activation prolongs allograft survival in ADAP-deficient mice. *Transplantation*, **84**, 400–6.
109. Tian, J., Rodriguez-Barbosa, J.-I., Pabst, O., et al. 2010, ADAP deficiency combined with costimulation blockade synergistically protects intestinal allografts. *Transpl. Int.*, **23**, 71–9.

110. Engelmann, S., Togni, M., Thielitz, A., et al. 2013, T Cell-Independent Modulation of Experimental Autoimmune Encephalomyelitis in ADAP-Deficient Mice. *J. Immunol.*, **191**, 4950–9.
111. Fiege, J. K., Burbach, B. J., and Shimizu, Y. 2015, Negative Regulation of Memory Phenotype CD8 T Cell Conversion by Adhesion and Degranulation-Promoting Adapter Protein. *J. Immunol.*, **195**, 3119–28.
112. Li, C., Li, W., Xiao, J., et al. 2015, ADAP and SKAP55 deficiency suppresses PD-1 expression in CD8+ cytotoxic T lymphocytes for enhanced anti-tumor immunotherapy. *EMBO Mol. Med.*, **7**, 754–69.
113. Li, C., Jiao, S., Wang, G., et al. 2015, The Immune Adaptor ADAP Regulates Reciprocal TGF-β1-Integrin Crosstalk to Protect from Influenza Virus Infection. *PLoS Pathog.*, **11**, e1004824.
114. Parzmair, G. P., Gereke, M., Haberkorn, O., et al. 2016, ADAP plays a pivotal role in CD4+ T cell activation but is only marginally involved in CD8+ T cell activation, differentiation, and immunity to pathogens. *J. Leukoc. Biol.*, **101**.
115. Levin, C., Koren, A., Pretorius, E., et al. 2015, Deleterious mutation in the FYB gene is associated with congenital autosomal recessive small-platelet thrombocytopenia. *J. Thromb. Haemost.*, **13**, 1285–92.
116. Hamamy, H., Makrythanasis, P., Al-Allawi, N., Muhsin, A. A., and Antonarakis, S. E. 2014, Recessive thrombocytopenia likely due to a homozygous pathogenic variant in the FYB gene: case report. *BMC Med. Genet.*, **15**, 135.
117. Levin, C., Zalman, L., Tamary, H., et al. 2013, Small-platelet thrombocytopenia in a family with autosomal recessive inheritance pattern. *Pediatr. Blood Cancer*, **60**, E128-30.
118. Wang, H., Lu, Y., and Rudd, C. E. 2010, SKAP1 is dispensable for chemokine-induced migration of primary T-cells. *Immunol. Lett.*, **128**, 148–53.
119. Zhou, L., Zhang, Z., Zheng, Y., et al. 2011, SKAP2, a novel target of HSF4b, associates with NCK2/F-actin at membrane ruffles and regulates actin reorganization in lens cell. *J. Cell. Mol. Med.*, **15**, 783–95.
120. Marie-Cardine, A., Verhagen, A. M., Eckerskorn, C., and Schraven, B. 1998, SKAP-HOM, a novel adaptor protein homologous to the FYN-associated protein SKAP55. *FEBS Lett.*, **435**, 55–60.
121. Marie-Cardine, A., Bruyns, E., Eckerskorn, C., Kirchgessner, H., Meuer, S. C., and Schraven, B. 1997, Molecular cloning of SKAP55, a novel protein that associates with the protein tyrosine kinase p59fyn in human T-lymphocytes. *J. Biol. Chem.*, **272**, 16077–80.
122. Ophir, M. J., Liu, B. C., and Bunnell, S. C. 2013, The N terminus of SKAP55 enables T cell adhesion to TCR and integrin ligands via distinct mechanisms. *J. Cell Biol.*, **203**, 1021–41.
123. Timms, J. F., Swanson, K. D., Marie-Gardine, A., et al. 1999, SHPS-1 is a scaffold for assembling distinct adhesion-regulated multi-protein complexes in macrophages. *Curr. Biol.*, **9**, 927–30.
124. Raab, M., Smith, X., Matthess, Y., Strebhardt, K., and Rudd, C. E. 2011, SKAP1 protein PH domain determines RapL membrane localization and Rap1 protein complex formation for T cell receptor (TCR) activation of LFA-1. *J. Biol. Chem.*, **286**, 29663–70.
125. Swanson, K. D., Tang, Y., Ceccarelli, D. F., et al. 2008, The Skap-hom dimerization and PH domains comprise a 3′-phosphoinositide-gated molecular switch. *Mol. Cell*, **32**, 564–75.
126. Togni, M., Swanson, K. D., Reimann, S., et al. 2005, Regulation of in vitro and in vivo immune functions by the cytosolic adaptor protein SKAP-HOM. *Mol. Cell. Biol.*, **25**, 8052–63.
127. Schraven, B., Marie-Cardine, A., and Koretzky, G. 1997, Molecular analysis of the fyn-complex: cloning of SKAP55 and SLAP-130, two novel adaptor proteins which associate with fyn and may participate in the regulation of T cell receptor-mediated signaling. *Immunol. Lett.*, **57**, 165–9.
128. Raab, M., Wang, H., Lu, Y., et al. 2010, T cell receptor "inside-out" pathway via signaling module SKAP1-RapL regulates T cell motility and interactions in lymph nodes. *Immunity*, **32**, 541–56.
129. Ménasché, G., Kliche, S., Chen, E. J. H., Stradal, T. E. B., Schraven, B., and Koretzky, G. 2007, RIAM links the ADAP/SKAP-55 signaling module to Rap1, facilitating T-cell-receptor-mediated integrin activation. *Mol. Cell. Biol.*, **27**, 4070–81.
130. Wu, L., Fu, J., and Shen, S. H. 2002, SKAP55 coupled with CD45 positively regulates T-cell receptor-mediated gene transcription. *Mol Cell Biol*, **22**, 2673–86.

131. Meineke, B. 2011, Molekulare Eigenschaften des Integrin regulierenden ADAP-SKAP55-Signalkomplexes. Dissertation, Otto-von-Guericke Universität Magdeburg.
132. Katagiri, K., Maeda, A., Shimonaka, M., and Kinashi, T. 2003, RAPL, a Rap1-binding molecule that mediates Rap1-induced adhesion through spatial regulation of LFA-1. *Nat. Immunol.*, **4**, 741–8.
133. Yang, J., Zhu, L., Zhang, H., et al. 2014, Conformational activation of talin by RIAM triggers integrin-mediated cell adhesion. *Nat. Commun.*, **5**, 5880.
134. Lim, D., Lu, Y., and Rudd, C. E. 2016, Non-cleavable talin rescues defect in the T-cell conjugation of T-cells deficient in the immune adaptor SKAP1. *Immunol. Lett.*, **172**, 40–6.
135. Wang, H., Liu, H., Lu, Y., Lovatt, M., Wei, B., and Rudd, C. E. 2007, Functional defects of SKAP-55-deficient T cells identify a regulatory role for the adaptor in LFA-1 adhesion. *Mol. Cell. Biol.*, **27**, 6863–75.
136. Jo, E.-K., Wang, H., and Rudd, C. E. 2005, An essential role for SKAP-55 in LFA-1 clustering on T cells that cannot be substituted by SKAP-55R. *J. Exp. Med.*, **201**, 1733–9.
137. Alenghat, F. J., Baca, Q. J., Rubin, N. T., et al. 2012, Macrophages require Skap2 and Sirpα for integrin-stimulated cytoskeletal rearrangement. *J. Cell Sci.*, **125**, 5535–45.
138. Hivroz, C., and Saitakis, M. 2016, Biophysical Aspects of T Lymphocyte Activation at the Immune Synapse. *Front. Immunol.*, **7**, 46.
139. Nicolls, M. R., and Gill, R. G. 2006, LFA-1 (CD11a) as a therapeutic target. *Am. J. Transplant*, **6**, 27–36.
140. Wang, H., and Rudd, C. E. 2008, SKAP-55, SKAP-55-related and ADAP adaptors modulate integrin-mediated immune-cell adhesion. *Trends Cell Biol.*, **18**, 486–93.
141. DiNitto, J. P., and Lambright, D. G. 2006, Membrane and juxtamembrane targeting by PH and PTB domains. *Biochim. Biophys. Acta*, **1761**, 850–67.
142. Lemmon, M. a. 2007, Pleckstrin homology (PH) domains and phosphoinositides. *Biochem. Soc. Symp.*, **93**, 81–93.
143. Lemmon, M. A. 2008, Membrane recognition by phospholipid-binding domains. *Nat. Rev. Mol. Cell Biol.*, **9**, 99–111.
144. Hammond, G. R. V, and Balla, T. 2015, Polyphosphoinositide binding domains: Key to inositol lipid biology. *Biochim. Biophys. Acta*, **1851**, 746–58.
145. Platre, M. P., and Jaillais, Y. 2016, Guidelines for the Use of Protein Domains in Acidic Phospholipid Imaging. *Methods Mol. Biol.*, **1376**, 175–94.
146. Kuropka, B., Witte, A., Sticht, J., et al. 2015, Analysis of Phosphorylation-dependent Protein Interactions of Adhesion and Degranulation Promoting Adaptor Protein (ADAP) Reveals Novel Interaction Partners Required for Chemokine-directed T cell Migration. *Mol. Cell. Proteomics*, **14**, 2961–72.
147. Fischer, A., Picard, C., Chemin, K., Dogniaux, S., le Deist, F., and Hivroz, C. 2010, ZAP70: a master regulator of adaptive immunity. *Semin. Immunopathol.*, **32**, 107–16.
148. Wang, H., Kadlecek, T. A., Au-Yeung, B. B., et al. 2010, ZAP-70: an essential kinase in T-cell signaling. *Cold Spring Harb. Perspect. Biol.*, **2**, a002279.
149. Kaur, M., Singh, M., and Silakari, O. 2014, Insight into the therapeutic aspects of "Zeta-Chain Associated Protein Kinase 70 kDa" inhibitors: a review. *Cell. Signal.*, **26**, 2481–92.
150. Bleul, C. C., Farzan, M., Choe, H., et al. 1996, The lymphocyte chemoattractant SDF-1 is a ligand for LESTR/fusin and blocks HIV-1 entry. *Nature*, **382**, 829–33.
151. Soede, R. D., Driessens, M. H., Ruuls-Van Stalle, L., Van Hulten, P. E., Brink, A., and Roos, E. 1999, LFA-1 to LFA-1 signals involve zeta-associated protein-70 (ZAP-70) tyrosine kinase: relevance for invasion and migration of a T cell hybridoma. *J. Immunol.*, **163**, 4253–61.
152. Goda, S., Quale, A. C., Woods, M. L., Felthauser, A., and Shimizu, Y. 2004, Control of TCR-mediated activation of beta 1 integrins by the ZAP-70 tyrosine kinase interdomain B region and the linker for activation of T cells adapter protein. *J. Immunol.*, **172**, 5379–87.
153. García-Bernal, D., Parmo-Cabañas, M., Dios-Esponera, A., Samaniego, R., Hernán-P de la Ossa, D., and Teixidó, J. 2009, Chemokine-induced Zap70 kinase-mediated dissociation of the Vav1-talin complex activates alpha4beta1 integrin for T cell adhesion. *Immunity*, **31**, 953–64.
154. Lin, Y.-P., Cheng, Y.-J., Huang, J.-Y., Lin, H.-C., and Yang, B.-C. 2010, Zap70 controls the interaction of talin with integrin to regulate the chemotactic directionality of T-cell migration. *Mol. Immunol.*, **47**, 2022–9.

155. Evans, R., Lellouch, A. C., Svensson, L., McDowall, A., and Hogg, N. 2011, The integrin LFA-1 signals through ZAP-70 to regulate expression of high-affinity LFA-1 on T lymphocytes. *Blood*, **117**, 3331–42.
156. Di Bartolo, V., Mège, D., Germain, V., et al. 1999, Tyrosine 319, a newly identified phosphorylation site of ZAP-70, plays a critical role in T cell antigen receptor signaling. *J. Biol. Chem.*, **274**, 6285–94.
157. Deswal, S., Schulze, A. K., Höfer, T., and Schamel, W. W. A. 2011, Quantitative analysis of protein phosphorylations and interactions by multi-colour IP-FCM as an input for kinetic modelling of signalling networks. *PLoS One*, **6**, e22928.
158. Alon, R., and Shulman, Z. 2011, Chemokine triggered integrin activation and actin remodeling events guiding lymphocyte migration across vascular barriers. *Exp. Cell Res.*, **317**, 632–41.
159. Förster, R., and Sozzani, S. 2013, Emerging aspects of leukocyte migration. *Eur. J. Immunol.*, **43**, 1404–6.
160. Pfaff, M., Liu, S., Erle, D. J., and Ginsberg, M. H. 1998, Integrin beta cytoplasmic domains differentially bind to cytoskeletal proteins. *J. Biol. Chem.*, **273**, 6104–9.
161. Witte, A., Meineke, B., Sticht, J., et al. 2017, D120 and K152 within the PH domain of T cell adapter SKAP55 regulate plasma membrane targeting of SKAP55 and LFA-1 affinity modulation in human T lymphocytes. *Mol. Cell. Biol.*, MCB.00509-16.
162. Landgraf, K. E., Pilling, C., and Falke, J. J. 2008, Molecular mechanism of an oncogenic mutation that alters membrane targeting: Glu17Lys modifies the PIP lipid specificity of the AKT1 PH domain. *Biochemistry*, **47**, 12260–9.
163. Shan, X., Czar, M. J., Bunnell, S. C., et al. 2000, Deficiency of PTEN in Jurkat T cells causes constitutive localization of Itk to the plasma membrane and hyperresponsiveness to CD3 stimulation. *Mol. Cell. Biol.*, **20**, 6945–57.
164. Freeburn, R. W., Wright, K. L., Burgess, S. J., Astoul, E., Cantrell, D. A., and Ward, S. G. 2002, Evidence That SHIP-1 Contributes to Phosphatidylinositol 3,4,5-Trisphosphate Metabolism in T Lymphocytes and Can Regulate Novel Phosphoinositide 3-Kinase Effectors. *J. Immunol.*, **169**, 5441–50.
165. Arcaro, a, and Wymann, M. P. 1993, Wortmannin is a potent phosphatidylinositol 3-kinase inhibitor: the role of phosphatidylinositol 3,4,5-trisphosphate in neutrophil responses. *Biochem. J.*, **296 (Pt 2**, 297–301.
166. Okada, T., Sakuma, L., Fukui, Y., Hazeki, O., and Ui, M. 1994, Blockage of chemotactic peptide-induced stimulation of neutrophils by wortmannin as a result of selective inhibition of phosphatidylinositol 3-kinase. *J. Biol. Chem.*, **269**, 3563–7.
167. Costello, P. S., Gallagher, M., and Cantrell, D. a. 2002, Sustained and dynamic inositol lipid metabolism inside and outside the immunological synapse. *Nat. Immunol.*, **3**, 1082–9.
168. Garcia, P., Gupta, R., Shah, S., et al. 1995, The pleckstrin homology domain of phospholipase C-delta 1 binds with high affinity to phosphatidylinositol 4,5-bisphosphate in bilayer membranes. *Biochemistry*, **34**, 16228–34.
169. Várnai, P., Bondeva, T., Tamás, P., et al. 2005, Selective cellular effects of overexpressed pleckstrin-homology domains that recognize PtdIns(3,4,5)P3 suggest their interaction with protein binding partners. *J. Cell Sci.*, **118**, 4879–88.
170. Bozulic, L., and Hemmings, B. A. 2009, PIKKing on PKB: regulation of PKB activity by phosphorylation. *Curr. Opin. Cell Biol.*, **21**, 256–61.
171. Vlahos, C. J., Matter, W. F., Hui, K. Y., and Brown, R. F. 1994, A specific inhibitor of phosphatidylinositol 3-kinase, 2-(4-morpholinyl)-8-phenyl-4H-1-benzopyran-4-one (LY294002). *J. Biol. Chem.*, **269**, 5241–8.
172. Ward, S. G., Westwick, J., Hall, N. D., and Sansom, D. M. 1993, Ligation of CD28 receptor by B7 induces formation of D-3 phosphoinositides in T lymphocytes independently of T cell receptor/CD3 activation. *Eur. J. Immunol.*, **23**, 2572–7.
173. Yao, L., Janmey, P., Frigeri, L. G., et al. 1999, Pleckstrin homology domains interact with filamentous actin. *J. Biol. Chem.*, **274**, 19752–61.
174. Macia, E., Partisani, M., Favard, C., et al. 2008, The pleckstrin homology domain of the Arf6-specific exchange factor EFA6 localizes to the plasma membrane by interacting with phosphatidylinositol 4,5-bisphosphate and F-actin. *J. Biol. Chem.*, **283**, 19836–44.

175. Lee, S. H., and Dominguez, R. 2010, Regulation of actin cytoskeleton dynamics in cells. *Mol. Cells*, **29**, 311–25.
176. Wang, H., Moon, E.-Y., Azouz, A., et al. 2003, SKAP-55 regulates integrin adhesion and formation of T cell-APC conjugates. *Nat. Immunol.*, **4**, 366–74.
177. da Silva, A. J., Raab, M., Li, Z., and Rudd, C. E. 1997, TcR zeta/CD3 signal transduction in T-cells: downstream signalling via ZAP-70, SLP-76 and FYB. *Biochem. Soc. Trans.*, **25**, 361–6.
178. Dransfield, I., Cabañas, C., Craig, A., and Hogg, N. 1992, Divalent cation regulation of the function of the leukocyte integrin LFA-1. *J. Cell Biol.*, **116**, 219–26.
179. Katagiri, K., Hattori, M., Minato, N., and Kinashi, T. 2002, Rap1 functions as a key regulator of T-cell and antigen-presenting cell interactions and modulates T-cell responses. *Mol. Cell. Biol.*, **22**, 1001–15.
180. Shimonaka, M., Katagiri, K., Nakayama, T., et al. 2003, Rap1 translates chemokine signals to integrin activation, cell polarization, and motility across vascular endothelium under flow. *J. Cell Biol.*, **161**, 417–27.
181. Lafuente, E. M., van Puijenbroek, A. A. F. L., Krause, M., et al. 2004, RIAM, an Ena/VASP and Profilin ligand, interacts with Rap1-GTP and mediates Rap1-induced adhesion. *Dev. Cell*, **7**, 585–95.
182. De Bruyn, K. M. T., Rangarajan, S., Reedquist, K. A., Figdor, C. G., and Bost, J. L. 2002, The small GTPase Rap1 is required for Mn2+- and antibody-induced LFA-1- and VLA-4-mediated cell adhesion. *J. Biol. Chem.*, **277**, 29468–76.
183. Lee, H. S., Lim, C. J., Puzon-McLaughlin, W., Shattil, S. J., and Ginsberg, M. H. 2009, RIAM activates integrins by linking talin to Ras GTPase membrane-targeting sequences. *J. Biol. Chem.*, **284**, 5119–22.
184. Okabe, S., Tauchi, T., Ohyashiki, K., and Broxmeyer, H. E. 2006, Stromal-cell-derived factor-1/CXCL12-induced chemotaxis of a T cell line involves intracellular signaling through Cbl and Cbl-b and their regulation by Src kinases and CD45. *Blood Cells, Mol. Dis.*, **36**, 308–14.
185. Deindl, S., Kadlecek, T. A., Brdicka, T., Cao, X., Weiss, A., and Kuriyan, J. 2007, Structural Basis for the Inhibition of Tyrosine Kinase Activity of ZAP-70. *Cell*, **129**, 735–46.
186. Hatada, M. H., Lu, X., Laird, E. R., et al. 1995, Molecular basis for interaction of the protein tyrosine kinase ZAP-70 with the T-cell receptor. *Nature*, **377**, 32–8.
187. Sigalov, A. B., Aivazian, D. A., Uversky, V. N., and Stern, L. J. 2006, Lipid-binding activity of intrinsically unstructured cytoplasmic domains of multichain immune recognition receptor signaling subunits. *Biochemistry*, **45**, 15731–9.
188. Lupas, A. N., and Bassler, J. 2016, Coiled Coils – A Model System for the 21st Century. *Trends Biochem. Sci.*, **42**, 1–11.
189. Labadia, M. E., Ingraham, R. H., Schembri-King, J., Morelock, M. M., and Jakes, S. 1996, Binding affinities of the SH2 domains of ZAP-70, p56lck and Shc to the zeta chain ITAMs of the T-cell receptor determined by surface plasmon resonance. *J. Leukoc. Biol.*, **59**, 740–6.
190. O'Brien, R., Rugman, P., Renzoni, D., et al. 2000, Alternative modes of binding of proteins with tandem SH2 domains. *Protein Sci.*, **9**, 570–9.
191. Ottinger, E. A., Botfield, M. C., and Shoelson, S. E. 1998, Tandem SH2 domains confer high specificity in tyrosine kinase signaling. *J. Biol. Chem.*, **273**, 729–35.
192. Balagopalan, L., Kortum, R. L., Coussens, N. P., Barr, V. A., and Samelson, L. E. 2015, The linker for activation of T cells (LAT) signaling hub: from signaling complexes to microclusters. *J. Biol. Chem.*, **290**, 26422–9.
193. Yasuda, K., Kosugi, A., Hayashi, F., et al. 2000, Serine 6 of Lck tyrosine kinase: a critical site for Lck myristoylation, membrane localization, and function in T lymphocytes. *J. Immunol.*, **165**, 3226–31.
194. Busillo, J. M., and Benovic, J. L. 2007, Regulation of CXCR4 signaling. *Biochim. Biophys. Acta*, **1768**, 952–63.
195. Friedl, P., Entschladen, F., Conrad, C., Niggemann, B., and Zänker, K. S. 1998, CD4+ T lymphocytes migrating in three-dimensional collagen lattices lack focal adhesions and utilize β1 integrin-independent strategies for polarization, interaction with collagen fibers and locomotion. *Eur. J. Immunol.*, **28**, 2331–43.
196. Woolf, E., Grigorova, I., Sagiv, A., et al. 2007, Lymph node chemokines promote sustained T lymphocyte motility without triggering stable integrin adhesiveness in the absence of shear forces. *Nat. Immunol.*, **8**, 1076–85.

197. Lämmermann, T., Bader, B. L., Monkley, S. J., et al. 2008, Rapid leukocyte migration by integrin-independent flowing and squeezing. *Nature*, **453**, 51–5.
198. Park, M.-J., Sheng, R., Silkov, A., et al. 2016, SH2 Domains Serve as Lipid-Binding Modules for pTyr-Signaling Proteins. *Mol. Cell*, **62**, 7–20.
199. Callan-Jones, A. C., and Voituriez, R. 2016, Actin flows in cell migration: from locomotion and polarity to trajectories. *Curr. Opin. Cell Biol.*, **38**, 12–7.
200. Ward, S. G., and Marelli-Berg, F. M. 2009, Mechanisms of chemokine and antigen-dependent T-lymphocyte navigation. *Biochem. J.*, **418**, 13–27.
201. Coppolino, M. G., Krause, M., Hagendorff, P., et al. 2001, Evidence for a molecular complex consisting of Fyb/SLAP, SLP-76, Nck, VASP and WASP that links the actin cytoskeleton to Fcgamma receptor signalling during phagocytosis. *J. Cell Sci.*, **114**, 4307–18.
202. Galler, A. B., García Arguinzonis, M. I., Baumgartner, W., et al. 2006, VASP-dependent regulation of actin cytoskeleton rigidity, cell adhesion, and detachment. *Histochem. Cell Biol.*, **125**, 457–74.
203. Chen, H., Bernstein, B. W., and Bamburg, J. R. 2000, Regulating actin-filament dynamics in vivo. *Trends Biochem. Sci.*, **25**, 19–23.
204. Samstag, Y., John, I., and Wabnitz, G. H. 2013, Cofilin: a redox sensitive mediator of actin dynamics during T-cell activation and migration. *Immunol. Rev.*, **256**, 30–47.
205. Arber, S., Barbayannis, F. A., Hanser, H., et al. 1998, Regulation of actin dynamics through phosphorylation of cofilin by LIM-kinase. *Nature*, **393**, 805–9.
206. Yang, N., Higuchi, O., Ohashi, K., et al. 1998, Cofilin phosphorylation by LIM-kinase 1 and its role in Rac-mediated actin reorganization. *Nature*, **393**, 809–12.
207. Niwa, R., Nagata-Ohashi, K., Takeichi, M., Mizuno, K., and Uemura, T. 2002, Control of actin reorganization by Slingshot, a family of phosphatases that dephosphorylate ADF/cofilin. *Cell*, **108**, 233–46.
208. Ohta, Y., Kousaka, K., Nagata-Ohashi, K., et al. 2003, Differential activities, subcellular distribution and tissue expression patterns of three members of Slingshot family phosphatases that dephosphorylate cofilin. *Genes Cells*, **8**, 811–24.
209. Nishita, M., Tomizawa, C., Yamamoto, M., Horita, Y., Ohashi, K., and Mizuno, K. 2005, Spatial and temporal regulation of cofilin activity by LIM kinase and Slingshot is critical for directional cell migration. *J. Cell Biol.*, **171**, 349–59.
210. Nishita, M., Aizawa, H., and Mizuno, K. 2002, Stromal cell-derived factor 1alpha activates LIM kinase 1 and induces cofilin phosphorylation for T-cell chemotaxis. *Mol. Cell. Biol.*, **22**, 774–83.
211. Klemke, M., Kramer, E., Konstandin, M. H., Wabnitz, G. H., and Samstag, Y. 2010, An MEK-cofilin signalling module controls migration of human T cells in 3D but not 2D environments. *EMBO J.*, **29**, 2915–29.
212. Kurita, S., Watanabe, Y., Gunji, E., Ohashi, K., and Mizuno, K. 2008, Molecular dissection of the mechanisms of substrate recognition and F-actin-mediated activation of cofilin-phosphatase slingshot-1. *J. Biol. Chem.*, **283**, 32542–52.
213. Tomiyoshi, G., Horita, Y., Nishita, M., Ohashi, K., and Mizuno, K. 2004, Caspase-mediated cleavage and activation of LIM-kinase 1 and its role in apoptotic membrane blebbing. *Genes to Cells*, **9**, 591–600.
214. Wagner, M. J., Stacey, M. M., Liu, B. A., and Pawson, T. 2013, Molecular mechanisms of SH2- and PTB-Domain-containing proteins in receptor tyrosine kinase signaling. *Cold Spring Harb. Perspect. Biol.*, **5**, 1–19.
215. Bravo-Cordero, J. J., Magalhaes, M. A. O., Eddy, R. J., Hodgson, L., and Condeelis, J. 2013, Functions of cofilin in cell locomotion and invasion. *Nat. Rev. Mol. Cell Biol.*, **14**, 405–15.
216. Riedl, J., Crevenna, A. H., Kessenbrock, K., et al. 2008, Lifeact: a versatile marker to visualize F-actin. *Nat. Methods*, **5**, 605–7.
217. Kavran, J. M., Klein, D. E., Lee, A., et al. 1998, Specificity and promiscuity in phosphoinositide binding by pleckstrin homology domains. *J. Biol. Chem.*, **273**, 30497–508.
218. Ponuwei, G. A. 2016, A glimpse of the ERM proteins. *J. Biomed. Sci.*, **23**, 35.
219. Hao, J.-J., Liu, Y., Kruhlak, M., Debell, K. E., Rellahan, B. L., and Shaw, S. 2009, Phospholipase C-mediated hydrolysis of PIP2 releases ERM proteins from lymphocyte membrane. *J. Cell Biol.*, **184**, 451–62.

220. Stirnweiss, A., Hartig, R., Gieseler, S., et al. 2013, T cell activation results in conformational changes in the Src family kinase Lck to induce its activation. *Sci. Signal.*, **6**, ra13.
221. Philipsen, L., Reddycherla, A. V, Hartig, R., et al. 2017, De novo phosphorylation and conformational opening of the tyrosine kinase Lck act in concert to initiate T cell receptor signaling.
222. Mason, J. M., and Arndt, K. M. 2004, Coiled coil domains: stability, specificity, and biological implications. *Chembiochem*, **5**, 170–6.
223. Wu, L., Yu, Z., and Shen, S.-H. 2002, SKAP55 recruits to lipid rafts and positively mediates the MAPK pathway upon T cell receptor activation. *J. Biol. Chem.*, **277**, 40420–7.
224. Schmits, R., Kündig, T. M., Baker, D. M., et al. 1996, LFA-1-deficient mice show normal CTL responses to virus but fail to reject immunogenic tumor. *J. Exp. Med.*, **183**, 1415–26.
225. Shier, P., Otulakowski, G., Ngo, K., et al. 1996, Impaired immune responses toward alloantigens and tumor cells but normal thymic selection in mice deficient in the beta2 integrin leukocyte function-associated antigen-1. *J. Immunol.*, **157**, 5375–86.
226. Berlin-Rufenach, C., Otto, F., Mathies, M., et al. 1999, Lymphocyte migration in lymphocyte function-associated antigen (LFA)-1-deficient mice. *J. Exp. Med.*, **189**, 1467–78.
227. Semmrich, M., Smith, A., Feterowski, C., et al. 2005, Importance of integrin LFA-1 deactivation for the generation of immune responses. *J. Exp. Med.*, **201**, 1987–98.
228. Hüser, N., Fasan, A., Semmrich, M., Schmidbauer, P., Holzmann, B., and Laschinger, M. 2010, Intact LFA-1 deactivation promotes T-cell activation and rejection of cardiac allograft. *Int. Immunol.*, **22**, 35–44.
229. Nourshargh, S., and Alon, R. 2014, Leukocyte migration into inflamed tissues. *Immunity*, **41**, 694–707.
230. Slaney, C. Y., Kershaw, M. H., and Darcy, P. K. 2014, Trafficking of T cells into tumors. *Cancer Res.*, **74**, 7168–74.
231. Weigelin, B., Krause, M., and Friedl, P. 2011, Cytotoxic T lymphocyte migration and effector function in the tumor microenvironment. *Immunol. Lett.*, **138**, 19–21.
232. Hogg, N., and Selvendran, Y. 1985, An anti-human monocyte/macrophage monoclonal antibody, reacting most strongly with macrophages in lymphoid tissue. *Cell. Immunol.*, **92**, 247–53.
233. Bazil, V., Stefanová, I., Hilgert, I., Kristofová, H., Vaněk, S., and Horejsí, V. 1990, Monoclonal antibodies against human leucocyte antigens. IV. Antibodies against subunits of the LFA-1 (CD11a/CD18) leucocyte-adhesion glycoprotein. *Folia Biol. (Praha).*, **36**, 41–50.
234. Gomez, T. S., McCarney, S. D., Carrizosa, E., et al. 2006, HS1 functions as an essential actin-regulatory adaptor protein at the immune synapse. *Immunity*, **24**, 741–52.
235. Astoul, E., Watton, S., and Cantrell, D. 1999, The Dynamics of Protein Kinase B Regulation during B Cell Antigen Receptor Engagement. *J. Cell Biol.*, **145**, 1511–20.
236. Rullo, J., Becker, H., Hyduk, S. J., et al. 2012, Actin polymerization stabilizes α4β1 integrin anchors that mediate monocyte adhesion. *J. Cell Biol.*, **197**, 115–29.
237. Bradford, M. M. 1976, A rapid and sensitive method for the quantitation of microgram quantities of protein utilizing the principle of protein-dye binding. *Anal. Biochem.*, **72**, 248–54.
238. Laemmli, U. K. 1970, Cleavage of structural proteins during the assembly of the head of bacteriophage T4. *Nature*, **227**, 680–5.
239. Zhang, K., and Chen, J. 2012, The regulation of integrin function by divalent cations. *Cell Adh. Migr.*, **6**, 20–9.
240. Berry, N., Ase, K., Kikkawa, U., Kishimoto, A., and Nishizuka, Y. 1989, Human T cell activation by phorbol esters and diacylglycerol analogues. *J. Immunol.*, **143**, 1407–13.
241. Sanger, F., Nicklen, S., and Coulson, a R. 1977, DNA sequencing with chain-terminating inhibitors. *Proc. Natl. Acad. Sci. U. S. A.*, **74**, 5463–7.
242. Beck, S., and Pohl, F. M. 1984, DNA sequencing with direct blotting electrophoresis. *EMBO J.*, **3**, 2905–9.

ABBREVIATIONS

°C	degree Celsius
2pY-ITAM	doubly phosphorylated ITAM
α	alpha
αβ-TCR	alpha and beta chain of the T cell receptor
β	beta
γ	gamma
δ	delta
μ	my
μg	microgram
μL	microliter
μm	micrometer
μM	micromolar
θ	theta
ζ	zeta
A	
A (Ala)	alanine
Ab	antibody
Ac	actin cytoskeleton
AC	adenylate cyclase
ADAP	adhesion and degranulation-promoting adapter protein
$ADAP_{Y571}$	Y571 of ADAP
$ADAP_{Y571F}$	Y571F-mutated ADAP
AKT	Ak thymoma
APC	antigen-presenting cell
APC	allophycocyanin
Arp2/3	actin-related protein 2/3
B	
bp	base pair
Bcl10	B-cell lymphoma/leukemia 10
BglII	restriction endonuclease enzyme isolated from *Bacillus globigii*
BSA	bovin serum albumin
Btk	bruton's tyrosine kinase
C	
Ca^{2+}	calcium ion
cAMP	cyclic adenosine monophosphate
CARMA-1	Caspase recruitment domain-containing membrane-associated guanylate kinase protein-1
CBM complex	CARMA-1/Bcl10/MALT1 complex
Cdk2	cyclin-dependent kinase 2
cDNA	complementary DNA
CCL19	C-C motif chemokine ligand 19
CCL21	C-C motif chemokine ligand 21
CCR7	C-C motif chemokine receptor 7
CD3	cluster of differentiation 3

CD4	cluster of differentiation 4
CD8	cluster of differentiation 8
CD11a	cluster of differentiation 11a
CD18	cluster of differentiation 18
CD25	cluster of differentiation 25
CD28	cluster of differentiation 28
CD45	cluster of differentiation 45
CD69	cluster of differentiation 69
CFP	cyan fluorescent protein
cfu	colony-forming unit
C-hSH3$_{ADAP}$	C-terminal hSH3 domain of ADAP
CLSM	confocal laser-scanning microscopy
CMVp	*Cytomegalovirus* promoter
CP	cytoplasm
C-pYBP$_{ZAP70}$	C-terminal phospho-tyrosine binding pocket of ZAP70
CR	chemokine receptor
C-SH2$_{ZAP70}$	C-terminal SH2 domain of ZAP70
cSMAC	central supramolecular activation cluster
CXCL12	C-X-C motif chemokine ligand 12
CXCR4	C-X-C motif chemokine receptor 4
D	
D (Asp)	aspartic acid
D120	aspartic acid 120 (SKAP55)
D129	aspartic acid 129 (SKAP-HOM)
D120K	D120 to K mutation
D129K	D129 to K mutation
Da	Dalton
DAG	diacylglycerol
DAGK-δ	diacylglycerol kinase-δ
DC	dendritic cell
DM domain	dimerization domain
DM$_{SK55}$	DM domain of SKAP55
DM$_{SK-HOM}$	DM domain of SKAP-HOM
DM_PH$_{SK55}$	DM and PH domain of SKAP55 wild-type
DM_PH$_{SK55*D120K}$	DM and PH domain of SKAP55 D120K-mutated
DM_PH$_{SK55*D/K}$	DM and PH domain of SKAP55 D/K-mutated
DMSO	dimethyl sulfoxide
DN	double-negative
DNA	deoxyribonucleic acid
dNTPs	deoxynucleotide
DP	double-positive
dSMAC	distal supramolecular activation cluster
E	
E (Glu)	glutamic acid
EAE	experimental autoimmune encephalomyelitis
E. coli	*Escherichia coli*

EDTA	ethylenediaminetetraacetic acid
EFA6	exchange factor for Arf6
e.g.	*exempli gratia*; for example
Ena	*Drosophila* enabled
ERK1/2	extracellular signal-regulated kinase 1/2
ERM proteins	ezrin/radixin/moesin proteins
et al.	*et alii*; and other
etc.	*et cetera*; and the rest (of the things)
EVH1	Ena/VASP homology 1
F	
F (Phe)	phenylalanine
F-actin	filamentous actin
FCS	fetal calf serum
FERM	four-point-one/ezrin/radixin/moesin
FRC	fibroblastic reticular cell
FRET	Förster resonance energy transfer
FYB	Fyn-binding protein
Fyn	feline yes-related protein
G	
g	gram
g	multiplied by gravity (9.81m/s^2)
G	GFP
G_1 phase	gap 1 phase (cell cycle)
G-actin	globular/monomeric actin
GFP	green fluorescent protein
G_p	G protein
GPCR	G protein-coupled receptors
G-PH_{AKT}	GFP-tagged PH domain of AKT
G-$PH_{PLC\delta}$	GFP-tagged PH domain of PLCδ
G-PH_{SK55}	GFP-tagged wild-type PH domain of SKAP55
G-$PH_{SK55*K116M}$	GFP-tagged K116M-mutated PH domain of SKAP55
G-$PH_{SK55*R131M}$	GFP-tagged R131M-mutated PH domain of SKAP55
G-$PH_{SK55*K152E}$	GFP-tagged K152E-mutated PH domain of SKAP55
G-$PH_{SK55*K152M}$	GFP-tagged K152M-mutated PH domain of SKAP55
Grp1	general receptor for phosphoinositides 1
G-$SK55_{D120K}$	GFP-tagged D120K-mutated full-length SKAP55
G-$SK55_{D/K}$	GFP-tagged D120K/K152E-mutated full-length SKAP55
G-$SK55_{WT}$	GFP-tagged wild-type full-length SKAP55
GTP	guanosine triphosphate
H	
h	hour(s)
H1p	H1 promoter
HEPES	4-(2-hydroxyethyl)-1-piperazineethanesulfonic acid
HEV	high endothelial venule
HindIII	restriction endonuclease enzyme isolated from *Haemophilus influenzae*
HRP	horseradish peroxidase

hSH3 domain	helical src homology 3 domain
I	
I (Ile)	isoleucine
ICAM-1, 2, 3,4,5	intercellular adhesion molecule 1-5
IFNγ	interferone-γ
IL-2	interleukine-2
IP	immunoprecipitation
IP_3	inositol-1,4,5-trisphosphate
IPTG	isopropyl-β-D-thiogalactopyranoside
IS	immunological synapse
ITAM	immunoreceptor tyrosine-based activation motif
Itk	IL2 inducible T cell kinase
iTreg	induced Treg
K	
K (Lys)	lysine
K116	lysine 116 (SKAP55)
K116M	K116 to M mutation
K152	lysine 152 (SKAP55)
K152E	K152 to E mutation
K152M	K152 to M mutation
kb	kilobase
k_D	dissociation constant
kDa	kilodalton
ko	knockout
K*R-mutants	lysine and arginine mutants (SKAP55)
L	
l	liter
L (Leu)	leucine
LAD	leukocyte adhesion deficiency
LAT	linker for activation of T cells
Lck	lymphocyte-specific protein tyrosine kinase
l.exp.	long exposure
LFA-1	lymphocyte function-associated antigen-1
LIMK	LIM domain kinase
LN	lymph node
LPS	lipopolysaccharides
M	
M (Met)	methionine
mAb	monoclonal antibody
MALT1	mucosa-associated lymphoid tissue lymphoma translocation protein 1
MFI	mean fluorescence intensitiy
MHC	major histocompatibility complex
mg	milligram
Mg^{2+}	magnesium ion
min	minute
ml	milliliter

MluI	restriction endonuclease enzyme isolated from *Micrococcus luteus* I
Mn^{2+}	manganese ion
mRNA	messenger RNA
Mst1	mammalian sterile20-like kinase 1
N	
n	number of independent experiments
Nck	non-catalytic region of tyrosine kinase
NFAT	Nuclear factor of activated T cells
NF-κB	nuclear factor kappa B
ng	nanogram
$N\text{-}hSH3_{ADAP}$	N-terminal hSH3 domain of ADAP
NK cell	natural killer cell
nm	nanometer
nM	nanomolar
NMR	nuclear magnetic resonance
NotI	restriction endonuclease enzyme isolated from *Nocardia otitidis-caviarum* I
$N\text{-}pYBP_{ZAP70}$	N-terminal phospho-tyrosine binding pocket of ZAP70
$N\text{-}SH2_{ZAP70}$	N-terminal SH2 domain of ZAP70
nTreg	natural Treg
O	
OD	optical density
OSBP	oxysterol-binding protein
P	
p	propability
P (Pro)	proline
PAMPs	pathogen-associated molecular pattern
PBS	phosphate-buffered saline
PCR	polymerase chain reaction
PD-1	programmed death-1
pH	*potentia Hydrogenii*
PH domain	pleckstrin homology domain
PH_{AKT}	PH domain of AKT
$PH_{PLC\delta}$	PH domain of PLCδ
PH_{SK55}	PH domain of SKAP55
$PH_{SK\text{-}HOM}$	PH domain of SKAP-HOM
PI	phosphatidylinositol
PI3K	phosphatidylinositol-3-kinase
PIP_2	phosphatidylinositol-(4,5)-bisphosphate
PIP_3	phosphatidylinositol-(3,4,5)-trisphosphate
PKCθ	protein kinase C theta
PLCγ	phospholipase C gamma
pLN	peripheral lymph node
PM	plasma membrane
PMA	phorbol-12-myristate-13-acetat
pmol	picomol
PNAd	peripheral lymph node addressin

PRO domain	proline-rich domain
PRRs	pattern-recognition receptors
pS473	phosphorylated S473 (AKT)
pSMAC	peripheral supramolecular activation cluster
PTEN	phosphatase and tensin homolog
pY319	phosphorylated Y319 (ZAP70)
pY571	phosphorylated Y571 (ADAP)
R	
R (Arg)	arginine
R131	arginine 131 (SKAP55)
R131M	R131 to M mutation
R140	arginine 140 (SKAP-HOM)
R140M	R140 to M mutation
RA domain	Ras-associating domain
Rap1	Ras proximity 1
RapL	regulator for cell adhesion and polarization enriched in lymphoid tissues
RE-AD/SK55$_{WT}$	suppression/re-expression vector encoding shRNA against ADAP/SKAP55 (shAD/shSK), shRNA-resistant FLAG-tagged wild-type ADAP/SKAP55, and GFP
RE-AD$_{Y571F}$	suppression/re-expression vector encoding shRNA against ADAP (shAD), shRNA-resistant FLAG-tagged Y571F-mutated ADAP, and GFP
RE-SK55$_{D120K}$	suppression/re-expression vector encoding shRNA against SKAP55 (shSK), shRNA-resistant FLAG-tagged D120K-mutated SKAP55, and GFP
RE-SK55$_{D/K}$	suppression/re-expression vector encoding shRNA against SKAP55 (shSK), shRNA-resistant FLAG-tagged D120K/K152E-mutated SKAP55, and GFP
RE-SK55$_{K152E}$	suppression/re-expression vector encoding shRNA against SKAP55 (shSK), shRNA-resistant FLAG-tagged K152E-mutated SKAP55, and GFP
RE-SK55$_{R131M}$	suppression/re-expression vector encoding shRNA against SKAP55 (shSK), shRNA-resistant FLAG-tagged R131M-mutated SKAP55, and GFP
RIAM	Rap1-GTP-interacting adapter molecule
RNA	ribonucleic acid
RT	room temperature
S	
S (Ser)	serine
S473	serine 473 (AKT)
SA	superantigen
SARAH domain	Sav/Rassf/Hpo domain
SD	standard deviation
SDS-PAGE	sodium dodecyl sulfate polyacrylamide gel electrophoresis
s.exp.	short exposure
SFK	src family kinase
SH2 domain	src homology 2 domain
SH3 domain	src homology 3 domain
SH4 domain	src homology 4 domain

shAD	suppression/re-expression vector encoding shRNA (shAD) against ADAP and GFP
shC	suppression/re-expression control vector encoding GFP
SHIP-1	SH2 domain-containing inositol 5-phosphatase 1
SHP-2	Src homology phosphatase 2
shRNA	small hairpin RNA
shSK	suppression/re-expression vector encoding shRNA (shSK) against SKAP55 and GFP
siRNA	small interfering RNA
siC	control siRNA
siRap1	siRNA against Rap1
siTalin	siRNA against Talin
$SKAP55_{\Delta PH}$	PH domain deletion mutant of SKAP55
SKAP55	src kinase-associated phosphoprotein of 55 kDa
SKAP-55R	SKAP55-related
SKAP-HOM	SKAP55-homolog
$SKAP\text{-}HOM_{\Delta PH}$	PH domain deletion mutant of SKAP-HOM
SLAP-130	SLP-76-associated protein of 130 kDa
SLOs	secondary lymphoid organs
SLP-76	SH2 domain-containing leukocyte phosphoprotein of 76kDa
SOC	super optimal broth
Src	
S phase	synthesis phase
SSH1L	slingshot protein phosphatase 1L
SV40p	simian virus 40 promoter
syk	spleen tyrosine kinase
T	
TAK1	transforming growth factor β-activated kinase
T-APC	T cell and antigen-presenting cell
Tc	cytotoxic T cell
TCR	T cell receptor
TGF-β1	transforming growth factor beta 1
Th	helper T cell
TRAF6	TNF receptor-associated factor 6
Treg	regulatory T cell
TRITC	tetramethylrhodamine
tRNA	transfer RNA
$tSH2_{ZAP70}$	tandem SH2 domains of ZAP70
U	
U	unit
V	
V (Val)	valin
VASP	vasodilator-stimulated phosphoprotein
VAV1	vav guanine nucleotide exchange factor 1
VCAM-1	vascular cell adhesion molecule-1
VLA-4	very late antigen-4

v/v	volume per volume
W	
W333	tryptophane 333 (SKAP55)
WASp	Wiskott-Aldrich syndrome protein
WAVE	WASp-family verprolin-homologous protein
WB	Western Blot
WIP	WASp-interacting protein
WL	whole lysate
w/o	without
w/v	weight per volume
Y	
Y (Tyr)	tyrosine
Y319	tyrosine 319 (ZAP70)
Y493	tyrosine 493 (ZAP70)
Y571	tyrosine 571 (ADAP)
Y571F	Y571 to F mutation
YFP	yellow fluorescent protein
Z	
ZAP70	ξ-chain associated protein of 70 kDa

LIST OF FIGURES AND TABLES

List of figures

Figure 1.1	Homing and activation of T cells in lymph nodes.	4
Figure 1.2	CXCR4-mediated signaling in T cells.	5
Figure 1.3	TCR-induced signaling pathways in T cells.	7
Figure 1.4	The actin cytoskeleton in T cells.	8
Figure 1.5	LFA-1 affinity and avidity regulation.	10
Figure 1.6	LFA-1-activating complexes.	13
Figure 1.7	Structure of ADAP.	14
Figure 1.8	Structure of SKAP55 and its homolog SKAP-HOM.	17
Figure 1.9	Model of a PIP_3-responsive molecular switch that controls the targeting of SKAP-HOM to actin-rich membrane ruffles.	21
Figure 2.1.1	ZAP70 inducibly interacts with ADAP upon TCR and CXCR4 stimulation.	24
Figure 2.1.2	Suppression/re-expression vectors of ADAP.	25
Figure 2.1.3	Tyrosine 571 (Y571) of ADAP mediates the ADAP-ZAP70 interaction.	26
Figure 2.1.4	Tyrosine 571 (Y571F) mutation has no effect on TCR-induced adhesion, interaction with APCs, CD69 upregulation and F-actin content.	28
Figure 2.1.5	Tyrosine 571 (Y571) phosphorylation of ADAP regulates CXCR4-induced migration and F-actin content but not adhesion.	30
Figure 2.2.1	The isolated PH domain of SKAP55 localizes at the plasma membrane of T cells.	33
Figure 2.2.2	Plasma membrane localization of the isolated PH domain of SKAP55 is independent of PIP_3 in Jurkat T cells.	34
Figure 2.2.3	Plasma membrane localization of the isolated PH domain of SKAP55 is independent of PIP_3 in primary human T cells.	35
Figure 2.2.4	Lysine 152 (K152) of SKAP55 mediates the interaction of the isolated PH of SKAP55 with the actin cytoskeleton.	37
Figure 2.2.5	Lysine 152 (K152) regulates plasma membrane targeting of SKAP55.	38
Figure 2.2.6	Suppression/re-expression vectors of arginine and lysine (K*R) mutants of SKAP55.	39
Figure 2.2.7	Lysine 152 (K152) of SKAP55 regulates adhesion and T-APC interaction.	40
Figure 2.2.8	Lysine 152 (K152) of SKAP55 mediates the interaction with Talin, LFA-1 and actin.	42

Figure 2.2.9	Full-length SKAP55 primarily localizes in the cytoplasm of non-stimulated Jurkat T cells but translocates to the plasma membrane upon TCR stimulation.	43
Figure 2.2.10	Comparison of the amino acid sequence of the PH domains of human SKAP55 and SKAP-HOM.	44
Figure 2.2.11	Mutation of aspartic acid 120 (D120K) leads to constitutive plasma membrane localization of SKAP55.	45
Figure 2.2.12	Suppression/re-expression vectors of aspartic acid 120 (D120K) mutants of SKAP55.	46
Figure 2.2.13	Mutation of aspartic acid 120 (D120K) induces constitutive adhesion, interaction with APCs and LFA-1 activation.	48
Figure 2.2.14	The lysine 152 (K152E) mutation interferes with the constitutive association of the D120K mutant of SKAP55 with Talin, LFA-1, and actin.	50
Figure 2.2.15	TCR-independent adhesion triggered by the D120K mutant of SKAP55 depends on Talin but not Rap1.	52
Figure 3.1.1	Model of ZAP70 tandem SH2 domain engagement with doubly-phosphorylated ITAMs of the CD3ξ chains or tyrosine 571-phosphorylated ADAP.	57
Figure 3.1.2	Two pools of ZAP70 are involved in the regulation of T cell migration.	61
Figure 3.1.3	Model of ADAP phospho-tyrosine 571-mediated F-actin polymerization.	62
Figure 3.2.1	Model of how SKAP55 auto-inhibition regulates plasma membrane recruitment and LFA-1 activation.	70
Figure 3.2.2	Model of a unimolecular FRET sensor to visualize the auto-inhibitory regulation of SKAP55.	71
Figure 4.1	Model of the ADAP and SKAP55 suppression/re-expression vectors.	86
Figure 4.2	Analysis of plasma membrane localization of GFP and the GFP-tagged isolated PH domain of PLCδ in Jurkat T cells.	96

List of tables

Table 1.1	Key players of integrin signaling.	12
Table 3.1	Summary of PI-binding affinities of relevant PH domains.	64
Table 4.1	Pipetting scheme for SDS-PAGE gels.	91
Table 4.2	Pipetting scheme for chemical transformation.	98
Table 4.3	Pipetting scheme for PCR.	101
Table 4.4	PCR program.	101
Table 4.5	Pipetting scheme for site-directed *in vitro* mutagenesis.	102
Table 4.6	*In vitro* mutagenesis programm.	102
Table 4.7	Scheme of the shRNA oligonucleotide annealing.	103
Table 4.8	Pipetting scheme for restriction.	103
Table 4.9	Pipetting schema for ligation.	104

ACKNOWLEDGEMENTS

First, I would like to thank Prof. **Burkhart Schraven**, the head of our institute and the lead researcher of the CRC854 project B12. I am thankful for all our enriching discussions after my progress reports and the intensive brainstorming during our project meetings. Your constructive feedback in our seminars helped me to improve my presentation skills, which I could further refine in workshops and conferences you allowed me to attend. I am very grateful for the financial support you kindly provided in the last year. Last but not least, I would like to thank you for all the time you spent proofreading my thesis and for your insightful comments.

Second of all, I would like to thank my supervisor Dr. **Stefanie Kliche** for the interesting projects and the invaluable guidance that led me through the whole "becoming a PhD" thing. You helped me to learn all these methods and introduced me into the big riddle of molecular immunology. Our discussions and your ideas concerning my projects were irreplaceable. I am thankful for the precious experiences I gained at workshops and on conferences (particularly for the one in italy). I couldn't have done it without your intensive support - especially in the last two years.

I'd also like to thank the structural biology part of the B12 project: Prof. **Christian Freund**, Dr. **Benno** Kuropka and Dr. **Bernhard** Meineke (AG Freund, Berlin). Thanks for all your MS and NMR studies and our fruitful discussions.

Thanks I like to give to Prof. **Thomas Schüler** who gave me the opportunity to work in his lab and expand my scientific horizon. I am very grateful for your support in the last two years.

A BIG THANKS goes to all former and present members of the two working groups I had/have the pleasure to be part of: AG Kliche (**Anke** Ramonat, **Janine** Degen, **Lisa** Podlasly, **Natalie** Waldt, and my Bachelor students (**Christopher** Theele, **Juliane** Nitschke, and **Michelle** Butzlaff)) and AG Schüler (Dr. **Kathrin** Deiser, **Jana** Giese, **Elena** Denks, Dr. **Ute** Bank, **Laura** Knop, **Robert** Jänsch, **Felix** Richter, and **Fabian** Plambeck). I thank you for teaching me all the practical stuff, for supporting me and for making me ☺ when I was in need of it.

I also would like to thank all the unmentioned former and present members of the **IMKI**. I am thankful for all your help with knowledge, useful ideas or reagents/materials. A special thanks goes to **Lars** Philipsen for providing me with the DisplayOverlay04 software that allowed me to quantify my microscopic pictures and all your help related to computers and analysis.

❊ ❊ ❊

Additionally, I would like to thank those institutions that funded my work. The **German society for Immunology** (DGfI; CRC854 project B12) and the Medical faculty of the **Otto-von-Guericke University** Magdeburg for giving me a LOM stipend.

❊ ❊ ❊

Ein RIESENGROSSES Dankeschön auch an meine Familie (meinen **Eltern**, **Großeltern** und meiner Schwester **Kathleen**). Euer Glaube an mich und eure Unterstützung bei all meinen Entscheidungen bedeuten mir unglaublich viel.

CURRICULUM VITAE

Der Lebenslauf ist in der Online-Version aus Datenschutzgründen nicht enthalten.

Der Lebenslauf ist in der Online-Version aus Datenschutzgründen nicht enthalten.